



The
University
Of
Sheffield.

*Identifying stomatal signalling genes to improve
plant water use efficiency*

by

Mahsa Movahedi

**Submitted to the University of Sheffield for the degree of Doctor of
Philosophy**

Department of Molecular Biology and Biotechnology

The University of Sheffield

August 2013

Acknowledgements

First and foremost, my utmost gratitude to Prof. Julie E. Gray for all her advice, encouragement and support without which this project would not have been materialized.

I would like to express my appreciation for all my collaborators' and colleagues', Prof. Michael Holdsworth, Dr. Daniel Gibbs, Dr. Caspar Chater and Dr. Lee Hunt, guidance and assistance. I would also like to acknowledge many members of the Department of Molecular Biology and Biotechnology and the Department of Animal and plant Science whose support was offered to me through my studies including Nagat Ali, Timothy Doheny Adams, Jennifer Sloan and Carla Turner.

I gratefully acknowledge the Sheffield University for funding my PhD studentship.

My deepest regards and blessings to my family and friends who provided unwavering emotional support and encouragement, including, Mahvash Nekoui, Behrooz Movahedi, Masood Maraghehchi and Mahroo Movahedi.

Abstract

Water is lost from higher plants via transpiration through stomatal pores the aperture of which is regulated by pairs of guard cells. Genetic engineering of the guard cell abscisic acid (ABA) signalling network that induces stomatal closure under drought stress is a key target for improving crop water use efficiency. In this study experiments were designed to investigate whether the biochemical mechanisms associated with the N-end rule pathway of targeted proteolysis could be involved in the regulation of stomatal apertures. The results indicate that the gene encoding the plant N-recogin, *PRT6* (*PROTEOLYSIS6*), and the N-end rule pathway, are important in regulating stomatal ABA-responses in addition to their previously described roles in germination and hypoxia. Direct measurements of stomatal apertures showed that plants lacking *PRT6* exhibit hypersensitive stomatal closure in response to ABA, and IR thermal imaging revealed reduced evapotranspiration under drought-stress. Together with a reduction in stomatal density, these properties result in drought tolerant plants. Plants lacking *PRT6* are able to synthesis NO but their stomata do not close in response to NO suggesting that *PRT6* is required for stomatal aperture responses to NO. Double mutant studies suggested that *PRT6* (and by implication the N-end rule pathway) genetically interacts with known guard cell ABA signalling components *OST1* and *ABI1*, and that it may act either downstream in the same signalling pathway or in an independent pathway. Several other enzymatic components of the plant N-end rule pathway were also shown to be involved in controlling stomatal ABA sensitivity including arginyl transferase and methionine amino peptidase activities. These results indicate that at least one of the N-end rule protein substrates which mediates ABA sensitivity has a methionine-cysteine motif at its N-terminus. A separate set of experiments were designed to investigate whether stomatal ABA-signalling pathways could have been conserved throughout land plant evolution. Cross-genetic complementation experiments were carried out to determine whether *Physcomitrella* stomatal apertures are able to respond to ABA and CO₂ using a similar signalling pathway to that of flowering plants. The results demonstrated involvement of OST1 and ABI1 orthologues indicating that the stomata of the moss respond to ABA and CO₂ using a signalling pathway that appears to be directly comparable to that of the model flowering plant *Arabidopsis thaliana*. This evidence would be consistent with a monophyletic origin for stomata.

Table of Contents

Table of figures-----	ix
1 Chapter 1- Introduction -----	1
1.1 Stomatal Biology-----	1
1.1.1 Structure and significance of stomata-----	1
1.2 Ion Channels and their Function in the regulation of stomatal aperture-----	3
1.3 Stomatal light responses -----	3
1.4 ABA Signalling -----	5
1.4.1 ABA biosynthesis-----	5
1.4.2 Network model of ABA-induced stomatal movement-----	6
1.4.3 ABA signalling, components and mechanisms-----	7
1.4.4 Transcription factors involved in ABA signalling -----	7
1.4.5 Protein kinases and protein phosphatases are involved in ABA-signalling-----	8
1.4.6 Interaction of a protein kinase-phosphatase pair with anion channels in ABA signalling 8	8
1.4.7 Mechanism of ABA perception by PYL receptors -----	10
1.4.8 Evolution of ABA signalling pathways -----	11
1.5 Guard cell CO ₂ responses-----	12
1.5.1 Mechanisms of CO ₂ signalling in guard cells-----	13
1.6 Establishing a role for nitric oxide (NO) in signalling stomatal closure-----	14
1.7 Functions of the N-end rule pathways in plants-----	16
1.7.1 N-end rule pathway and its substrates in plants-----	17
1.7.2 26S proteasome-dependent protein degradation in ABA responses -----	18
1.8 Aim and objectives of the investigation -----	20
2 Chapter 2- Materials and Methods-----	21
2.1 Materials -----	21
2.1.1 Chemicals, enzymes, vectors etc.-----	21
2.2 Growth conditions -----	21
2.2.1 Plant material-----	21
2.3 Nucleic acid techniques-----	22
2.3.1 Plant Genomic DNA isolation -----	22
2.3.2 Total plant RNA extraction -----	22
2.3.3 RNA and DNA quantification-----	23
2.3.4 Reverse transcription/ first strand cDNA synthesis using superscript II RT-----	23

2.4	Polymerase Chain Reaction (PCR)	24
2.4.1	<i>Taq</i> DNA polymerase PCR	24
2.4.2	PCR using a polymerase with proofreading activity	24
2.5	Agarose gel electrophoresis	26
2.5.1	Extraction of DNA fragments from agarose gels	26
2.6	Cloning of DNA fragments	26
2.6.1	Cloning vectors	26
2.6.2	LR Clonase	27
2.7	DNA ligation	28
2.7.1	Transformation of competent <i>Escherichia coli</i>	28
2.7.2	Bacterial storage	28
2.7.3	Analysing transformants by PCR	29
2.7.4	Plasmid DNA preparation using Sigma Gen Elute™ Miniprep Kit	29
2.7.5	Analysing plasmid DNA by restriction	30
2.7.6	Recombination of entry vector and destination vectors LR using Clonase	30
2.7.7	Transformation of <i>Arabidopsis thaliana</i> using <i>Agrobacterium tumefaciens</i>	30
2.7.8	Preparation of <i>Agrobacterium</i> for floral dipping	31
2.7.9	Transformation of <i>Arabidopsis</i> by floral dipping	31
2.7.10	Histochemical localization of GUS activity	31
2.8	Stomatal phenotyping	32
2.8.1	Stomatal density and index measurement	32
2.8.2	Stomatal aperture measurements	33
2.8.2.3	Light induced stomatal opening	34
2.9	Relative water content measurements.	35
2.10	Analysis of leaf temperature in response to drought stress	35
2.10.1	Infrared Thermal imaging	35
2.11	Statistical analysis	36
3	Chapter 3- The N-recognin PRT6 mediates ABA-induced stomatal closure and drought susceptibility	37
3.1	Introduction	37
3.2	ABA-induced stomatal closure	37
3.3	Light induced stomatal opening	38
3.4	Effects of CO ₂ on stomatal aperture	38
3.5	Expression pattern of the PRT6 gene	39

3.6	Investigation of PRT6 gene expression in guard cells using a pPRT6::GUS reporter gene fusion	42
3.7	GUS histochemical staining of <i>pPRT6::GUS</i> transformed plants	45
3.8	Studies of <i>Arabidopsis prt6</i> T-DNA insertional mutant plants	49
3.9	Phenotypic characterisation of <i>prt6</i> plants	50
3.9.1	Stomatal aperture analysis	50
3.9.2	<i>prt6</i> stomatal aperture responses to ABA	50
3.9.3	<i>prt6</i> stomatal aperture responses to CO ₂ concentration	51
3.9.4	<i>prt6</i> stomatal opening in response to light	51
3.9.5	Analysis of stomatal development in <i>prt6</i>	52
3.9.6	Relative water content of <i>prt6</i>	52
3.10	Thermal imaging of <i>prt6</i> leaf evapotranspiration	59
3.11	Nitric oxide is an endogenous signalling intermediate in ABA-induced stomatal closure	62
3.11.1	<i>Prt6</i> stomatal aperture responses to NO	62
3.11.2	ABA induces NO synthesis in <i>Arabidopsis</i> guard cells	63
3.12	Genetic interactions of <i>PRT6</i> with ABA signal transduction components	66
3.13	Conclusion	69
4	Chapter 4-The N-end rule pathway of protein degradation regulates ABA-induced stomatal closure	70
4.1	The role of methionine aminopeptidases in the N-end rule pathway and stomatal ABA signalling	70
4.2	Expression of methionine aminopeptidase genes in guard cells	71
4.3	Stomatal aperture response of <i>map1a</i> to ABA	72
4.4	<i>Arabidopsis</i> NTAN and NTAQ amidases	74
4.4.1	The expression of <i>NTAN</i> and <i>NTAQ</i> genes in guard cells	75
4.4.2	The role of <i>NTAN1</i> and <i>NTAQ1</i> in stomatal ABA-responses.	75
4.5	N-terminal arginylation in the N-end rule pathway	79
4.5.1	The expression of arginyl transferases genes in guard cells	79
4.5.2	Role of arginyl transferases in stomatal ABA-signalling	80
4.5.3	Analysis of stomatal numbers	81
4.6	Putative substrates of the N-End Rule Pathway	83
4.7	The role of MC-ERFs in stomatal ABA-responses	84
4.8	Conclusion	86
5	Chapter- 5 The mechanisms of ABA and CO ₂ induced stomatal closure appears to have been conserved throughout land plant evolution.	87

5.1	Introduction	87
5.2	Moss stomata respond to ABA and CO ₂	89
5.3	Methods Summary.....	90
5.3.1	<i>Atost1-4</i> complementation with <i>PpOST1-1</i>	91
5.4	PpABI1A Complementation of <i>Arabidopsis</i> <i>hab1-1abi1-2</i>	92
5.5	CO ₂ Signalling.....	94
5.6	Conclusion	95
6	Chapter 6– Discussion	97
6.1	Discussion	97
6.1.1	The N-recognin <i>PRT6</i> mediates ABA-induced stomatal closure and drought susceptibility	97
6.1.2	The N-end rule pathway of protein degradation is a mediator of ABA-induced stomatal closure	99
6.1.3	The mechanisms of ABA and CO ₂ induced stomatal closure appears to have been conserved throughout land plant evolution.....	99
6.2	Prospects for future work.....	100
7	References.....	103

Table of figures

Figure 1-1 the position of guard cell in a leaf	2
Figure 1-2 Processes of stomatal opening and closing in response to blue light and ABA	5
Figure 1-3 Stomata regulate gas exchange between leaves and the atmosphere.	9
Figure 1-4 Model to illustrate the molecular components of the ABA-activated signalling pathway that regulates gene expression.	11
Figure 1-5 CO ₂ signalling in regulation of stomatal movements	14
Figure 1-6 the hierarchical structure of the N-end rule pathway of protein degradation.	17
Figure 1-7 Regulation of abiotic stress signalling pathways by ABA and the possible role of the N-end rule pathway.	19
Figure 2-1 Equipment used to incubate epidermal fragments at optimum conditions for opening Arabidopsis stomatal pores (Diagram reproduced from Dr Sarah Clements thesis)	36
Figure 3-1 Expression pattern of PRT6 in mesophyll and guard cells from a transcriptomic analysis of protoplast extracts	40
Figure 3-2 Expression pattern of PRT6 at different growth stages	41
Figure 3-3 Expression pattern of PRT6 in seedlings treated with ABA	42
Figure 3-4 Generation of the pPRT6::GUS promoter fusion construct	43
Figure 3-5 Entry vector used for pPRT6 promoter cloning	44
Figure 3-6 Destination vector used to create pPRT6::GUS	45
Figure 3-7 GUS histochemical localisation in guard cells of pPRT6::GUS	47
Figure 3-8 histochemical localization of expression directed by PRT6 promoter regions in T1 generation pPRT6::GUS seedlings treated with ABA	47
Figure 3-9 GUS histochemical localization in pPRT6::GUS rosette leaves	48
Figure 3-10 GUS histochemical localisation in pPRT6::GUS inflorescence tissues	48
Figure 3-11 Stomatal aperture measurements taken from epidermal peels of prt6-5, prt6-1 and control plants in response to A) ABA; B) expressing the same data as a ratio of ABA-treated to control (no added ABA) for each genotype; C) pore length of open stomata of prt6 and control plants (no added ABA)	54
Figure 3-12 Stomatal aperture measurements taken from epidermal peels of prt6-5, prt6-1 and control plants in response to A) CO ₂ B) Light	55
Figure 3-13 Stomatal and epidermal cell densities of Col-0, prt6-1, prt6-5 and abh-1 leaves	56
Figure 3-14 Stomatal indices of Col-0, prt6-1, prt6-5 and abh-1 leaves	57
Figure 3-15 Measurements of leaf relative water content of control, prt6-1 and prt6-5	58
Figure 3-16 prt6-5 mutants are defective in the regulation of transpiration during water stress	61
Figure 3-17 Effects of ABA and NO donor on stomatal closure of prt6-5 and control plants	63
Figure 3-18 Effects of ABA and NO scavenger on stomatal closure of prt6 and control plants	64
Figure 3-19 ABA induces NO synthesis in Arabidopsis guard cells.	65
Figure 3-20 Stomatal ABA-responses of the ost1-4 mutant in combination with prt6-1	68
Figure 3-21 Stomatal ABA-responses of snrk2 mutants in combination with prt6-1	68
Figure 3-22 Stomatal ABA-responses of abi1-1 mutant in combination with prt6-4	69
Figure 4-1 Simplified representation of Arginine branch of the N-end rule pathway associated with Cysteine oxidation of MC-substrate proteins (S).	71
Figure 4-2 Expression patterns of MAP1A, MAP2A and MAP2B genes in guard and mesophyll cells from a transcriptomic analysis of protoplast extracts	73
Figure 4-3 Stomatal aperture measurements taken from epidermal peels of map1a, prt6-5 and control plants in response to ABA	74
Figure 4-4 Expression patterns of the NTAN1 and NTAQ1 genes in mesophyll and guard cells from a transcriptomic analysis of protoplast extracts	77
Figure 4-5 Stomatal aperture measurements taken from epidermal peels of ntan1-1, ntaq1-1, ntaq1-2 and control plants in response to ABA.	78

<i>Figure 4-6 Expression patterns of the ATE1 and ATE2 genes in mesophyll and guard cells from a transcriptomic analysis of protoplast extracts</i> -----	80
<i>Figure 4-7 Stomatal aperture measurements taken from epidermal peels of ate1-2ate2-1, prt6-5, prt6-1 and control plants in response to ABA</i> -----	81
<i>Figure 4-8 Analysis of stomatal density in Col-0, ate1-2ate2-1, prt6-1 and prt6-5</i> -----	82
<i>Figure 4-9 Analysis of stomatal indices in Col-0, ate1-2ate2-1, prt6-1 and prt6-5</i> -----	82
<i>Figure 4-10 Expression patterns of the HRE1, HRE2, RAP2.12 and RAP2.2 genes in mesophyll and guard cells from a transcriptomic analysis of protoplast extracts</i> -----	85
<i>Figure 4-11 Stomatal aperture measurements taken from epidermal peels of rap2.2-1, rap2.12, hre1hre2 and control plants in response to ABA</i> -----	86
<i>Figure 5-1 Moss stomata</i> -----	88
<i>Figure 5-2 Moss stomatal responses to ABA and increasing [CO₂].</i> -----	89
<i>Figure 5-3 Stomatal aperture measurements of cross-species complementation of ost1 mutant with PpOST1-1 in Arabidopsis response to ABA.</i> -----	91
<i>Figure 5-4 Stomatal aperture measurements of cross-species complementation of double mutant hab1-labi1-2 with PpABI1A in Arabidopsis response to ABA.</i> -----	93
<i>Figure 5-5 Stomatal aperture measurements of Cross-species complementation of ost1 mutant with PpOST1-1 in Arabidopsis response to CO₂.</i> -----	94
<i>Figure 5-6 Stomatal aperture measurements of Cross-species complementation of ABA hypersensitive hab1-labi1-2 mutant with PpABI1A in Arabidopsis response to CO₂.</i> -----	95
<i>Figure 5-7 Stomatal aperture measurements and RT-PCR verification of Physcomitrella wild-type and Ppost1-1 sporophytes</i> -----	96
<i>Figure 6-1 Model to illustrate how the N-end rule pathway and its currently unknown substrates may interact with known components of the core guard cell ABA signalling pathway to regulate stomatal aperture.</i> -----	102

1 Chapter 1- Introduction

A significant global environmental concern for the twenty-first century is water availability. Plant growth accounts for approximately 65% of global fresh water use and therefore it is important to understand how they control water uptake and loss (Morison *et al.*, 2008). Water is lost from plants via transpiration through stomatal pores whose aperture is regulated by pairs of guard cells. Genetic engineering of the guard cell abscisic acid (ABA) signalling network that induces stomatal closure under drought stress is a key target for improving crop water use efficiency (Schroeder *et al.*, 2001). Much scientific research has been directed towards providing novel tools to increase drought tolerance, crop yields and crop quality (Morison *et al.*, 2008). The major aim of the research described in Chapters 3 and 4 of this thesis was to investigate whether the biochemical mechanisms associated with the N-end rule pathway of targeted proteolysis could be involved in the regulation of stomatal apertures. A separate set of experiments, described in Chapter 5, were designed to investigate whether ABA-regulation of stomatal apertures arose before the evolution of vascular land plants.

1.1 Stomatal Biology

1.1.1 Structure and significance of stomata

Stomata are microscopically small pores found on the surface of leaves and stems and other plant aerial tissues, bounded by a pair of specialized cells in the epidermis called guard cells (See reviews by (Hetherington and Woodward, 2003) (**Figure 1-1**). These guard cells are responsible for controlling stomatal apertures. They regulate exchange of oxygen and carbon dioxide between the inside of the leaf and the external environment and also enhance water use efficiency by controlling water loss (Hetherington, 2001; Schroeder *et al.*, 2001). Before discussing the different features of stomatal behaviour, it is important to note that the rate of the transpiration (the loss of water by evaporation from plants, especially through the stomata) may amount to approximately 70% of an identical structure without a cuticle. Several internal (physiological) and external (environmental) signals play key roles in regulating stomatal opening and closing such as atmospheric carbon dioxide concentration, atmospheric humidity, light intensity, drought stress, and the hormone abscisic acid that is produced on drought stress (reviewed by Hetherington and Woodward, 2003). Regulation of stomatal apertures in response to these environmental signals depends

on a complex network of signalling components that affect guard cell turgor (ionic fluxes, organic acids and sugars) including the activity of ion channels in the plasma membrane, cytoskeletal organization and gene expression (Heichel and Anagnostakis, 1978).

A



B

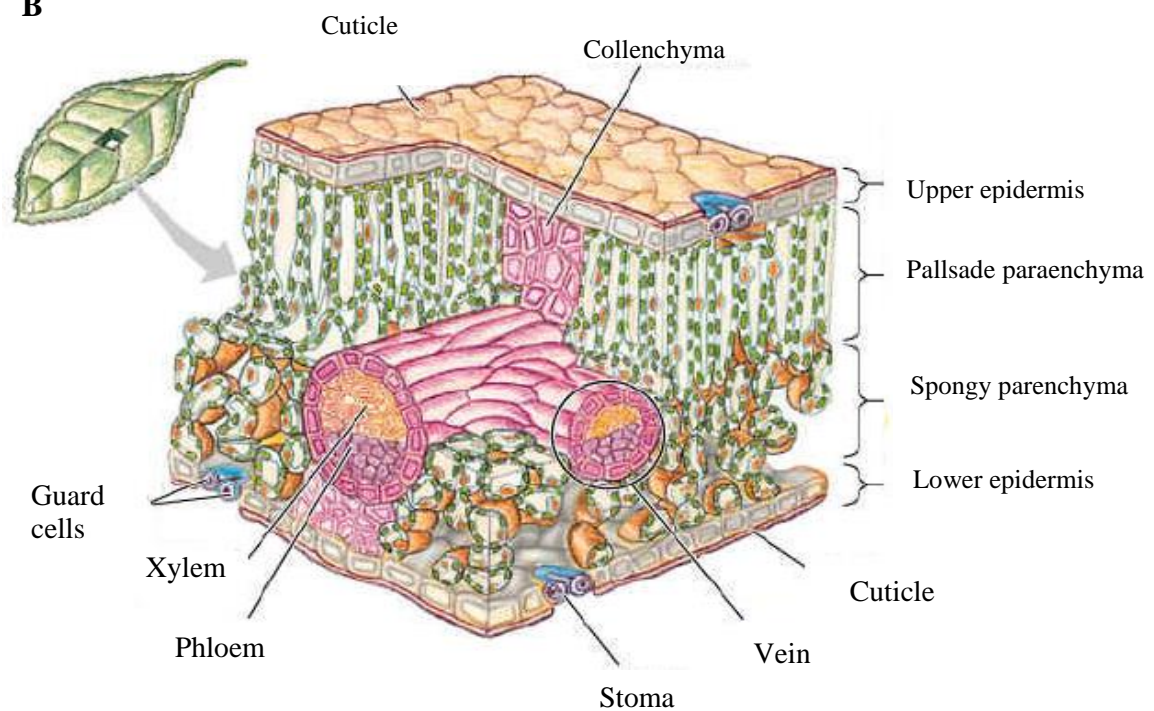


Figure 1-1 the position of guard cell in a leaf

A) Light micrograph of an *Arabidopsis* mature leaf abaxial epidermal peel. Scale bar = 50 μm .

B) Schematic diagram showing the organization of cells inside a leaf. All the parts of the inside of a typical leaf, including, cuticle, upper and lower epidermis, xylem, phloem, guard cells and the palisade mesophyll/spongy mesophyll. Guard cells are positioned in the upper (adaxial) and lower (abaxial) epidermis. **Figure 1-1B** taken from Photosynthesis - leaf and pigments <http://fhs-bio-wiki.pbworks.com>.

1.2 Ion Channels and their Function in the regulation of stomatal aperture

The adjustment of stomatal aperture is brought about by changes in guard cell turgor which is in turn regulated by the plants responses to internal and external stimuli. Increasing stomatal apertures result from hyperpolarization of the guard cell plasma membrane, which is caused by H⁺-ATPase-dependent proton efflux. Inward – rectifying K⁺_{in} channels are activated by membrane hyperpolarization and allow solute influx and water uptake into guard cells. Two mutant alleles of *Arabidopsis* *AHA1/OST2* (*ARABIDOPSIS* H⁺ ATPASE1/*OPEN STOMATA* 2) have been characterised and offer genetic evidence supporting the role of H⁺-ATPases in stomatal regulation. The dominant mutants *ost2-1* and *ost2-2* constitutively activate the guard cell H⁺-ATPase resulting in persistent stomatal opening and therefore stomatal ABA-insensitivity (Yoshida *et al.*, 2006). ABA is responsible for releasing and increasing cytosolic [Ca²⁺] (Kim *et al.*, 2010) which stimulates two different kinds of anion channels, slow (S-type) and rapid-transient (R-type) anion channels (Na and Metzger, 2005). S-type anion channels bring about slow and sustained anion efflux, leading in the long term to membrane depolarization lasting several minutes. Genetic studies have shown that S-type anion channels play a significant role in inducing stomatal closure. The guard cell expressed gene, *SLAC1* (*SLOW ANION CHANNEL-ASSOCIATED 1*) is responsible for encoding the major anion-transporting components of S-type anion channels in guard cells (Vahisalu *et al.*, 2008). *SLAC1* anion channels (and their *SLAH* homologues) play a key role in driving K⁺ efflux from guard cells through outward-rectifying K⁺_{out} channels (Hosy *et al.*, 2003; Na and Metzger, 2005). R-type anion channels are activated rapidly within 50 ms. Recently Meyer *et al.* shown that *AtALMT12*, a member of the aluminium activated malate transporter family in *Arabidopsis*, is a guard cell R-type anion channel. *AtALMT12* is highly expressed in guard cells and is targeted to the plasma membrane (Hedrich, 2012; Meyer *et al.*, 2010; Schroeder and Keller, 1992).

1.3 Stomatal light responses

The stomata of most plants (CAM being an exception) open in response to light and close in response to darkness. Stomatal apertures show two different light responses, in the blue and red wavelength ranges, (Shimazaki *et al.*, 2007). Blue and red light

induce stomatal opening via a complex signalling network, however, blue light is more efficient than red light in stomatal opening (Mott, 2009). Light is absorbed by several classes of photoreceptors of phytochromes (PHYT1 and PHYT2), cryptochromes (CRY1 and CRY2), zeitlupes (ZTL, FKF1 and LKP2) family members and phototropins (PHOT1 and PHOT2). PHOT1 and PHOT2 blue light receptor-type Ser/Thr protein kinases, are responsible for promoting stomatal opening and enhancing photosynthetic CO₂ fixation by eliminating the stomatal restriction to CO₂ entry (Shimazaki *et al.*, 2007) (**Figure 1-2**). These blue light photoreceptors have two Light, Oxygen, Voltage domains (LOV1 and LOV2) which perceive blue light and undergo autophosphorylation, mediating a signalling cascade through 14-3-3 proteins in response to blue light (Inoue *et al.*, 2010; Shimazaki *et al.*, 2007). 14-3-3 proteins bind to the phosphorylated C terminus of the H⁺-ATPase which induces H⁺-ATPase phosphorylation and pumping of H⁺ from the guard cell. This drives K⁺ uptake through voltage-gate K⁺ channels, and thereby stomatal opening (Shimazaki *et al.*, 2007). These blue receptors could be the target of H₂O₂, as phototropins have cysteine residues which are significant for their activity (Salomon *et al.*, 2000). The cryptochrome (CRY1 and CRY2) blue light receptors negatively regulate COP1 (CONSTITUTIVE PHOTOMORPHOGENIC 1), a repressor of photomorphogenesis and stomatal opening which acts downstream of both CRY and PHOT receptors (Mao *et al.*, 2005). The blue light receptors also control chloroplast accumulation, leaf expansion, and leaf movement (Briggs and Christie, 2002). Red light stimulated stomatal opening is based on the accumulation of sugars and a combination of guard cell responses to a decrease in the intercellular CO₂ concentration and photosynthetic activity (Roelfsema and Hedrich, 2005). Because of the same absorption of the spectrum for the red light response and the action spectrum for chlorophyll, it seems likely that chlorophyll is the red light photoreceptor, Studies indicate that the red light response is repressed when 3-(3,4-dichlorophenyl)-1,1-dimethylurea (DCMU), inhibits photosynthetic electron transport (Mott, 2009; Zeiger *et al.*, 2002). However, Wang *et al.* 2010 demonstrated that PHYB is a positive regulator of stomatal opening under red light and also functions together with PHYA, CRY and PHOT to increase stomatal opening in blue light. Furthermore, the ABA signalling network inhibits blue-light- induced phosphorylation of the H⁺-ATPase and the inhibition mediated by H₂O₂ that is produced by ABA in guard cells (Shimazaki *et al.*, 2007). In summary,

the current evidence indicates that red and blue light induced guard cell signalling are separate from each other but are intimately synergistic (Shimazaki *et al.*, 2007) (Figure 1-2).

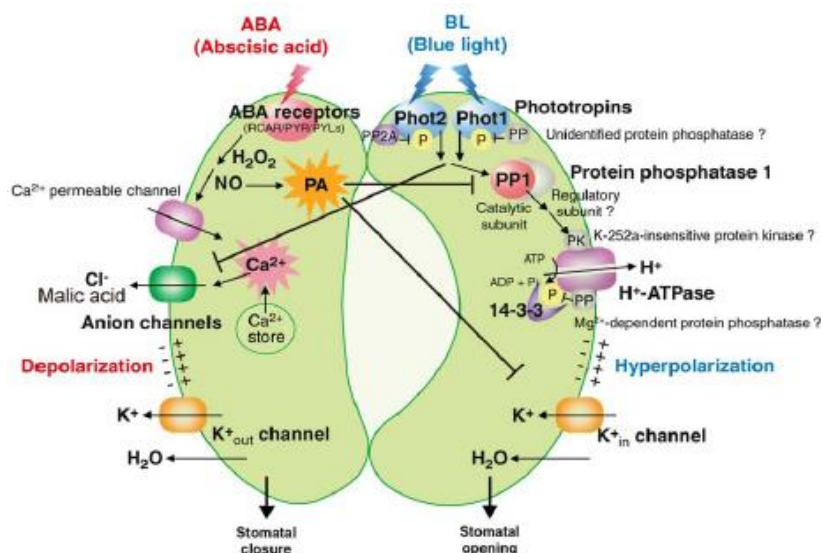


Figure 1-2 Processes of stomatal opening and closing in response to blue light and ABA

Schematic model of blue-light signalling pathway in stomatal guard cells and signalling of ABA-induced stomatal closure (left). Photoreceptors perceive blue light and autophosphorylation mediates a signalling cascade through binding of 14-3-3 proteins to the phosphorylated C terminus of the H⁺-ATPase inducing H⁺-ATPase phosphorylation and pumping H⁺ from the guard cell, driving K⁺ uptake, increasing turgor pressure and stomatal opening. Arrows and T-bars show positive and negative regulation, respectively. The P in the yellow-colored disks indicates a phosphorylated protein. Unknown signalling components are shown in grey. As shown in Figure 1-3 below, ABA stimulates stomatal closure through ABA receptors proteins (PYR/PYL/RCAR) with subsequent production of H₂O₂ and NO, and eventually activates anion channels which induce stomatal closure Figure taken from Inoue *et al.*, 2010.

1.4 ABA Signalling

1.4.1 ABA biosynthesis

To prevent extreme water loss through the stomata, the plant stress hormone ABA induces stomatal closure and inhibits stomatal opening. Thus, modifying the biosynthesis and perception of ABA has been investigated as a means of enhancing drought resistance in crops (Wasilewska *et al.*, 2008). ABA is synthesised by cleavage of carotenoids. Several ABA biosynthesis genes are required in the conversion of carotenoids to ABA. The ABA deficient mutants (known as the *aba* series of mutants) in *Arabidopsis* which are each deficient in one of the essential enzymes show reduced resistance to drought (Xiong and Zhu, 2003). ABA biosynthesis genes are highly expressed in roots for the duration of drought stress, suggesting that root tissues are

the most important source of ABA production (Wasilewska *et al.*, 2008). However, recent evidence proposes that ABA biosynthesis enzymes are also expressed in *Arabidopsis* guard cells which suggests that guard cells contain all the components necessary for ABA biosynthesis (Melhorn *et al.*, 2008). In the short-term enhanced ABA levels in response to drought, induce stomatal closure to avoid water loss. In the medium-term, ABA is also responsible for modifying gene expression levels and stimulating the accumulation of proteins which defend cells against drought damage (Woodward *et al.*, 2002; Zeiger *et al.*, 2002). In the longer-term, ABA affects plant development and a reduced number of stomata are produced on the surface of newly emerging leaves. Indeed, ABA has several physiological roles in non-stress states even when water is plentiful. Plants deficient in ABA show phenotypic abnormalities and reduced growth, even in well-watered conditions (Barrero *et al.*, 2005). Thus ABA is a major regulator of several plant stress and developmental responses.

1.4.2 Network model of ABA-induced stomatal movement

As described above, stomatal opening requires the stimulation of H⁺-ATPases in the plasma membrane of guard cells. H⁺-ATPases play a significant role in membrane hyperpolarization by inducing K⁺ uptake through inward-rectifying K⁺_{in} channels. Accumulation of K⁺, Cl⁻, NO₃⁻, and production of malate from starch metabolism enhances guard cells turgor and volume, and induces stomatal opening. In response to water deficit, the stress hormone abscisic acid plays a major role in inducing stomatal closure (Hetherington and Quatrano, 1991; Israelsson *et al.*, 2006; Schroeder *et al.*, 2001). A network model of ABA response factors and the role of ion channels in regulating stomatal closure have been analyzed to identify an upstream ABA signal transduction system (Kim *et al.*, 2010). In brief, ABA binds receptor proteins in guard cells, probably both in the plasma membrane and in the cytosol (Zhu *et al.*, 2010). The hormone induces several changes: first of all, an increase in cytoplasmic pH and secondly, enhancement of cytosolic Ca²⁺ levels (Kim *et al.*, 2010). Cytoplasmic Ca²⁺ levels increase when the membrane potential is hyperpolarized below ~ -120mV, although, ABA moves the threshold for influx to above -80mV, which suggests that voltage-dependent Ca²⁺ channels and ABA signalling are intimately linked (Grabov and Blatt, 1999). Consequently, the uptake of any additional K⁺ into the cells is inhibited. This causes chloride and other anions to exit the cells. Also sucrose is removed and malate converted to osmotically inactive starch (MacRobbie, 1998). The

loss of these solutes leads to a reduction in guard cell turgor and volume, causing stomatal closure (MacRobbie, 1998; Schroeder *et al.*, 2001; Zhu *et al.*, 2010). Stomata respond to a wide variety of environmental stimuli using a multitude of signalling intermediates. This complexity has been likened to a scale-free network and is believed to provide ‘robustness’ in stomatal responses (Hetherington & Woodward, 2003).

1.4.3 ABA signalling, components and mechanisms

Large-scale gene expression studies from seedlings and guard cell extracts of *Arabidopsis* has led to the recognition of a great number of genes whose expression levels are regulated by ABA (Hoth *et al.*, 2002). However, stomatal responses are very fast and early ABA signalling events must be initiated by rapid alterations in enzymes and ion channel activities (Finkelstein *et al.*, 2002). The application of ABA-induced reporter gene systems has shown that drought stress plays a major role in inducing ABA synthesis in leaves and in roots (Christmann *et al.*, 2005). Further genetic analyses have revealed many components that are involved in ABA signalling including a complex network of both positive and negative regulators of protein kinase and phosphatase enzyme activities (Finkelstein *et al.*, 2002; Fujii *et al.*, 2009) which are described below.

1.4.4 Transcription factors involved in ABA signalling

ABA is recognized having a key role in regulating transcription of target genes. The identification of ABA-responsive elements (ABREs) within target gene promoters helped to identify major downstream targets of ABA signalling responses. AREB1/ABF2 (ABSCISIC ACID RESPONSE ELEMENT BINDING FACTOR 1) is a bZIP family transcription factor which was identified as a DNA binding protein and shown to be phosphorylated by ABA-activated SnRK2 kinases. The AREB proteins play a central role in regulating the transcription of factors that regulate ABA-mediated gene expression under osmotic stress conditions (Fujita *et al.*, 2011). The bZIP domain consists of two motifs: a leucine zipper mediating transcription factor dimerization and a central section implicated in the specific binding of the transcription factor to its target DNA (Fujita *et al.*, 2011). In addition to ABREs, MYBRs (MYB recognition sites) and MYCRs (MYC-recognition sites) are known to be present in the promoters of ABA-regulated genes. Two guard cell-expressed MYB transcription factors, MYB60 and MYB61 (Liang *et al.*, 2005), function in light-

induced stomatal opening (Cominelli *et al.*, 2005). The expression of MYB60 is up-regulated by light and down-regulated by ABA. NUCLEAR FACTOR Y, SUBUNIT A5 (NFYA5) was recently described as a positive regulator of drought-stress responses (Nelson *et al.*, 2007), indicating a potential role for CCAAT box element and its binding partner NF/Y in ABA/abiotic stress signalling (Kim *et al.*, 2010). Transcription factors such as AtERF7 (ETHYLENE RESPONSE FACTOR 7) and NPX1 (NUCLEAR PROTEIN X 1) have been shown to negatively regulate ABA-signalling. Over expression of negative regulators AtERF7 and NPX1 leads to decreased sensitivity to ABA and an enhanced wilting phenotype under drought stress (Song *et al.*, 2005). Thus, there is much evidence that the control of gene expression, in addition to changes in enzyme and ion channel activities, is important in regulating stomatal apertures in response to ABA.

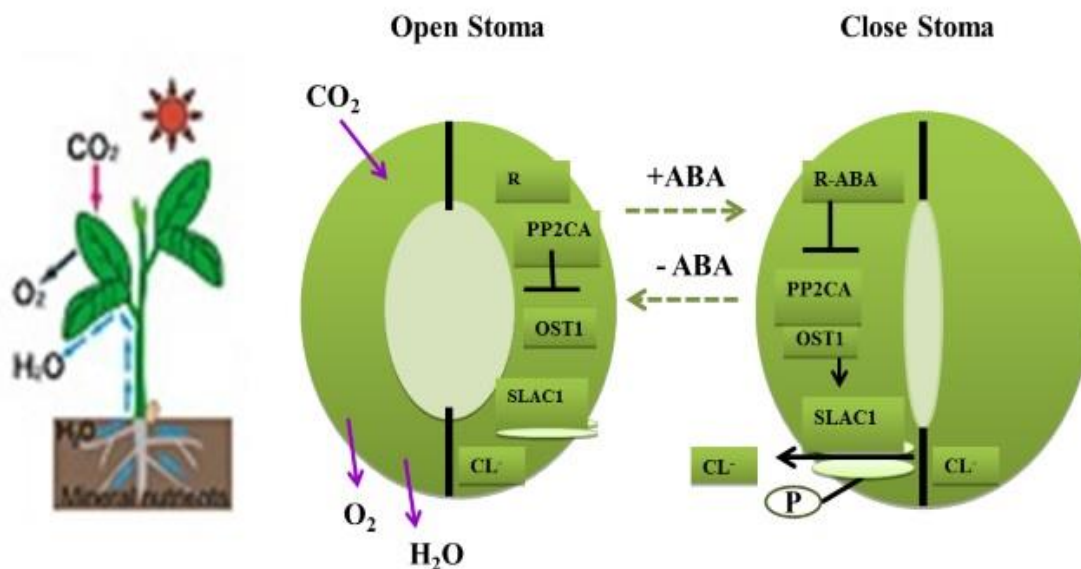
1.4.5 Protein kinases and protein phosphatases are involved in ABA-signalling

The core ABA signalling cascade relies on directly altering the activity of a number of protein components. A subfamily of ABA-activated SNF1-related protein kinases (known as SnRK2.2, SnRK2.3 and SnRK2.6 or OST1 in Arabidopsis) play a central role as positive regulators of ABA signalling (Fujii *et al.*, 2009; Miyazono *et al.*, 2009a). In addition, Mg²⁺ - and Mn²⁺ -dependent serine-threonine protein phosphatases (PP2Cs, known as ABI1, ABI2, HAB1 and PP2CA/AHG3 in Arabidopsis) negatively regulate ABA-responses, including gene expression (Rubio *et al.*, 2009). The role of ABI1 and ABI2 in ABA signalling was revealed from studies of ABA insensitive *Arabidopsis* mutants *abi1-1* and *abi2-1*. Merlot and colleagues proposed that (ABA-INSENSITIVE 1) ABI1 and its closest structural homologue ABI2 genes both encode PP2Cs that act as key negative regulators at an early step of the ABA-signalling cascade (Christmann *et al.*, 2005; Leung *et al.*, 1997; Ma *et al.*, 2009; Merlot *et al.*, 2001; Park *et al.*, 2009). It is now known that, in the absence of ABA, the guard cell expressed PP2Cs inhibit the activity of the guard cell SnRK2s as described below.

1.4.6 Interaction of a protein kinase-phosphatase pair with anion channels in ABA signalling

Numerous studies in anion channel mechanisms have demonstrated interactions between the regulation of ion channels and ABA-linked kinase and phosphatase activities in inducing stomatal closure (Lee *et al.*, 2009). OPEN STOMATA 1 (OST1

or SnRK2-6) encodes a protein kinase involved in guard cell ABA signalling (Mustilli *et al.*, 2002; Yoshida *et al.*, 2006). SLOW ANION CHANNEL 1 (SLAC1) has a key role in closing stomata which is induced by either ABA or high CO₂ (Negi *et al.*, 2008; Vahisalu *et al.*, 2008). Genetic and biochemical analyses have revealed that both the protein kinase OST1 and type 2C protein phosphatases directly interact with SLAC1 anion channel, and each other, and adjust its activity (Lee *et al.*, 2009). Finally, OST1 kinase and SLAC1 channels are responsible for releasing anions and depolarizing the guard cell plasma membrane (Lee *et al.*, 2009). While ABA concentration is low, ABI1 family protein phosphatases interact with OST1 and autophosphorylation activity is inhibited. In the absence of OST1 phosphorylation activity the SLAC1 anion channel has only basal activity. By contrast, at high concentrations ABA binds to the recently characterized PYL family ABA receptors and also interacts with PP2C protein to inhibit its activity (Ma *et al.*, 2009; Park *et al.*, 2009). The PYL ABA receptors interact with the PP2Ca and dissociate them from the OST1-PP2C complex (Ma *et al.*, 2009; Park *et al.*, 2009) (**Figure 1-3**). OST1 kinase can then autophosphorylate to activate itself, and activate the SLAC1 anion channel by phosphorylation, initiating stomatal closure. This pathway for ABA perception is now well accepted and recently has even been reconstituted *in vivo* (Brandt *et al.*,



2012). Figure 1-3 Stomata regulate gas exchange between leaves and the atmosphere.

A model for the activity of ABA-linked kinases and phosphatases to ion channel regulation (Lee *et al.*, 2009). R-ABA receptors, PP2CA, serine-threonine protein phosphatases, OST1, OPEN STOMATA 1 SLAC1, SLOW ANION CHANNEL 1, P stands for phosphorylation.

1.4.7 Mechanism of ABA perception by PYL receptors

ABA-interacting proteins recently proposed to be ABA receptors are known by a variety of names including REGULATORY COMPONENT of ABA RECEPTOR (RCAR) (Saez *et al.*, 2006), or PYROBACTIN RESISTANCE (PYR), or PYROBACTIN LIKE proteins (PYL). Together these constitute a subfamily of novel START domain proteins that are also known as RCARs or PYR/PYLs (Fujii *et al.*, 2007; Fujii *et al.*, 2009). The PYR/PYL/RCAR family of proteins play a crucial role in interacting with and inhibiting PP2Cs by the ligand-bound receptor (Sheard and Zheng, 2009). Therefore, they act as regulators of the ABA-signalling kinases and phosphatases and the downstream ABA-responsive transcriptional regulators, by influencing phosphorylation and dephosphorylation of substrate proteins (Sheard and Zheng, 2009). In the absence of the phytohormone ABA, PP2C is free to repress autophosphorylation and activation of the SnRK2 kinases (including OST1). In the presence of ABA, PYR/PYL/RCARs bind to PP2Cs. Subsequently, SnRK2s become auto-activated and can then phosphorylate and activate downstream substrates such as downstream transcription factors to start transcription at ABA-responsive promoter elements (ABREs), or other ABA-related phosphorylation targets such as the SLAC1 anion channel (Miyazono *et al.*, 2009; Sheard and Zheng, 2009) (**Figure 1-4**).

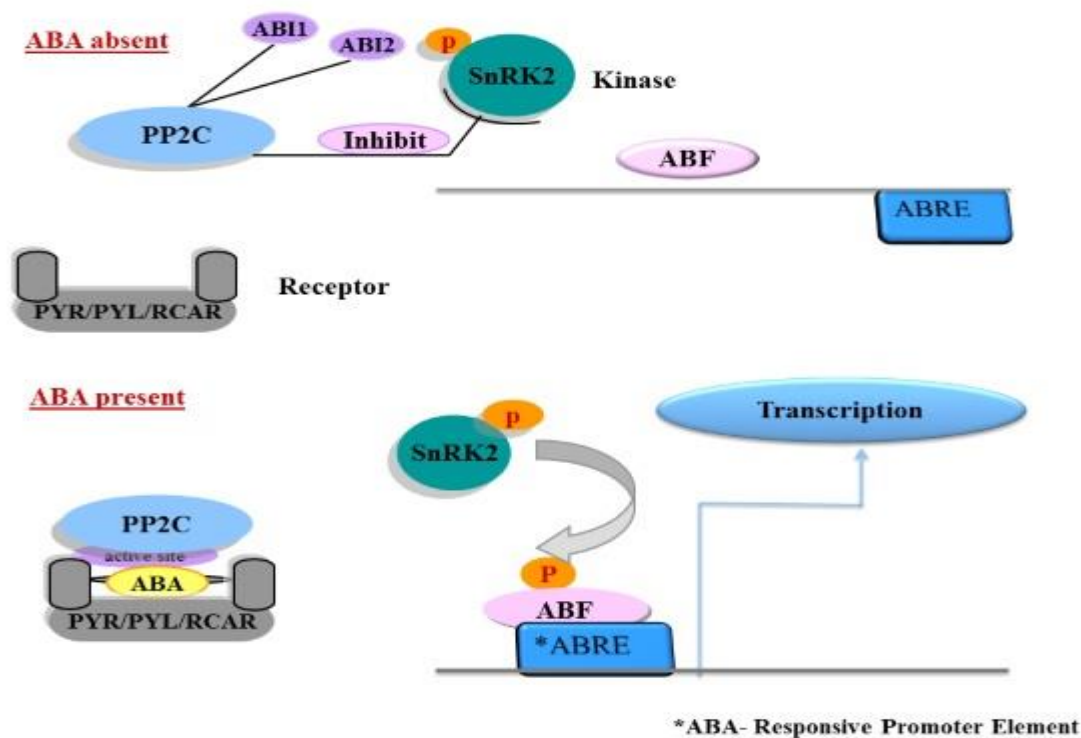


Figure 1-4 Model to illustrate the molecular components of the ABA-activated signalling pathway that regulates gene expression.

In the absence of ABA, PP2Cs are free to repress SnRK2 kinases. In the presence of ABA, PYR/PYL/RCARs bind to and inhibit PP2Cs. SnRK2 becomes auto-activated and activates downstream substrates including transcription factors (ABF) to start transcription at ABA-responsive promoter elements (ABREs) or other ABA-related responses (Miyazono *et al.*, 2009; Sheard and Zheng, 2009).

1.4.8 Evolution of ABA signalling pathways

There is strong evidence that the same key signalling components involved in ABA responses to a range of osmotic stresses which are present in *Arabidopsis* and higher plants are also involved in ABA responses in mosses (Cuming *et al.*, 2007; Rensing *et al.*, 2008). In addition, there is confirmation that the same core module of ABA functions in liverwort gametophytes (Tougan *et al.*, 2010). Transcriptomic analyses of the moss *Physcomitrella patens* stress responses strongly suggest similarities between bryophyte and higher plant responses (Cuming *et al.*, 2007; Hauser *et al.*, 2007). The interaction between ABA, the transcription factor families involved in ABA signalling, a negative regulatory role for PP2Cs and interaction with the SnRK2s, which are well characterized in ABA signalling in higher plants, are all encoded in the *Physcomitrella* genome (Hauser *et al.*, 2011; Rensing *et al.*, 2008). The dominant *abi1-1 Arabidopsis* has been shown to disrupt ABA signalling and decrease abiotic stress tolerance in *Physcomitrella* (Komatsu *et al.*, 2009), and this is

reversible by co-expression of the transcription factor ABI3 (Marella *et al.*, 2006) which is a transcriptional enhancer of ABA responsive promoters in *Arabidopsis* and in *Physcomitrella* (PpABI3A). Further experiments in *Physcomitrella* showed that the transient expression of PpABI1A obstructs expression of LEA genes and causes ABA hypersensitivity (Komatsu *et al.*, 2009). PpABI1A is also known to be involved in gametophyte development (Sakata *et al.*, 2009). Together, these results suggest that ABI1 is a negative regulator of ABA signalling involved in both abiotic stress responses and developmental regulation in *Physcomitrella*. ABA responses were well characterised in the leafy structures (gametophyte generation) of mosses at the start of this project but little was known about the ABA responses of moss stomata, which are found on the spore capsule (sporophyte). Even less was known of moss stomatal CO₂ responses. The signalling intermediates involved in moss stomatal aperture responses are explored in Chapter 5 of this thesis.

1.5 Guard cell CO₂ responses

High concentrations of atmospheric CO₂ lead to high intercellular CO₂ concentrations which reduce stomatal conductance through rapid physiological responses. In the short term, changes in CO₂ concentration induce alterations in stomatal aperture as described below. Additionally, long-term exposure of many plant species to high levels of CO₂ reduces stomatal density in newly developing leaves, further decreasing stomatal conductance (Kim *et al.*, 2010; Raschke *et al.*, 2003; Woodward *et al.*, 2002). During stomatal closure an elevated intercellular concentration of CO₂ activates anion channels and K⁺_{out} efflux channels in guard cells, and this is responsible for releasing Cl⁻ from guard cells and membrane depolarization (Raschke *et al.*, 2003) in a similar manner to that described above for ABA. Moreover, CO₂ requires Ca²⁺ for inducing stomatal closure and a change in cytosolic pH can be detected when CO₂ levels are elevated in *V.faba*. Analysis of stomatal apertures in epidermal fragments, removed from the mesophyll, indicates that high CO₂ can induce stomatal closure, showing a direct functional role for guard cells in mediating in the response to CO₂ (Mott *et al.*, 2008; Weyers and Hillman, 1980) but these experiments also suggested that the effect of CO₂ on stomatal closure could be enhanced by contact with the mesophyll. Identification of particular CO₂ signalling components and mechanisms by genetic manipulation is essential for additional insights into the cell type specificity of CO₂ signalling mechanisms (Kim *et al.*, 2010).

1.5.1 Mechanisms of CO₂ signalling in guard cells

Brearley *et al.*, 1997; Hedrich and Marten, 1993 suggested that malate is released from mesophyll cells in response to high concentrations of CO₂ (Vankirk and Raschke, 1978) and activates anion channels S-type and R-type anion channel activity of guard cells, resulting in anion loss and subsequently stomatal closure thus suggesting a mechanism for CO₂-induced stomatal closure. CO₂-induced stomatal closure has been shown to involve several signalling components in common with ABA-induced closure including the phosphatase ABI1 (Webb and Hetherington, 1997) and the kinase OST1 (Xue *et al.*, 2011). The HT1 (HIGH LEAF TEMPERATURE 1) kinase was the first regulatory component to be identified specifically in the high CO₂-induced stomatal closure pathway (Kim *et al.*, 2010). Although, HT1 protein kinase activity is highly decreased in *ht1-1 ht1-2* mutants, they retain responsiveness to blue light and ABA, showing that HT1 may function upstream of the convergence of the CO₂ and ABA promoted stomatal closure pathways (Kim *et al.*, 2010). CO₂ binding/interacting proteins that are involved in CO₂ regulated stomatal movements have not been identified and genetic redundancy may have prevented their recognition (Kim *et al.*, 2010). Recent research demonstrated that *Arabidopsis* mutant plants disrupted in two carbonic anhydrases β CA1 (BETA CARBONIC ANHYDRASE 1) and β CA4 (BETA CARBONIC ANHYDRASE 4)- are effectively impaired in stomatal CO₂ responses (Hu *et al.*, 2011). Carbonic anhydrases catalyze the conversion of carbon dioxide (and water) to bicarbonate (and protons). Specific expression of carbonic anhydrase in guard cells indicates that these two carbonic anhydrases can mediate the CO₂ response directly in guard cells (**Figure 1-5**). Thus it appears that guard cells respond to solubilized bicarbonate rather than directly to dissolve CO₂.

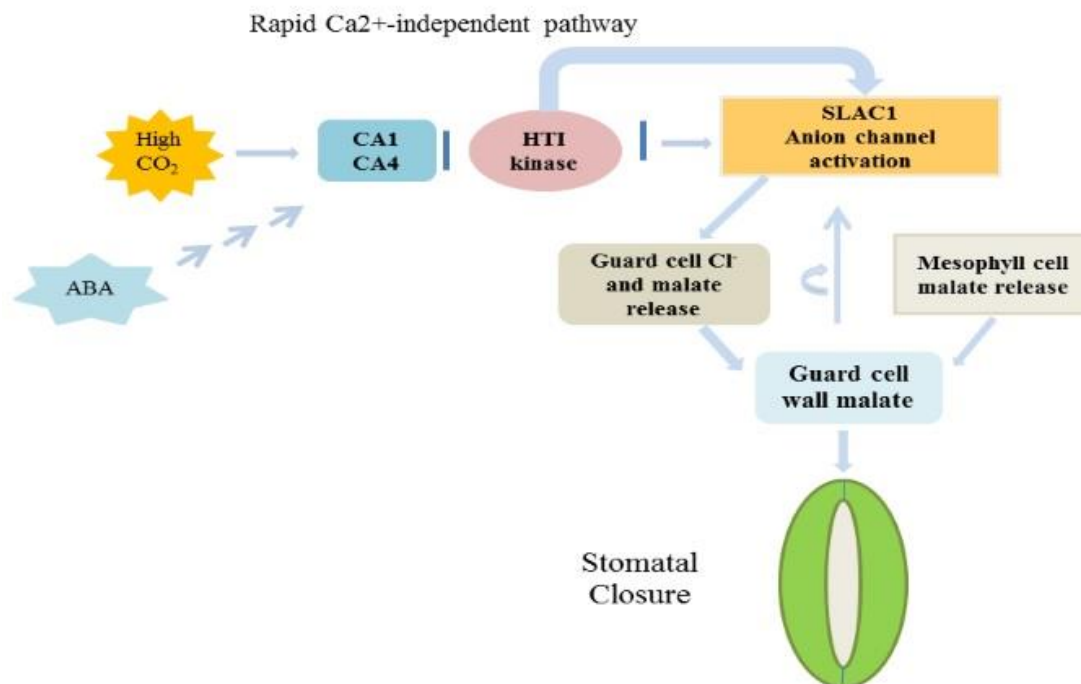


Figure 1-5 CO₂ signalling in regulation of stomatal movements

A proposed simplified model demonstrating the functions of recently recognized guard cell components that mediate CO₂ regulation of stomatal movements. The HT1 protein kinase and ABCB14 proteins function as negative mediators (red) whilst CA1, CA4, GCA2, and SLAC1 function as positive regulators (blue) of elevated CO₂ mediated stomatal closing. Convergence with abscisic acid signalling is also indicated. Abbreviations: CA, CARBONIC ANHYDRASE; HT1, HIGH LEAF TEMPERATURE 1; SLAC1, SLOW ANION CHANNEL ASSOCIATED 1 Figure taken from (Kim *et al.*, 2010).

1.6 Establishing a role for nitric oxide (NO) in signalling stomatal closure

The intracellular signalling networks that mediate the effects of ABA on stomatal closure are complex, with numerous new signalling intermediates having been recognized recently (Desikan *et al.*, 2002; Hancock *et al.*, 2011). One such component is the gaseous signal nitric oxide (NO), a significant signalling molecule in plants. Treatment of plants with sodium nitroprusside (SNP), a NO donor, has been shown to increase drought tolerance by reducing stomatal apertures (Desikan *et al.*, 2002). As ABA induces NO production in guard cells it has been proposed that NO acts downstream of ABA in the ABA-induced stomatal closure pathway. This is supported by experiments showing that the NO scavenger PTIO inhibits ABA-induced stomatal closure (reviewed by (Hancock *et al.*, 2011)). However, the role of nitric oxide in promoting stomatal closure is not clear cut. It was recently demonstrated that plants lacking NO synthesis enzymes (*nia1nia2noal* triple mutants) are ABA hypersensitive, resistant to water deficit and show increased drought tolerance

(Lozano-Juste and Leon, 2010). Intriguingly, these plants that are unable to generate NO were found to have enhanced ABA-induced stomatal closure. Electrophysiological experiments suggest that nitric oxide mediates ABA-induced changes in stomatal aperture by altering the activity of potassium ion channels. At low levels (<10nM), NO inactivates K_{in} preventing guard cell K^+ uptake, and stimulating calcium-mediated stomatal closure. However, at slightly higher levels (>20nM), NO has essentially the opposite effect; inactivating K_{out} activity by a mechanism that is believed to involve oxidation, and perhaps nitrosylation, of cysteine residues in unidentified intracellular protein target(s) (Sokolovski and Blatt, 2004). In plants, NO is believed to be generated by NO synthase (NOS) and nitrate reductase (Desikan *et al.*, 2002; Hancock *et al.*, 2011). Biochemical and pharmacological research has demonstrated NOS activity in several plant tissues. However, NOS inhibitors have variable effects in *Arabidopsis* and no NOS-like sequences have been discovered in the *Arabidopsis* genome (Delledonne *et al.*, 1998; Hancock *et al.*, 2011). Two enzymatic pathways have been linked to NO synthesis in plants NOA1 (Nitric Oxide Associated 1) which was originally believed to be a plant nitric oxide synthase but is now believed to be involved in the synthesis of nitrite in mitochondria. Nitrate reductase (NR) is a central enzyme of nitrogen assimilation in plants and there is genetic evidence that NR-mediated NO synthesis is essential for ABA-stimulated stomatal closure in *Arabidopsis* (Desikan *et al.*, 2002). This molecule has a key role, as either a stressor or regulator in response to various abiotic and biotic stresses (Hu *et al.*, 2005). Pharmacological studies show that NO signalling in plant cells involves a transient increase in the concentration of the second messenger molecule cyclic GMP (cGMP). Inhibition of cGMP synthesis inhibits NO reactions (Neill *et al.*, 2003). Neill *et al.* 2003. also revealed that in pea guard cells, inhibition of cGMP synthesis with the guanylyl cyclase inhibitor ODQ inhibited stomatal closure stimulated by either ABA or NO. Evidence for cGMP as a mediator of NO signalling has been found in several systems (Delledonne, 2005; Neill *et al.*, 2003). Both salt and osmotic conditions which are expected to induce ABA synthesis, stimulated a fast increase in the cGMP content of *Arabidopsis* seedlings (Donaldson *et al.*, 2004). This suggests that ABA stimulates the enzyme responsible for cGMP synthesis. It is possible that the biological effects of NO are mediated at least in part by the N-end rule pathway as explored in Chapter 3 of this thesis. NO is believed to be responsible for *oxidising* amino acid residues particularly cysteine residues (Graciet and Wellmer, 2010).

Although NO is well established as an important regulator in stomatal movement, further work is required to understand if and how it effects with other signalling components such as the N-end rule pathway which is involved in inducing stomatal closure in response to ABA.

1.7 Functions of the N-end rule pathways in plants

The N-end rule pathway has an essential role in regulating the protein-degradation system in eukaryotes. In all organisms, substrates for the N-end rule pathway which contain an N-degron are targeted for ubiquitination and proteasomal degradation (Choi *et al.*, 2010). N-degrons are amino-terminal destabilizing residues of proteins which are recognized by N-recognin E3 ligases which target them for proteolysis via the 26S proteasome (Holman *et al.*, 2009). This pathway has a hierarchical system in plants which is similar to the mammalian systems (Graciet and Wellmer, 2010) (**Figure 1-6**). Asparagine (Asn) and glutamine (Gln) residues are N-terminal tertiary destabilizing residues since they are enzymatically deamidated by two distinct N-terminal amidases, NTAN1 and NTAQ1, to yield aspartic acid (Asp) and glutamic acid (Glu) which are secondary destabilizing N-terminal residues (Graciet *et al.*, 2010; Sriram *et al.*, 2011). The activity of the secondary destabilizing N-terminal residues are mediated by two distinct Arg-tRNA-protein transferases (ATE1 and ATE2) which transfer arginine (Arg) to one of the primary destabilizing residues (Graciet and Wellmer, 2010; Sriram *et al.*, 2011) (**Figure 1-6**). A substrate of the proteolytic system is ubiquitylated through the action of three different enzymes, ubiquity-activating enzyme (E1), ubiquitin-conjugating enzyme (E2) and ubiquitin ligase (E3) before degradation by the 26S proteasome (Tasaki and Kwon, 2007). E3 ligases specifically identify a degradation signal (degron) of the target protein. An efficient N-degron can be generated by N-terminal modifications (deamidation, oxidation, and/or arginylation) of a pre-N-degron (Lee and Kim, 2011). Primary destabilizing residues are identified by E3 ligases of the N-end rule pathway, termed recognins. In *Arabidopsis*, two N-recognins, PROTEOLYSIS 1 (PRT1) and PRT6, have been described (Garzon *et al.*, 2007; Tasaki *et al.*, 2009). PRT1 contains two RING domains and one ZZ domain; it was discovered in a genetic screen and analysis of its sequence indicates that it has no strong sequence homology with other known N-recognins (Sriram *et al.*, 2011). In contrast, PRT6 was found to have sequence homologous to UBR1 (the yeast and human N-recognin) including the characteristic

UBR domain and RING finger motif (Garzon *et al.*, 2007). PRT6 identifies only basic amino acids, whilst PRT1, which has no UBR box, recognizes aromatic amino acids in *Arabidopsis* (Garzon *et al.*, 2007). The presence of the N-end rule pathway enzymatic components as well as whole sets of stabilizing and destabilizing residues in plants, illustrates that the organization of N-end rule pathway is most probably similar to that of animals and yeast (Graciet and Wellmer, 2010).

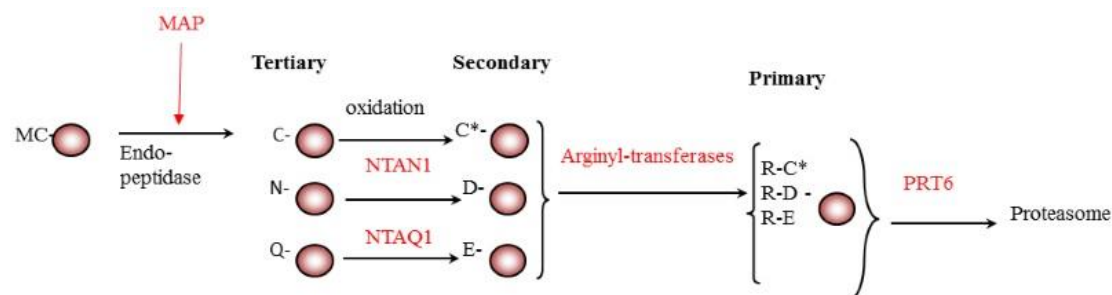


Figure 1-6 the hierarchical structure of the N-end rule pathway of protein degradation.

Schematic representation of the N-end rule pathway in plants. Ovals denote a protein substrate. N-terminal residues are indicated by single-letter abbreviations. N-terminal methionine residues (M) may be removed by an endo-peptidase (e.g. MAP1A) to reveal tertiary destabilising residues. The tertiary destabilizing N-terminal residues asparagine and glutamine (N and Q) are deamidated through two distinct enzymes NTAN1 and NTAQ1 into aspartic acid and glutamic acid (D and E) respectively. C denotes N-terminal cysteine residues. Cysteine residues may be oxidised by oxygen and/or nitric oxide (shown as C*). Arginyl-tRNA:protein arginyltransferase (e.g. ATE1) is responsible for converting N-terminal aspartate and glutamate secondary destabilizing residues to the primary destabilizing N-terminal residues through arginylation. Figure taken from Hu *et al.*, 2005.

1.7.1 N-end rule pathway and its substrates in plants

Even though the N-end rule pathway is known to regulate numerous cellular and developmental processes, our understanding of its substrates and their potential functions is not yet clear in plants (Gibbs *et al.*, 2011). Transcriptional regulators belonging to the ERF (transcription factor family) play a key role in numerous processes, including development and responses to biotic and abiotic stresses (Licausi *et al.*, 2010). Recent data demonstrates that several members of sub group VII ERFs in *Arabidopsis*, At1g53910 (RAP2.12), At3g14230 (RAP2.2), At1g72360 (HRE1), At2g47520 (HRE2) and At3g16770 (RAP2.3 also known as AtEREBP) are substrates of the N-end rule pathway during hypoxic stress (Gibbs *et al.*, 2011; Licausi *et al.*, 2011). ERF proteins are characterised by a conserved DNA-binding domain the highly conserved N-terminal motif MCGGAV/IISD and by tryptophan and leucine/isoleucine residues at the C-terminus (Licausi *et al.*, 2010). Typically, most proteins are synthesized with an N-terminal Met stabilizing residue, and degradation is precluded

by the N-end rule pathway (Bradshaw *et al.*, 1998). Methionine aminopeptidase (MetAP) is responsible for removing the N-terminal Met from proteins, if the second residue has a relatively small side chain (Graciet and Wellmer, 2010). MetAP exposes the tertiary destabilizing residue cysteine in proteins beginning with Met-Cys, which targets substrates for degradation by the N-end rule pathway. Amino peptidases have a diversity of localizations in plant cells. Green fluorescent protein (GFP) fusions of MetAPs, suggest that MAP1A, MAP2A and MAP2B are cytosolic and also redundant in function. MAP1B is localized in plastids, whilst MAP1C and MAP1D are present in both the plastid and mitochondrion (Giglione *et al.*, 2004).

1.7.2 26S proteasome-dependent protein degradation in ABA responses

Proteolysis by the 26S proteasome is a common regulatory mechanism for degrading specific target proteins. Several enzymes are involved in tagging specific proteins with small ubiquitin modifiers to tag them for degradation (Kim *et al.*, 2010). E3 ligases are responsible for selecting specific target proteins by direct protein-protein interactions (Vierstra, 2009). RING or U-box type E3 ligases have been recognized as regulatory components, during abiotic and ABA stress signalling. However as has been demonstrated in other phytohormone response pathways (eg auxin, gibberellic acid, and jasmonic acid) targeted degradation of repressors is implicated in ABA responses. AIP2 (ABI3 INTERACTING PROTEIN 2) is a RING finger motif containing E3 ligase and modulates protein stability of ABI3 (ABA –INSENSITIVE 3) transcription factor (Zhang *et al.*, 2005). In a similar way, a RING E3 ligase has been shown to ubiquitylate ABI5 (ABA-INSENSITIVE 5) (Stone *et al.*, 2006). A direct interaction of the RING E3 with ABI5, has been established (Stone *et al.*, 2006). In addition to, degradation of positive transcription factors such as ABI3 and ABI5, the degradation of ABA signalling regulators in the modulation of ABA signalling has been implicated (Kim *et al.*, 2010). Genetic mutants of the *SDIRI* (*SALT-AND DROUGHT-INDUCED RING FINGER 1*) have decreased ABA responses in stomatal closure as well as in seed germination, suggesting that *SDIRI* is a specific negative regulator of ABA signalling (Zhang *et al.*, 2007). These several lines of evidence show the significance of controlled protein degradation in regulating ABA responses. Further research is required to identify how these mechanisms may regulate ABA control of stomatal movements (**Figure 1-7**).

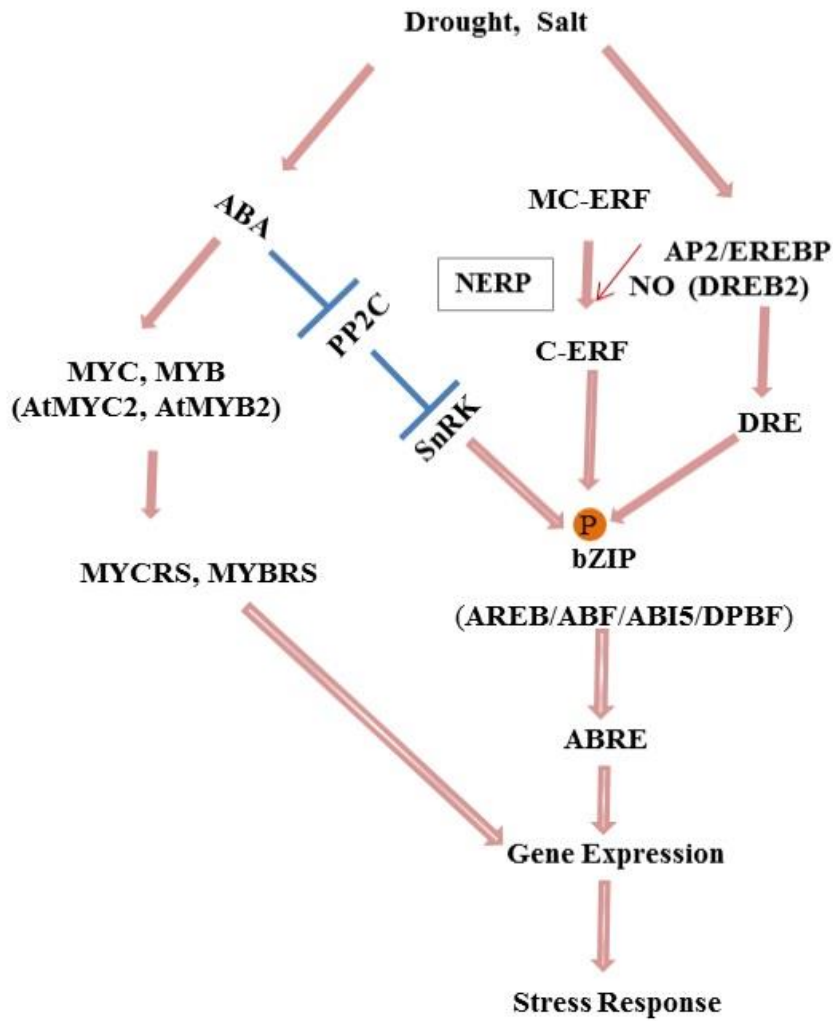


Figure 1-7 Regulation of abiotic stress signalling pathways by ABA and the possible role of the N-end rule pathway.

A simplified model to illustrate the biochemical and transcriptional regulatory steps in ABA signalling that are mediated via AREB/ABF/ABI5/ DPBF bZIP transcription factor families (data taken from Lee and Kim, 2011). The ‘NERP box’ indicates the possible role of the N-end-rule pathway and nitric oxide (NO) in controlling the stability of a subgroup of ERF transcription factors that initiate MC (MC-ERF) and are therefore potential targets for degradation

1.8 Aim and objectives of the investigation

This study aimed to investigate two aspects of stomatal ABA-responses at the molecular level. Firstly, the experiments described in Chapters 3 and 4 were designed to investigate whether the N-end rule pathway of protein degradation could be involved in regulating stomatal ABA signalling, and to analyse the components of this pathway. Secondly, the experiments presented in Chapter 5 were aimed at investigating the evolution of stomatal ABA-signalling mechanisms, and whether the components of stomatal ABA-signalling pathways could have been conserved throughout land plant evolution.

2 Chapter 2- Materials and Methods

2.1 Materials

2.1.1 Chemicals, enzymes, vectors etc.

General laboratory chemicals and reagents were purchased from Sigma, Bio Rad and BDH. Unless otherwise stated restriction enzymes were purchased from Roche (www.roche.com) or Promega (www.promega.com). Modification enzymes; Biotaq *Taq* and Hot start KOD polymerase were purchased from Bionline (www.bionline.com) or Invitrogen (www.invitrogen.com). MM-LV reverse transcriptase was purchased from Invitrogen or Bionline. Total plant RNA was extracted using the spectrum Plant Total RNA kit from Sigma (catalogue number STRN50). DNA size standards were purchased from Bionline. Custom oligonucleotides were designed using Primer3 (<http://www-genome.wi.mit.edu/cgi-bin/primer/primer3>) or TDNA primer software (<http://signal.salk.edu/tdnaprimers.2.htm>) which were synthesized by Sigma Genosys (www.sigmaaldrich.com).

2.2 Growth conditions

2.2.1 Plant material

Several ecotypes and mutants of *Arabidopsis thaliana* were used during this study. The *Landsberg erecta* (L.er), *Columbia-0* (Col0) and *Columbia-2* (Col2) were obtained from NASC (Nottingham *Arabidopsis* Stock Centre). All seeds were germinated on M3 commercial compost for soil based growth. Plants were propagated in the growth room under conditions of 10 hours photoperiod with light intensity of ($140\mu\text{mol m}^{-2}$), 20/16°C day/night temperature, Relative humidity 60% and ambient (approximately 400ppm) CO₂ for approximately six weeks until the rosettes were completely expanded but flowering had not commenced. Mutants and their controls were grown at the same time and in the same conditions. For plate based growth, seeds of *Arabidopsis thaliana* were surface sterilised before being plated on Murashige & Skoog (0.5X MS) media (4.12g l^{-1} MS salts, 1% sucrose, pH5.8) and 1% agar, autoclaved at 20lb/in at 120°C for 20 minutes, set in a sterile petri dish. Surface sterilisation of seed was carried out by soaking seed in 1ml 50% ethanol. The ethanol was then decanted and 1 ml 10 % bleach containing 0.05 % Tween 20 for 10 minutes. The bleach was poured off and seeds were washed three times with sterile deionised water and then 1 ml of sterilized 0.15% agar was added before pouring onto the top of agar plates. The plates were then sealed with porous micropore tape and stratified at

4°C for 72 hours. Following stratification the plates were moved to controlled environment growth conditions and allowed to germinate.

2.3 Nucleic acid techniques

2.3.1 Plant Genomic DNA isolation

Leaf tissue from *Arabidopsis* plants was used for DNA extraction. 6g of leaf tissue was macerated for 15 second without buffer. 700µl extraction buffer (200mM Tris-HCL, pH 8.0, 250 mM NaCl, 25 mM EDTA, pH 8.0 and 0.5% SDS) was added to the plant tissue. This was vortexed briefly and centrifuged for 1min at 18,000 rpm then 600 µl of the supernatant was transferred to a fresh Eppendorf tube. 600 µl of isopropanol was added and the sample immediately centrifuged at 18,000 rpm for 5 min. The supernatant was removed carefully without disturbing the pellet in the bottom of the tube. The DNA pellet was dried to eliminate any remaining liquid and resuspended in 100 µl sterile deionized water and stored at -20°C.

2.3.2 Total plant RNA extraction

Total RNA was extracted from all plant tissues using an RNA extraction kit from sigma. Approximately, 100mg of leaf tissue was harvested into liquid nitrogen and ground in a powder in microcentrifuge tubes. 500 µl extraction buffer (kit reagent mixed with 5µl 2-mercaptoethanol) was added and the sample transferred to a 2ml Eppendorf tube then centrifuged at 18,000 pm for 1 min. The lysate supernatant was transferred into a filtration column seated in a 2ml collection tube. This was centrifuged at full speed for 1 min and then 750 µl binding solution was added thoroughly to the clarified lysate by pipetting up and down. 700 µl of this mixture was pipetted into a binding column seated in a 2ml collection tube, centrifuged for 1min at 18,000 pm. The flow-through liquid was discarded and then the binding column was washed with 500 µl wash solution 1 (kit reagent) and centrifuged for 1 minute at full speed. After this the column was loaded with 500 µl wash solution 2 and microcentrifuged for 30 seconds. The last wash was then repeated. The empty column and microtube was centrifuged for 1 minute to dry and then it was placed into a clean microcentrifuge tube. 30 µl of Elution Solution (kit reagent) was transferred to the centre of the column, let to stand for 1 minute and after that eluted for 1 minute in the microcentrifuge. 5 µl of DNase buffer and 1 µl of DNase were added and then incubated at 37°C for 20 min. DNase inactivation solution was transferred and

centrifuged for 1 min at high speed. The supernatant (m RNA) was moved to a clean Eppendorf tube and maintained at -20°C for short term or -70°C for long term storage.

2.3.3 RNA and DNA quantification

5 µl of each RNA sample was examined by agarose gel electrophoresis for ribosomal RNA integrity. 2 µl of each sample was added to nuclease-free water and the optical density was measured at 260nm in an Eppendorf Biophometer. RNA has an optimal absorption at 260 nm and A_{260} of 1 is equal to an RNA concentration of 40 µg/ml. As a result, the reading at 260 nm gave an estimation of concentration of the sample as follows:

$$\text{RNA concentration (}\mu\text{g/ml)} = A_{260} \times \text{dilution factor} \times 40$$

A similar procedure assayed genomic and plasmid DNA quality and quantification except double stranded DNA has an A_{260} of 1 = 50µg/ml.

2.3.4 Reverse transcription/ first strand cDNA synthesis using superscript II RT

RT-PCR was used for the confirmation of knockout plant genotypes by demonstrating the absence of an amplifiable transcript. The total RNA extracted was used as a template to synthesise the first strand of complementary DNA (cDNA) by adding the following components as described below.

Oligo (dT) ₁₂₋₁₈ (0.5 µg/µl)	1µl
Total RNA	1 to 5µg
dNTP mix (10mM each)	1µl
Elution buffer to a final volume	12µl

The above reagents were heated at 65°C for 5min to breakdown secondary structure and then chilled quickly on ice.

Afterwards, the contents were briefly centrifuged, then the reagents below were added:

5X first-strand buffer	4µl
0.1 M DTT	2µl
Elution buffer	1µl

The contents of the tube was mixed gently and incubated at 42°C for 2 minutes. 1µl of SuperScript™ II was added after the two minutes and then mixed by gently pipetting

up and down. The mixture was incubated at 42°C for 50 mins then the reaction inactivated by heating the contents at 70°C for 15 min. Once inactivated the newly synthesised cDNA was stored at -20°C.

2.4 Polymerase Chain Reaction (PCR)

The polymerase chain reaction was mainly used to amplify specific DNA and cDNA fragments using *Taq* DNA polymerase (Biotaq, Bioline). The PCR was used for a variety of techniques for instance; two PCR reactions were used for isolating homozygous knockout plants. The first reaction included specific forward and reverse oligonucleotide primers to detect the wild type allele, and the second one included a Left Border (LB) primer complementary to the T-DNA insertion and reverse gene-specific primer to detect the mutant allele.

2.4.1 *Taq* DNA polymerase PCR.

This enzyme was used for most PCR applications. Typical reaction conditions were as follows, these components were added to a nuclease-free micro centrifuge tube:

Template DNA (50-1000ng)	3µl
primer 1 (25pmol)	1.5 µ
primer 2 (25pmol)	1.5 µ
dNTP mix (2mM each)	1 µl
PCR buffer	5 µl
MgCL ₂ (25mM)	2.5 µl
Tag DNA polymerase enzyme	0.2 µl
Sterile H ₂ O	up to 50 µl

dNTP mix contained equimolar amounts of dATP,dCTP,dGTP and dTTP, (10mM of each).

A standard thermal cycling programme was used:

In some cases following analysis of the reaction products by electrophoresis the annealing temperature was modified, to either make the reaction more specific by increasing the temperature or by decreasing the temperature to make the reaction less specific.

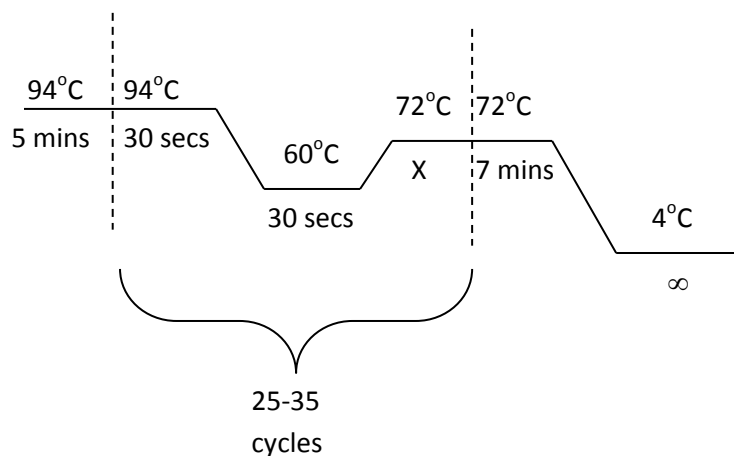
2.4.2 PCR using a polymerase with proofreading activity

To obtain DNA amplicons with high homology to the DNA template for cloning applications, a high fidelity proofreading KOD hot start DNA polymerase (serial

number 71086-5, Novagen.com) was used for producing gene constructs. The standard reaction set up was as follows

Template DNA (50-1000ng)	3µl
primer 1 (10pmol)	1.5 µ
primer 2 (10pmol)	1.5 µ
dNTP mix (2mM each)	2.5 µl
KOD buffer	2.5 µl
MgSO ₄ (25mM)	1 µl
KOD enzyme	0.5 µl
Sterile H ₂ O	up to 50 µl
Step	Target size 1000-3000 bp
Polymerase activation	95 °C for 2min
Denature	95 °C for 20s
Annealing	55 °C for 10s
Extension	70 °C for 25s

The standard thermal cycling conditions used were



Where X, the extension time, is 1 minute/kb size of the expected fragment.

25-35 thermal cycles were usually used for amplifying cDNA and specific genomic DNA fragments respectively.

2.5 Agarose gel electrophoresis

DNA samples were separated on 1% agarose gels by electrophoresis in a Bio Rad mini subcell. The agarose was dissolved in 1x TAE buffer which was prepared from 50x stock. (0.04M tris-acetate, 0.001 M EDTA; 50x stock/L, 2M tris base, 57.1ml glacial acetic acid, 0.05 M EDTA pH8.0) and then diluted to 1 L with H₂O. 40 mg of agarose was dissolved in 40 ml of 1xTAE buffer by heating then boiled and cooled to 50-60°C. 4µl Ethidium bromide solution was added to a final concentration of 0.5 µg/ml to visualize the DNA. The gel was submerged in 1xTAE buffer and the samples loaded into wells with with 6x loading buffer (0.2 % w/v bromophenol blue, 50 % v/v glycerol). In addition, to determine the size of DNA fragments, 5 µl of hyperladder1 (Bioline) was used. The gel electrophoresis was run at 100 V for approximately 25 minutes. The DNA/RNA was visualized on a UV trans-illuminator, and digital images taken by an UVitech trans-illuminator attached to a digital camera.

2.5.1 Extraction of DNA fragments from agarose gels

QIAquick Gel Extraction kit (Qiagen) was used for recovering DNA from agarose gels. A block of agarose containing the required fragment of DNA was excised with a clean, sharp scalpel blade from the TAE agarose gel after electrophoresis and visualisation under UV light and placed in a pre-weighed Eppendorf tube. Assuming the mass of the excised agarose is equal to its volume 3 volumes of Buffer QG (kit reagent) was added. The tube was then incubated at 50°C for 10 minutes, with vortexing of the tube every 2-3 minutes throughout the incubation. The Buffer QG should remain yellow in colour. If however it changed 10µl of 3M sodium acetate, pH 5.0 was added. The dissolved sample was then applied to the QIAquick spin column (supplied with kit) and the DNA bound to the column by centrifugation for 1 minute at 13,000 rpm. The flow-through was discarded and the column inserted back into the same tube to be washed by adding 0.75ml of Buffer PE (kit reagent) and centrifuged at 13,000 rpm for 1 minute. Again the flow-through was discarded and the column centrifuged for a further minute at 13,000 rpm. The DNA was eluted by the addition of 30µl of Buffer EB (kit reagent), which was left to stand for a further 1 minute and then centrifuged at 13,000 rpm for 1 minute.

2.6 Cloning of DNA fragments

2.6.1 Cloning vectors

PCR fragments were cloned into the pENTR/D-TOPO Gateway entry vector (Invitrogen) and then cloned into a gateway-compatible destination vector using LR

Clonase. Blunt–end DNA fragments were created by PCR using the pENTR/D-TOPO compatible oligonucleotide primers (altered to comprise the four base pair CACC motif 5'-3' on the forward primer) and a high fidelity proofreading KOD DNA polymerase. The pENTR/D-TOPO reaction was set up as described below, using a 1:2 to 2:1 molar ratio of eluted PCR product:TOPO vector;

Fresh PCR product	0.5 to 4µl
Salt solution (1.2M NaCl, 0.06M MgCl ₂)	1µl
Water to a final volume of	5µl
TOPO® vector	1µl
Total volume	6µl

The D-Topo reaction was stirred gently and incubated at room temperature for between 5 minutes and 3 hours. 1µl of this solution was then added to 25µl of One-shot TOP10 chemically competent *E.coli* cells and incubated on ice for 30 minutes. The culture was spread on a Luria-Bertani (LB) agar plate and incubated overnight. LB medium consisted of 1.0 % tryptone, 0.5% yeast extract and 1.0% NaCl, (pH 7.0) autoclaved for 20 minutes then left to cool to 55 °C and then supplemented with the appropriate antibiotic and stored at room temperature or at 4°C. Individual colonies selected on kanamycin 50mg/ml in H₂O LB plates were then incubated at 37°C overnight in 3ml of kanamycin-supplemented LB. Plasmid minipreps were then prepared. Insertion of the fragment into the TOPO vector was verified by PCR and restriction analysis, and glycerol stocks were prepared for cultures with confirmed insertions.

2.6.2 LR Clonase

Gateway LR Clonase mix was used to transfer DNA fragments inserted into the TOPO entry vector into a gateway compatible destination vector usually at a molar ratio of 1:1. The LR reaction was performed as described below:

Entry clone (100-300 ng)	1-10 µl
Destination vector (150 ng/ µl)	2µl
5 x LR Clonase Reaction Buffer	4µl
TE buffer, pH 8.0	To 16 µl

This mixture was vortexed twice briefly and then microcentrifuged, after that it was incubated at 25°C for 60 minutes. 2 µl of Proteinase K solution was added to each sample to stop the reaction. This mixture was vortexed and then incubated at 37°C for 10 minutes. 1µl of this reaction mix was then used to transform One-shot TOP10 chemically competent *E. coli* cells (Invitrogen) as described below. Cells were then incubated overnight in 3ml of the appropriate antibiotic-supplemented LB. Plasmid minipreps were then carried out and insertion of the fragment into the destination vector was first verified by PCR and restriction analysis and then sequences of the plasmid were obtained to identify any possible errors in the DNA sequence. Glycerol stocks were prepared from bacterial cultures with confirmed insertions and stored as described below.

2.7 DNA ligation

2.7.1 Transformation of competent *Escherichia coli*

A 200 µl aliquot of α -select competent Cells (DH5 α strain) was thawed on ice. Invitrogen TOP10 chemically competent cells were used for DNA manipulations. The cells were thawed and 1µl of the DNA ligation reaction mix was added and gently mixed with a pipette tip but not pipetted. The mixture was placed on ice for 5 to 30 minutes. The mixture was then heat shocked at 42°C for 30 seconds and then immediately the tube incubated on ice for 2 minutes. 250 µl of S.O.C. medium (2% Tryptone, 0.5% Yeast Extract, 10 mM NaCl, 2.5 mM KCl, 10 mM MgCl₂, 10 mM MgSO₄, 20mM glucose) was added to the cells. The capped tube was incubated with shaking at 200 rpm for 1 hour at 37 °C. 50-200 µl of the transformation mix was then plated on a pre-warmed appropriate antibiotic usually (spectomycin, Kanamycin) then incubated overnight at 37 °C.

2.7.2 Bacterial storage

Short-term storage of bacteria was on LB agar plates (autoclaved), supplemented with the appropriate antibiotics where required. Bacteria were streaked onto plates, cultured overnight at 37°C and the plates were stored at 4°C. Glycerol stocks of 200µl of sterile 80% glycerol was added to 800µl of an overnight culture grown from a single colony from a LB agar plate were vortexed and then flash frozen in liquid nitrogen for frozen long-term storage at -80°C.

2.7.3 Analysing transformants by PCR

10-15 colonies were chosen for analyzing positive transformants after growing bacterial cells on selective medium. The selected colonies were picked up and resuspended separately in 100 µl deionized water. The mixture was incubated for 10 minutes at 94°C to lyse the cells. A PCR was carried out using a forward primer including CACC nucleotides at the 5' end following the instructions of Gateway cloning (Invitrogen) and M13 reverse primer. PCR DNA amplification was run for 30-35 cycles and the DNA products were subjected to gel electrophoresis and visualized on a UV trans-illuminator. After verifying amplification of the estimated DNA band size, 2-3 colonies were selected and incubated overnight in LB medium containing 50 µg/ml kanamycin at 37°C for plasmid DNA preparation.

2.7.4 Plasmid DNA preparation using Sigma Gen Elute™ Miniprep Kit

Preparation of plasmid DNA was carried out from transformed cells using a commercial Miniprep kit from Sigma. Following the manufacturer's instructions. A 5ml overnight cultures of a single-colony of *E. coli* grown in antibiotic-supplemented LB medium at 37 °C with shaking at 200 rpm was harvested by centrifuging 1.5 ml of the culture in 1.5 ml Eppendorf tube at 14,000 for 1 minute. The supernatant was removed and a further 1.5ml of the culture was added to the same tube and centrifuged again. The cells were fully resuspended in 200 µl of Resuspension Solution (kit reagent) and vortexed. Then 200 µl of Lysis buffer (kit reagent) was added to the tube which was inverted 6-8 times to gently mix the solutions. 350 µl of Neutralization/Binding Solution was added immediately inverted gently 4-6 times. The lysate was centrifuged at 14,000 rpm for 10 minutes and then the cleared lysate was added to a Gene Elute™ miniprep binding column which had been placed into a centrifuge tube. 500 µl of preparation solution was transferred and centrifuged at 14,000 rpm for 1 minute. The flow-through was discarded and then the column was washed with 750µl of wash solution (kit reagent) and then centrifugation at 14,000 rpm for 1 minute. The flow through was discarded and the tube was centrifuged again for a further 2 minutes to remove any excess ethanol. To elute the DNA, the column was put in a clean 1.5 Eppendorf tube, 50 µl of Elution Solution (kit reagent) was added. The column was left to stand for 1 minute before being centrifuged at 14,000 rpm for 1 minute. The isolated plasmid DNA was then stored at -20 °C until further use.

2.7.5 Analysing plasmid DNA by restriction

Restriction enzyme digestion of plasmid DNA was used to verify the presence and correct orientation of the inserted DNA fragment. Single or multiple restriction digestions of DNA were performed at the temperature specified in the manufacturer's technical information provided with each restriction enzyme. A general reaction mix was:

DNA (1µg)	Xµl
10X Restriction digest buffer (supplied with enzyme)	1µl
Restriction enzyme (1U/µl)	1µl
Sterile H ₂ O	up to 10µl

The above reagents were mixed together and incubated at the suitable restriction enzyme digestion for 1-2 hours. If multiple digests were carried out multicore buffer was frequently used to give the greatest possible reaction conditions for both restriction enzymes. Analysis of the digested products was performed by agarose gel electrophoresis.

2.7.6 Recombination of entry vector and destination vectors LR using Clonase

The LR recombination reaction was carried out as described below:

LR Clonase™ II plus enzyme mix was defrosted on ice for around 2 minutes and vortexed briefly twice. 1µl of LR Clonase™ II plus were added to each LR reaction mixture (3:1ng of destination to entry vector) and mixed well by vortexing and centrifuged briefly. The recombination reaction was then placed at 25°C for at least 1 hour. To terminate the reaction, 1 µl of proteinase K solution was added to each sample, vortexed briefly and samples were incubated at 37°C for 10 minutes. The transformation to one shot® Chemically Competent *E.coli* was performed as described in 2.7.7 below.

2.7.7 Transformation of *Arabidopsis thaliana* using *Agrobacterium tumefaciens*

2.7.7.1 Transformation of *Agrobacterium* with plasmid DNA using electroporation

The *Agrobacterium* strain C58 which is rifampicin resistant was used for *Arabidopsis* transformation. Electrocompetent *Agrobacterium* cells were defrosted on ice and 1 µl plasmid DNA was added. Electroporation was carried out according to the instructions of the electroporator (capacitance: 25µF, voltage: 2.4 KV, resistance: 200 Ohm and pulse length: 5msec). The cells and DNA were mixed on ice and transferred to a pre-chilled electroporation cuvette. 1mL of LB medium was added to the cuvette directly after electroporation, and the bacterial suspension was transferred to 10mL LB and

cultured at 28°C for 4 hours. After collecting the cells by centrifugation, they were spread on an LB agar plate containing the appropriate antibiotic for the plasmid vector and *Agrobacterium* strain (rifampicin which was solubilized in diluted acid solution, plus usually kanamycin). Plates were incubated for 3 days at 28°C and were stored at 4°C.

2.7.8 Preparation of *Agrobacterium* for floral dipping

The *Arabidopsis* floral dipping technique described by Clough and Bent, 1998 was used for *Arabidopsis* transformation. 5mL of LB media containing a colony of *Agrobacterium* from an LB plate with the appropriate antibiotics was cultured overnight at 28°C. 0.5mL of this culture was then added with no antibiotics to 50mL LB media and cultured at room temperature overnight. The optical density of the solution was measured at 600nm on an Eppendorf Biophotometer to check that the optical density has reached approximately an OD₆₀₀ of 0.8. *Agrobacterium* cells were pelleted and resuspended in 5% sucrose after centrifugation at 4000g for 10 minutes.

2.7.9 Transformation of *Arabidopsis* by floral dipping

Plants were grown until they began flowering. Flower buds were dipped in the re-suspended *Agrobacterium* in sucrose solution for 5 seconds. Once all the flower buds had been dipped, the plants were enclosed in a bag in the dark to maintain high humidity for 1 hour. The plants were maintained until they produced seed. The seed was collected and positive transformants were selected by sowing seeds on medium containing an appropriate antibiotic.

2.7.10 Histochemical localization of GUS activity

Promoter GUS fusion activity is broadly used to analyse the expression pattern of specific genes driven by a particular cis-acting promoter region. The staining activity is based on an enzyme from the bacterium *Escherichia coli*, β -glucuronidase. When incubated with specific colorless substrate, β -glucuronidase converts this into coloured products. The PHGWFS7 vector contains the *E. coli* β -glucuronidase gene which encodes a hydrolase that catalyses cleavage of β -glucuronides, such as X-gluc to generate a blue precipitate giving an indication of where the GUS gene is being expressed. As the promoter GUS fusion gene construct is randomly inserted into the genome using *Agrobacterium* mediated transformation the position of the insertion in the genome may have an effect on the level of GUS expression. Plants tissues containing this vector were incubated with the X-Gluc substrate as described below

(Jefferson *et al.*, 1987), and the expression pattern of the GUS gene was investigated by histochemical staining.

X-Gluc reagent comprised of the following:

1M phosphate Buffer pH7	100µl
50mM potassium ferricyanide	10µl
50mM potassium ferrocyanide	10µl
250mM EDTA	40µl
10% Triton x 100	10µl
40mM X-Gluc in DMSO	50µl
Deionized water to a final volume of	1ml

Fresh tissue samples were placed in a 1.5 microcentrifuge tube. Enough reagent mix was added to completely cover the sample. The tissue and X-Gluc reagent was then vacuum infiltrated for 10 minutes. The sample with the reagent solution was placed in the dark at 37°C for 1-48 hours in a closed vessel, i.e. the tubes were capped. To improve visualisation of the staining the tissue was cleared of chlorophyll, which was performed by the removal of the reagent mix and the addition of enough 70% ethanol to cover the tissue. The tissue and ethanol was placed on a shaker at 100 rpm until all of the chlorophyll green colouration had been removed.

2.8 Stomatal phenotyping

2.8.1 Stomatal density and index measurement

For leaf epidermal cell and stomatal counting, impressions were taken from the abaxial and adaxial epidermes from fully-expanded leaves. Three mature fully expanded rosette leaves were cut from three different plants of each genotype (9 leaves in total). High definition Dental resin (Coltene Whaledent, Switzerland) was applied to the leaves and nail varnish peels were taken from set resin after removal of the leaf (e.g. Gray *et al.*, 2000). Clear nail polish was applied to the impressions and let to entirely dry. Nail polish patches were peeled then placed on clean microscope slides and a cover slip sited over. Cell counting was carried out using a microscope at 40x magnification, and an eyepiece grid with an area of 0.065 mm². For stomatal density, the number of stomata per square millimetre and for stomatal index, the number of stomata and epidermal cells were calculated from central areas of three leaves from three separate plants of each genotype using the equation.

$$\text{Stomatal index} = 100 \times \frac{\text{stomatal density}}{\text{stomatal density} + \text{epidermal cell density}}$$

2.8.2 Stomatal aperture measurements

The equipment used in stomatal bioassays for measuring stomatal apertures from leaf epidermal peels was originally created by Clements and based on a rig in Hetherington's University of Lancaster laboratory. This equipment was designed for the control of environmental factors influencing stomatal physiology. (McAinsh *et al.*, 1991; McAinsh *et al.*, 1996; McAinsh *et al.*, 1995; Webb and Hetherington, 1997). Strips were taken from the abaxial surface of *Arabidopsis* leaves from four to five week-old leaves of control and mutant plants using curved fine forceps. Three to five leaves of each plant were used and epidermal strips floated on resting buffer (10mM MES, pH 6.2). Epidermal strips were then transferred to opening buffer (10mM MES, 50mM KCl, pH 6.2), incubated in light and bubbled with CO₂ free air and kept at 20°C by placing Petri dishes containing the strips and opening buffer in a glass tank filled with water whose temperature was maintained by a cooling coil and heater. The Petri dishes were illuminated by a light box containing fluorescent bulbs located beneath the water tank. The light box was run with a dimmer switch allowing the light intensity to be set at 300µmol m⁻² s⁻¹. To allow the aeration of the opening buffer with CO₂-free air, an air pump was used to force air through self-indicating soda lime, and then through a manifold which was connected to Petri dishes via rubber tubing and syringe needles. Air flow was adjusted to 100ml min⁻¹ and set for each experiment to make sure that air perfused the opening buffer without displacing the epidermal peels from the buffer.

2.8.2.1 Preparation of ABA Standard Solutions

A stock solution (1mM) of ABA standard was prepared by dissolving 0.264 mg of ABA (Sigma Chemical Co) in 1 ml methanol. This stock solution was stable for more than three months when stored in a refrigerator at 4°C. The working standard of ABA (1 mg/l) was made by 100-fold dilution of the stock solution

2.8.2.2 ABA induced stomatal closure

Epidermal strips were incubated in resting buffer and transferred to stomatal opening buffer in light with CO₂ free air for 2 hours as described above. Then they were incubated for 2 h in the same buffer containing 0 to 5 µM ABA (McAinsh *et al.*, 1996).

2.8.2.3 Light induced stomatal opening

Plants were kept in the dark overnight and in the morning before the lights came on epidermal strips were prepared in dim-light and stored in resting buffer for one hour in the dark. Strips were then transferred to opening buffer and CO₂ free air and maintained at 20°C for up to three hours. Stomatal apertures of epidermal strips were measured every 45 minutes.

2.8.2.4 Inhibition of stomatal opening by CO₂

Epidermal strips were prepared as in 2.8.2 and incubated in opening solution in light with exposure to either CO₂-free air or ambient air bubbled to the solution for two hours and then stomatal aperture measurements were carried out.

2.8.2.5 Measurement the effects of NO (Nitric Oxide) on stomatal aperture

Epidermal peels prepared as in 2.8.2 above were incubated for 2 hours in opening buffer in light with CO₂ free air to induce stomatal opening, To increase NO concentration the exogenous NO donor, 100 µM sodium nitroprusside (SNP) was added to epidermal strips (in the presence or absence of added ABA) for 2 hours then stomatal apertures were measured.

2.8.2.6 Chemical inhibitor studies

To determine effects of methionine amino peptidase activity on stomatal responses to ABA, epidermal strips were harvested as above and incubated in resting buffer, before transfer to opening buffer under light and CO₂ free air for two hours to induce full opening. The methionine amino peptidase 1 inhibitor fumagillin (final concentration of 5 µM) and ABA (1 or 5 µM final concentration) were added and the tissues were incubated for a further 2 hours and the apertures were measured.

2.8.2.7 Stomatal aperture measurements

Following all the above epidermal strip incubations stomatal apertures were analysed by light microscopy (Olympus Bx51, Tokyo) using a fitted camera (Olympus digital camera unit) and graticule. Epidermal strips were transferred on to slides and transferred to the microscope to capture images as quickly as possible (i.e. within 0-5 minutes). The lengths and widths of apertures of 40 stomata per treatment per experiment were measured for each plant type. Stomatal apertures were measured using ImageJ software (National Institutes of Health). Each experiment was repeated on three separate occasions using fresh plant samples on three consecutive days so that 120 stomatal apertures were measured per treatment or genotype. Data were

expressed as μm and aperture areas were calculated using the formula for an ellipse ($\pi \frac{1}{2} (\text{length}) \frac{1}{2} (\text{width})$). Results were expressed as aperture mean \pm SE.

2.8.2.8 Assessment of nitric oxide accumulation using DAF2-DA

Nitric oxide accumulation was assessed using the specific NO dye DAF2-DA dissolved in Dimethyl sulfoxide DMSO (Calbiochem, Nottingham, UK) using the method described previously (Desikan *et al.*, 2002). Epidermal fragments prepared as above in opening buffer were loaded with 20 μM DAF2-DA for 20 minutes before washing with MES-KCL buffer for 20 min and then epidermal peels were incubated for a further 25 minutes in the presence of ABA, before images were visualized by fluorescent microscopy (Olympus BX51 microscope) and photomicrographs taken using an DD71 camera.

2.9 Relative water content measurements.

Leaves from the mature leaf rosette of at least five plants were excised, and their fresh weight was measured immediately. After floating them in deionized water at 4°C overnight, their rehydrated weight was determined. Finally, they were dried in an oven at 70°C overnight and weighed. The equation used to calculate the RWC follows as below:

$$RWC = \frac{(\text{fresh weight} - \text{dry weight})}{(\text{rehydrated weight} - \text{dry weight})}$$

2.10 Analysis of leaf temperature in response to drought stress

2.10.1 Infrared Thermal imaging

Infrared thermography is a powerful technique for measuring leaf temperature which does not require physical contact with the leaves (Wang *et al.*, 2004). Thermal images were obtained using a Thermacam FLIR 660 camera (Inframetrics, FLIR Systems, North Billerica, MA, USA) One. This infrared camera has a resolution of 640 x 480 (307200 pixels) and a maximum 0.03°C sensitivity. The camera was mounted vertically on a tripod approximately 40 cm above the leaf rosette, and was connected to a colour monitor to facilitate visualisation of individual plants. Infrared images were taken within the plant growth cabinets and were analysed using ThermaCAM™ Researcher™ 2.9 Professional version (FLIR systems).

2.11 Statistical analysis

One way analysis of variance *ANOVA* was used in the analysis of comparative experiments. Variance was considered significant for $p < 0.05$. One way analysis of variance *ANOVA* and Tukey's Multiple Comparison Test were conducted with Graph pad prism software.

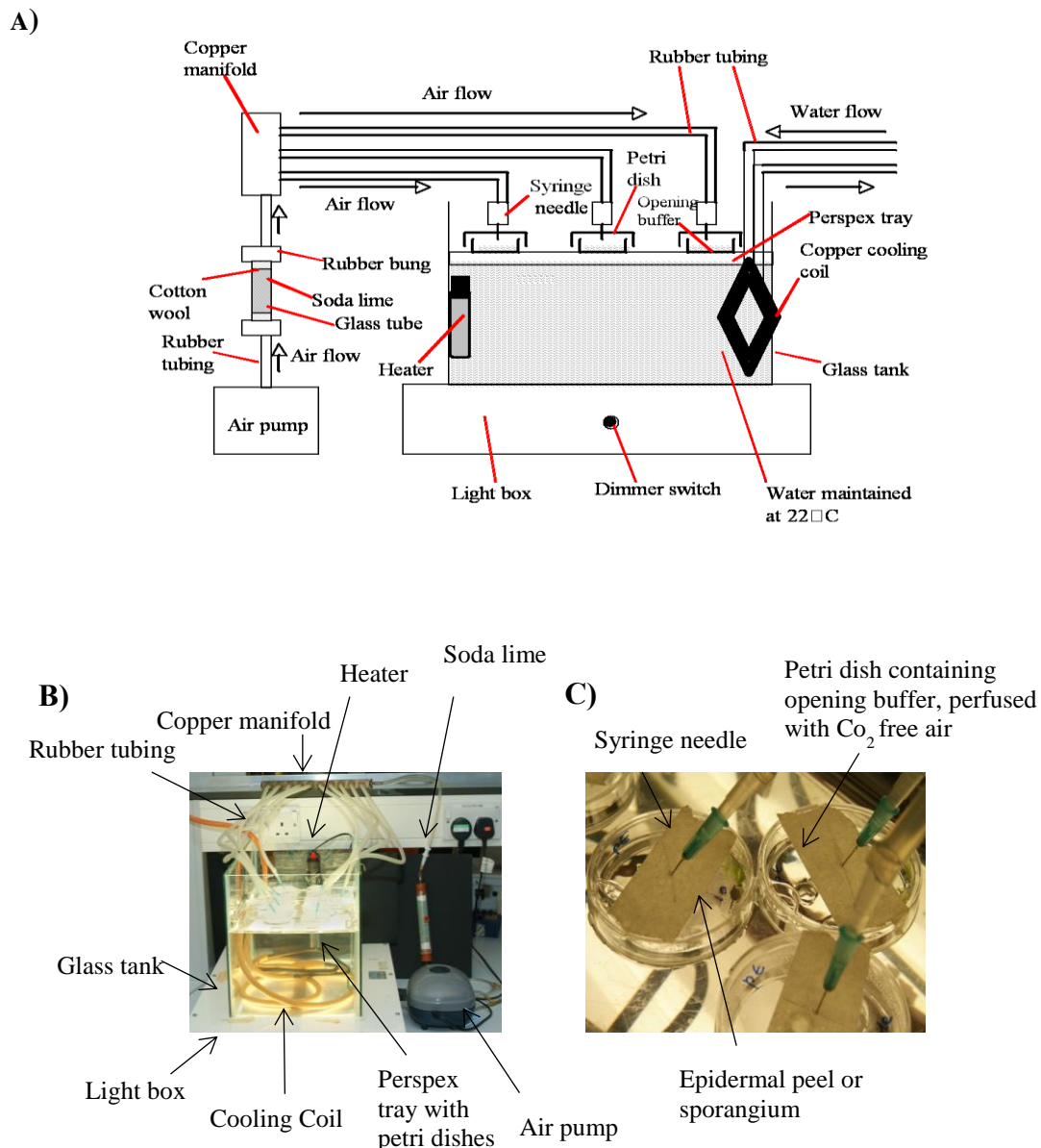


Figure 2-1 Equipment used to incubate epidermal fragments at optimum conditions for opening *Arabidopsis* stomatal pores (Diagram reproduced from Dr Sarah Clements thesis)

A) Schematic diagram of stomatal bioassay equipment. B) Photograph showing the illuminated water-filled tank and Petri dishes maintained at 22°C by the water and perfused with CO₂-free air. C) Photograph of Petri dishes filled with opening buffer with floating epidermal tissues.

3 Chapter 3- The N-recognin PRT6 mediates ABA-induced stomatal closure and drought susceptibility

3.1 Introduction

The N-end rule pathway of targeted proteolysis determines the half-life of proteins that contain destabilizing amino-terminal residues such as arginine (Bachmair *et al.*, 1986; Varshavsky, 2005, 2008). It is an ubiquitin (Ub) requiring system, responsible for ubiquitylating proteins through the action of three enzymes: E1 a ubiquitin activating enzyme; E2 a Ub-conjugating enzyme; and E3 a Ub ligase. This leads to degradation by the 26S proteasome. Over the past decade other related Ub-dependent processes have been shown to play important roles in the regulation of plant signalling by phytohormones, such as auxin, gibberellins and jasmonic acid (Tasaki and Kwon, 2007). In this chapter experiments are presented to investigate the role of the N-end rule pathway in stomata ABA-mediated responses. The N-end rule pathway has a hierarchic structure as described in chapter 1 (**Figure 1-6**). Primary destabilizing residues are identified by E3 Ub ligases of the N-end rule pathway, termed N-recognins. In *Arabidopsis*, two recognins of this pathway termed PROTEOLYSIS1 (PRT1) and PRT6 have been recognized (Garzon *et al.*, 2007; Moon *et al.*, 2004; Potuschak *et al.*, 1998) but PRT6 (encoded in *Arabidopsis* by At5g02310) is the important E3 ligase in the plant N-end rule pathway and a key regulator of seed ABA sensitivity during germination (Holman *et al.*, 2006). PRT6 and N-end pathway play a major role in seed ABA signalling, influencing the seed to seedling transition. The over-arching aim of the work presented in this chapter was to determine whether the N-end rule pathway is also important in another plant ABA response, the closure of stomatal pores. The experiments presented in section 3.5 below were designed to investigate the expression and function of *PRT6* in guard cells.

3.2 ABA-induced stomatal closure

Plants can sense water shortages in the rhizosphere and induce suitable adaptive responses by synthesising and transmitting chemical signals such as ABA which can inhibit stomatal opening in the shoots of transpiring plants (Karimi *et al.*, 2002). Thus, understanding ABA-signalling pathways and stomatal responses may help us to alleviate plant drought stress (Neumann, 2008). In the experiments described in section 3.2 below it was investigated whether the gene product of *PRT6*, an enzyme of

the N-end rule pathway, may act through key known components of ABA signalling such as PP2C and SnRK2 to regulate stomatal apertures. Previously, in seeds it has proved, difficult to determine whether the core ABA-signalling components function upstream or downstream of the N-end rule pathway (Holman *et al.*, 2009). Additionally, how the N-end rule pathway components influence ABA signalling mechanisms that control stomatal aperture have not previously been investigated.

3.3 Light induced stomatal opening

In section 3.3 the effect of the N-end rule pathway on light-induced stomatal opening was investigated. Blue light is known to be important for inducing stomatal opening and red light is also involved. Conversely, darkness, or the absence of light trigger stomatal closure. Blue light stimulates a signalling cascade resulting in guard cell membrane hyperpolarization and stomatal opening which involves activation of an H⁺ ATPase. H⁺ extrusion, drives K⁺ uptake, starch metabolism and malate synthesis to increase guard cell turgor and promote opening. Red light mediated stomatal opening acts through reduction of intercellular concentration of CO₂, which inhibits guard cell anion channels (Umezawa, 2011). ABA, which inhibits light-induced stomatal opening, has been shown to act through the inhibition of the H⁺ ATPase activation via phosphorylation (Roelfsema *et al.*, 2002).

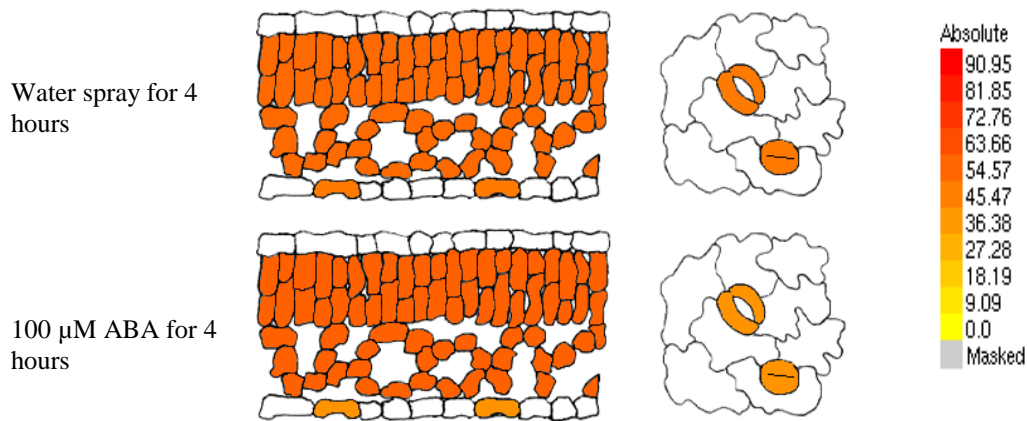
3.4 Effects of CO₂ on stomatal aperture

In section 3.4 the effect of the N-end rule pathway on CO₂-induced stomatal closure was investigated. Stomata respond to elevations in atmospheric CO₂ concentration by promoting stomatal closing and inhibiting stomatal opening. Elevated [CO₂] induces stomatal closure and external [CO₂] reductions induce opening (Roelfsema *et al.*, 2002; Zhang *et al.*, 2009). High [CO₂] leads to anion channel and K⁺ efflux channel activation and membrane depolarization. It has also been proposed that high levels of CO₂ induce malate synthesis which is important for activating guard cell anion channels causing anion efflux, and stomatal closure (Assmann, 1993). Several *Arabidopsis* genes products have been identified as acting in guard cell [CO₂] signalling, including some components in common with the stomatal ABA signalling pathway such as OST1 and ABI1 as described in Chapter 1. Thus, complex guard cell signalling pathways must interact to adjust stomatal apertures in response to a multitude of environmental signals. In this chapter the responses of guard cells lacking the N-recognin PRT6, to ABA, CO₂ and light stimuli were investigated.

3.5 Expression pattern of the *PRT6* gene

The evidence provided by Holman *et al.* (2009) indicating the importance of *PRT6* in the removal of ABA sensitivity during seed germination prompted an investigation of the role of the N-end rule pathway in ABA-induced stomatal aperture responses. The first step involved using a plant gene expression online analysis tool, the eFP-browser, to investigate whether the *PRT6* gene is expressed in guard cells. This tool was used to query available microarray datasets, and to create diagrammatic representations of the location and intensity of *PRT6* expression in guard cell and mesophyll protoplasts (Graciet *et al.*, 2010; Potuschak *et al.*, 1998; Stary *et al.*, 2003) and during *Arabidopsis* development (Graciet *et al.*, 2009) (**Figure 3-1**). In general, in these previously published microarray datasets, *PRT6* appeared to be expressed at a low level across most plant tissues. The data suggested that the *PRT6* gene was expressed at a relatively low level in guard cell and mesophyll protoplasts both before and after treatment with 100 μ M ABA. Although absolute levels were very low *PRT6* expression appeared to perhaps reduce slightly in guard cell protoplasts after treatment with ABA (**Figure 3-1**). The *PRT6* gene was expressed at relatively higher levels in seeds than siliques, and at moderately low levels in seedlings, cotyledons, hypocotyls and roots (**Figure 3-2**). *PRT6* was expressed at low levels at all leaf developmental stages and in dry and imbibed seeds. ABA-treated seedlings, showed a slight increase in *PRT6* expression after 30 minutes, however, after one hour and three hours of 10 μ M ABA treatment expression levels of *PRT6* decreased, suggesting that the expression of these genes may perhaps be slightly inhibited by ABA (**Figure 3-3**). Thus, in summary, the microarray data available online suggest that *PRT6* is expressed at relatively low levels throughout the plant, including in the guard cells.

A



B

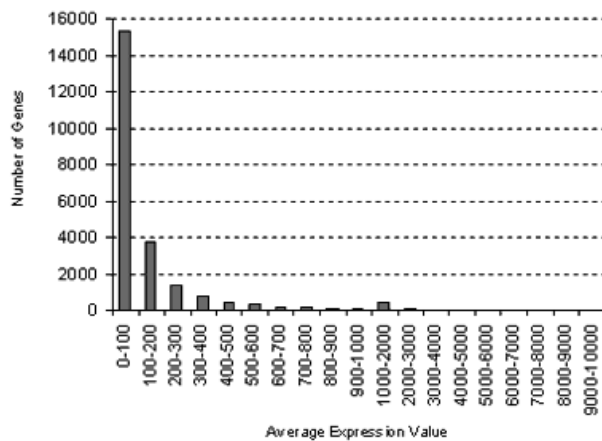


Figure 3-1 Expression pattern of PRT6 in mesophyll and guard cells from a transcriptomic analysis of protoplast extracts

A) Schematic illustration of the expression levels of the *PRT6* gene in the mesophyll and guard cells before and after treatment with 100 μ M ABA. Darker colours represent relatively higher gene expression levels as demonstrated in the scale bar to the right. Data was taken from the eFP-browser and is based on results from experiments carried out by (Schmid *et al.*, 2005). B) The distribution of *PRT6* gene expression levels across all experiments on TAIR reveals a relatively low expression level across most tissues (Winter *et al.*, 2007, Yang *et al.*, 2008).

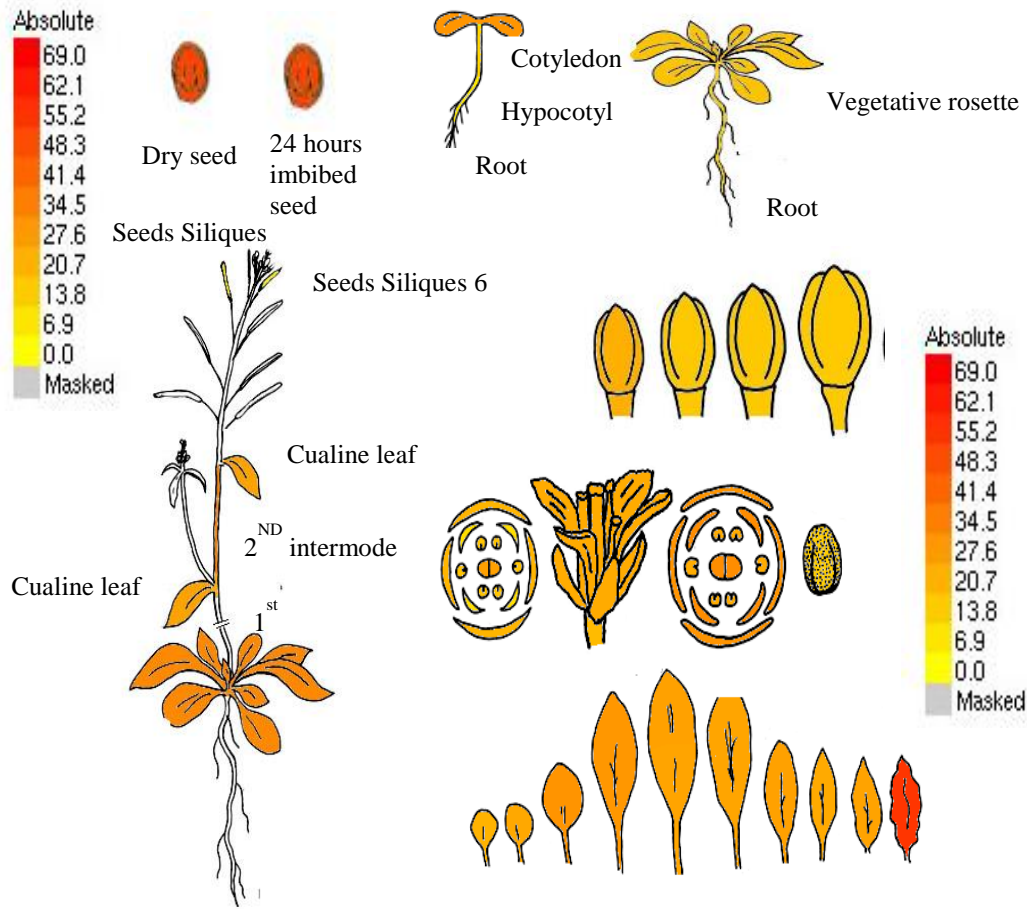


Figure 3-2 Expression pattern of PRT6 at different growth stages

Schematic illustration of the expression levels of the *PRT6* gene at different stages in the life cycle. Darker colour represents relatively for higher gene expression levels as demonstrated in the scale bar to the right. Data was taken from the eFP-browser and is based on results from experiments carried out by (Kilian *et al.*, 2007).

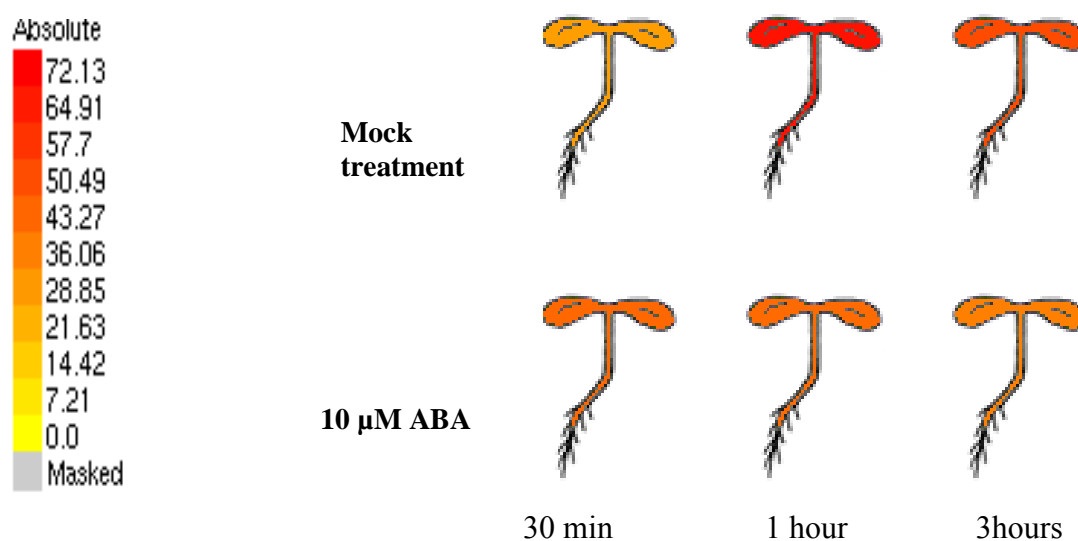


Figure 3-3 Expression pattern of *PRT6* in seedlings treated with ABA

Schematic illustration of the expression levels of *PRT6* in seedlings before and after treatment with ABA. Darker colours indicate higher gene expression levels as represented in the scale bars to the left. Data was obtained from the eFP-browser and is based on results from experiments carried out by (Schmid *et al.*, 2005; Yang *et al.*, 2008).

3.6 Investigation of *PRT6* gene expression in guard cells using a *pPRT6::GUS* reporter gene fusion

To investigate *PRT6* gene expression patterns further a *PRT6* promoter β -glucuronidase (GUS) fusion gene construct was produced. The construct contained the DNA region up-stream of the *PRT6* coding sequence fused to the GUS gene. The promoter gene construct, *pPRT6::GUS*, was stably transformed into *Arabidopsis* plants and the GUS expression pattern examined by histochemical staining for GUS activity at diverse developmental stages and after application of ABA. Approximately 2 kb of DNA upstream of the *PRT6* gene ATG translational start codon was PCR amplified from *Arabidopsis* genomic DNA and recombined with pENTR-D-TOPO (**Figure 3-4** and **Figure 3-5**). The resulting plasmid was transformed into competent cells of *E.coli*, as described in section 2.7.7 and verified using a PCR reaction containing a gene specific forward primer complementary to the insert, and the entry vector (M13) reverse primer. Restriction digestion was used to analyse the plasmids. The entry vector was recombined with the destination vector PHGWFS7 containing the GUS gene, using Gateway® LR Clonase™ II Enzyme Mix (**Figure 3-6**). A forward primer complementary to the insert and a GUS reverse primer were used to PCR amplify DNA from spectinomycin resistant colonies. Restriction digestion was

used to confirm the *PRT6* promoter insertion in the plasmid. Plasmid transformation to *Agrobacterium tumefaciens* cells was carried out using electroporation as described in section 2.8.11. Rifampicin resistant *Agrobacterium* cells were cultured and the floral dip method used to transform *Arabidopsis* plants. The seeds were collected from the *Agrobacterium*-treated plants and sown on MS agarose plates supplemented with hygromycin antibiotic. Hygromycin resistant seedlings were transferred to compost and grown to maturity. The presence of the transgene was confirmed by PCR using plant genomic DNA. Six verified T0 lines were subjected to GUS histochemical staining to examine *PRT6* gene promoter activity. Plants that had GUS expression were grown to maturity and seeds were collected. T1 lines were grown, and used to study the GUS location and expression level in different developmental stages and cell types. One *pPRT6::GUS* staining T1 line, with a typical GUS staining pattern, was examined in detail (**Figure 3-8**, **Figure 3-9** and **Figure 3-10**).

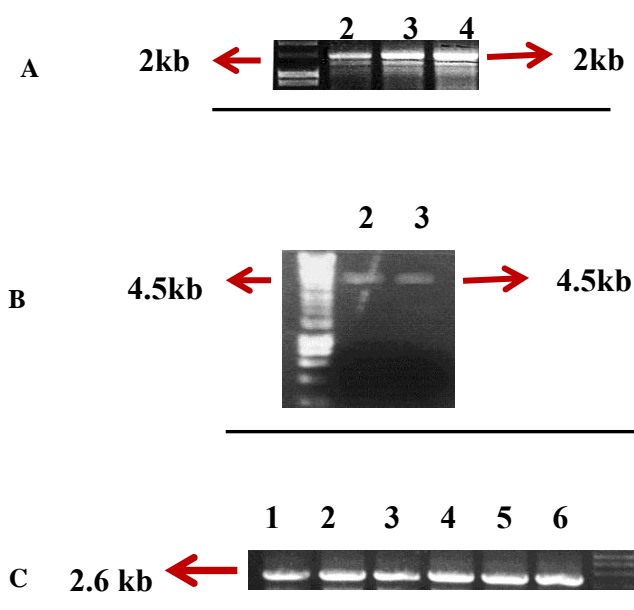


Figure 3-4 Generation of the *pPRT6::GUS* promoter fusion construct

A) PCR using forward and reverse specific gene primers were used to amplify a DNA fragment of approximately 2kb from the *PRT6* upstream ‘promoter region’ of *Arabidopsis* genomic DNA (lanes 2, 3, 4 are samples amplified from Col-0 plant DNA). B) Restriction digestion of recombinant *PRT6::pENTR-D-TOPO* entry vector plasmid. Gel lanes 2 and 3 contain DNA fragments from different digestions of the same plasmid DNA preparation. Lane 2 *SpeI* digest and lane 3 *SacI* digest. Both lanes are expected to cut the *PRT6::pENTR-D-TOPO* plasmid at one position in the inserted fragment to give a DNA band of approximately 4.5kb in size. C) Identification of *pPRT6::GUS* transformed plants from seedlings selected on MS plates supplemented with hygromycin. PCR reactions were carried out with a gene specific forward primer and GUS reverse primer on genomic DNA samples extracted from 6 independently transformed T0 generation plants labelled 1 to 6. DNA size markers (HyperLadder I) are shown on the side of the gels in lanes A1 B1 and C7.

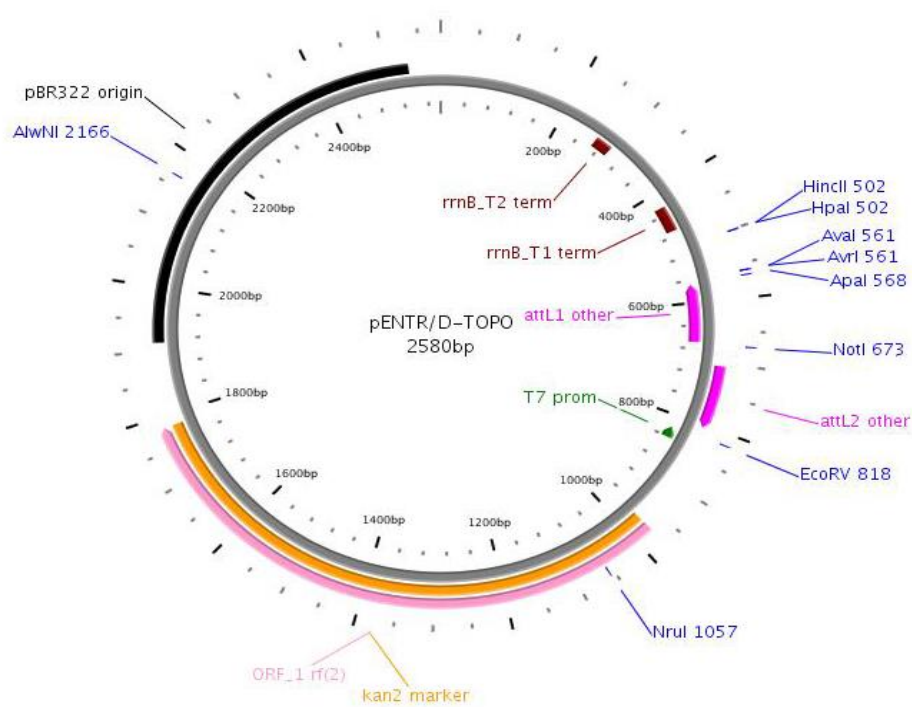


Figure 3-5 Entry vector used for *pPRT6* promoter cloning

The *PRT6* promoter region fragment (approximately 2kb upstream of the ATG translational start codon) was inserted into the *pENTR-D-TOPO* entry vector (Gateway recombination cloning kit, Invitrogen Cat. No. K2435-2) between the attL1 and attL2 recombination sites.

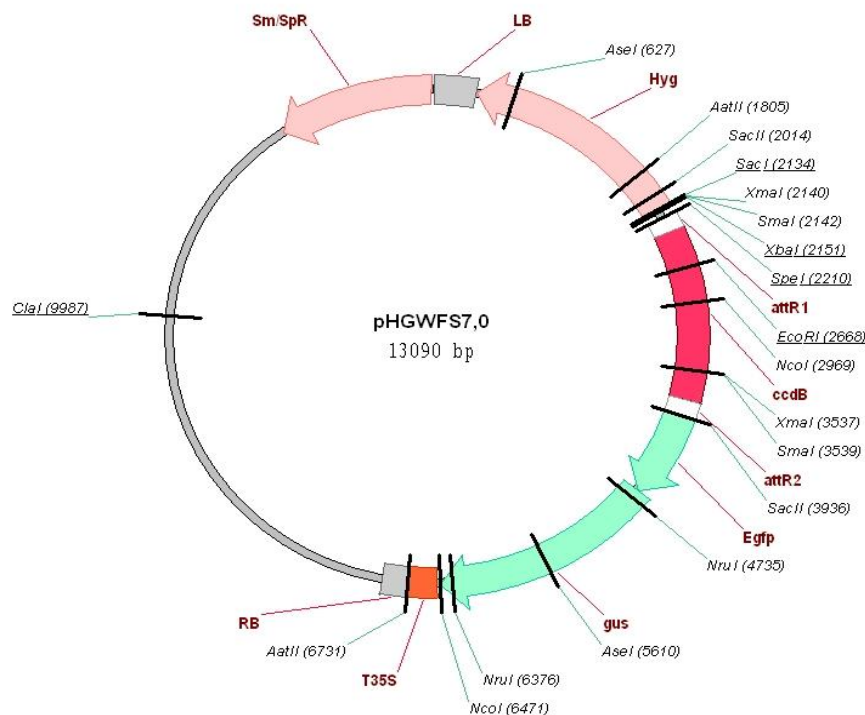


Figure 3-6 Destination vector used to create p*PRT6*::GUS

The p*GWFS7 plasmid destination vector was used for *PRT6* promoter cloning and analysis (Goda *et al.*, 2008). *pPRT6* was recombined into the attR1 and attR2 sites upstream of the EGFP and GUS genes, and between the LB and RB sequences necessary for *Agrobacterium* mediated transformation.

3.7 GUS histochemical staining of *pPRT6*::GUS transformed plants

To observe gene expression directed by the 2kb upstream *PRT6* gene promoter region, plant tissues at different developmental stages were exposed to the histochemical substrate X-gluc. Tissues were exposed to the X-gluc solution for 24-48 hours at 37°C after vacuum infiltration of the tissue to ensure that the X-gluc entered the cells. Histochemical GUS staining of *pPRT6*::GUS promoter-reporter plants revealed a low, but consistent, level of GUS activity in guard cells of leaf epidermal peels (**Figure 3-7**) in line with the available microarray data (**Figure 3-1**). This verification of *PRT6* expression in stomata strengthens the possibility that that *PRT6* activity could play a role in guard cell ABA-signalling. Treatment of leaves with ABA appeared to slightly increase guard cell *PRT6* expression (**Figure 3-7 B**). To explore whether *PRT6* expression is affected by ABA application, seedlings of *pPRT6*::GUS were exposed to distilled water or exogenous 30 µM ABA and histochemical localization X-gluc was observed. Three week old seedlings were incubated with distilled water for 1 hour, or a 30 µM solution of ABA for one or three hours before histochemical GUS

staining was carried out (**Figure 3-8**). It was observed that one and three hours of ABA treatment increased the histochemical GUS staining intensity in *pPRT6::GUS*. This result is not consistent with e-FP browser data where ABA caused, if anything, caused a slight decrease in seedling *PRT6* expression with these incubation times (**Figure 3-3**). In the experiment presented in (**Figure 3-8**), GUS expression increased after 1 hour and increased still further after three hours of ABA incubation treatment suggesting that *PRT6* expression may be ABA-inducible. The rosette leaves of five to six week old *pPRT6::GUS* plants were histochemically stained to investigate if the age of the leaf has an effect on the intensity and distribution of GUS expression. GUS activity was observed at low levels throughout the leaves, and was perhaps stronger in the main vein. In the older leaves, stronger and more widespread histochemical staining was detected across the whole leaf (**Figure 3-9**), suggesting that *PRT6* expression may be higher in older leaves. This result is consistent with the e-FP browser data which suggested increased *PRT6* expression in older cauline leaves (**Figure 3-2**). Histochemical GUS staining was also carried out on floral tissues. GUS expression was observed in cauline leaves, flowers and siliques of *pPRT6::GUS* plants (8-9 weeks old) (**Figure 3-10**). *PRT6* expression appeared to be strongest in the younger, more apical, inflorescence tissues. This floral staining pattern is consistent but perhaps stronger than that indicated by the e-FP browser data (**Figure 3-2**). However, in general, the expression pattern directed by the 2kb upstream *PRT6* promoter region could be described as a low level of expression throughout most plant tissues. This expression pattern was broadly similar to that previously found in microarray studies shown in (**Figure 3-1** and **Figure 3-2**) with the exception of the ABA-inducible *PRT6* expression revealed here. The experiments with *pPRT6::GUS* expressing plants presented here, unlike those on the e-FP browser, suggest that *PRT6* expression is strongly ABA inducible in seedlings (but probably not in guard cells). However, this result and all the results presented in (**Figure 3-7** and **Figure 3-10**) require further verification as the 2 kb promoter region used in these experiments may not fully reflect the expression pattern of the native *PRT6* gene.

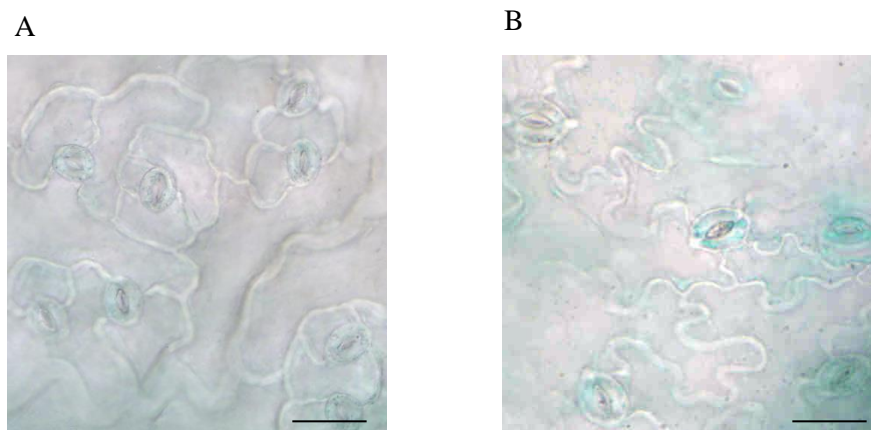


Figure 3-7 GUS histochemical localisation in guard cells of pPRT6::GUS

A) The Guard cell T2 generation *pPRT6::GUS* epidermal strips following GUS staining. B) Treated with 100 µM ABA for four hours. Scale bars: 50 µm.

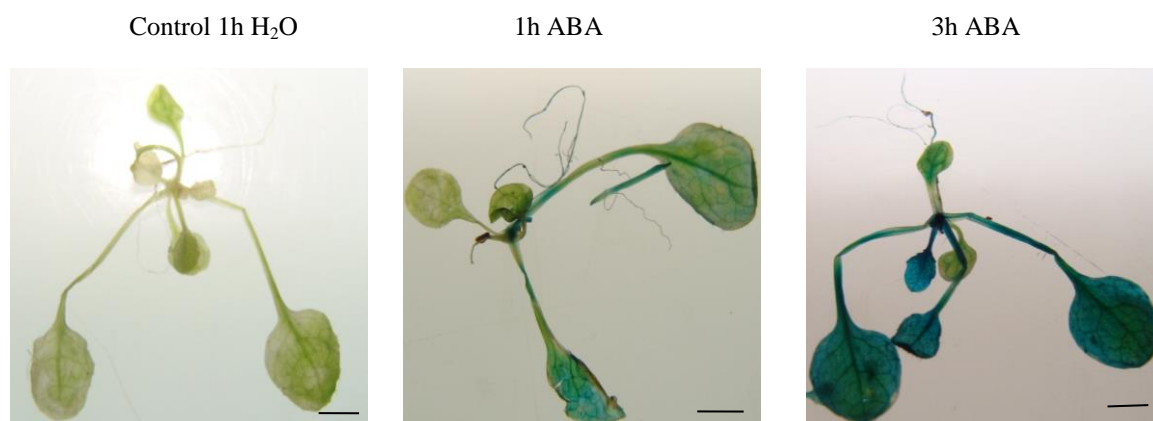


Figure 3-8 histochemical localization of expression directed by PRT6 promoter regions in T1 generation pPRT6::GUS seedlings treated with ABA

pPRT6::GUS transformed seedlings treated with distilled water and 30µM ABA. Control, 1h and 3h: indicate the incubation time was one and three hours respectively. Scale bar: 1cm.

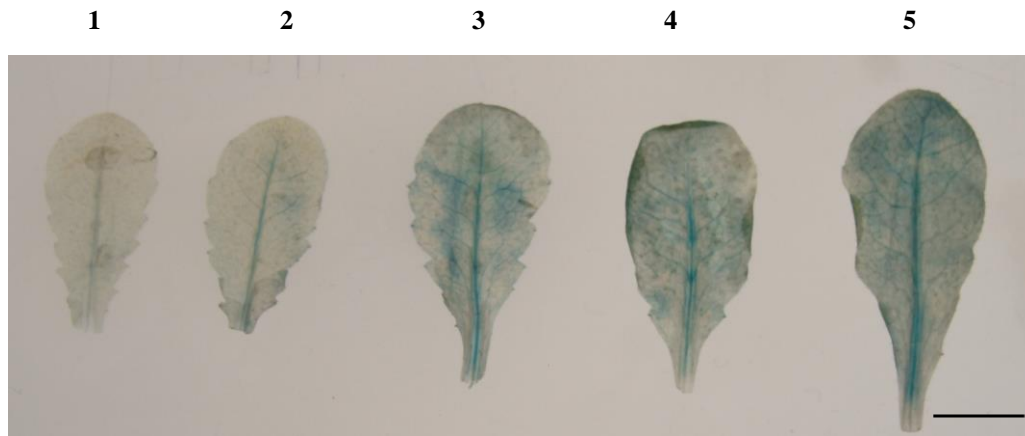


Figure 3-9 GUS histochemical localization in pPRT6::GUS rosette leaves

pPRT6::GUS Leaves were taken from 6 week old T1 generation plants and are displayed in order of maturity. The numbers indicate the position of the leaf within the rosette, number 1 being the youngest. Scale bar: 1cm.



Figure 3-10 GUS histochemical localisation in pPRT6::GUS inflorescence tissues

GUS activity was observed in *pPRT6::GUS* mature plant inflorescence tissues of a T1 generation plant. Scale bar: 1 cm.

3.8 Studies of *Arabidopsis prt6* T-DNA insertional mutant plants

To investigate a possible role for the N-end rule pathway in regulating stomatal responses to ABA, and plant responses to drought stress, T-DNA insertional mutant lines *prt6-1*, *prt6-2* and *prt6-5* were obtained from Professor Michael Holdsworth at the University of Nottingham and analysed (**Table 3-1**). The *prt6-4* mutant generated by EMS mutagenesis and identified by positional cloning in the Ler background ecotype (Holman *et al.*, 2009) was not used in this study with the exception of the double mutant studies presented in (**Figure 3-20**) Database information on the *Arabidopsis* Information Resource (TAIR) suggests that these three T-DNA insertions lines each have disruptions in the coding region of *PRT6*. PCR and RT-PCR reactions confirmed that each of these independently transformed plant lines have an insertion in the *PRT6* coding region and do not produce a detectable transcript (not shown). All the *Arabidopsis thaliana* mutant lines used in this study were present in the Columbia-0 (Col-0) background ecotype with the exception of *prt6-4* and *abi1-1* which were in the Landsberg erecta. (Ler) background.

Table 3-1 *Arabidopsis prt6* mutant seed stocks obtained for use in this study

<i>Arabidopsis</i> gene	allele	Origin	Reference	Background ecotype
At5g02310	<i>Proteolysis6-1</i> (<i>prt6-1</i>)	SAIL1278_H11	Garzon <i>et al.</i> , 2007	Col-0
	<i>Proteolysis6-2</i> (<i>prt6-2</i>)	GK270G04		
	<i>Proteolysis 6-5</i> (<i>prt6-5</i>)	SALK051088		
	<i>Proteolysis 6-4</i> (<i>prt6-4</i>)	EMS generated mutation	Holman <i>et al.</i> , 2009	Ler

3.9 Phenotypic characterisation of *prt6* plants

3.9.1 Stomatal aperture analysis

Studies of *Arabidopsis* guard cell signalling response pathways were performed by direct measurement of stomatal apertures using an epidermal peel bioassay as described in Chapter 2. Mature leaf abaxial epidermal strips were isolated from the mesophyll so that stomatal apertures were not affected by the leaf internal CO₂ concentration, C_i. The [CO₂] in the incubation media was controlled by supplying bathing solutions with CO₂-free air, or air at known [CO₂] in all experiments. The length and width of 40 stomatal apertures were measured for each plant genotype at each time point or treatment and every experiment was repeated 3 times (n=120 stomata). Mean stomatal aperture changes were calculated in response to ABA, light and [CO₂] in the following experiments.

3.9.2 *prt6* stomatal aperture responses to ABA

Leaf epidermal peels were taken from wild-type and mutant (*prt6-1*, *prt6-5*) plants at the start of the daily photoperiod and stored in resting buffer (10mM MES, pH 6.2) before transfer to stomatal opening buffer (10 mM MES, 50 mM KCl, pH 6.2) in 300 μmol m⁻²s⁻¹ light and with CO₂-free air at 22°C for 2 hours (essentially as described by McAinsh *et al.*, 1996). Stomatal apertures of both *prt6* lines tested were significantly smaller than wild-type after 2 hours incubation in the control solution (without addition of ABA, in light and CO₂-free air), suggesting that the *prt6* stomata may have impaired light-induced opening or sub-ambient CO₂ induced opening responses, or be hypersensitive to endogenous stomatal closure signals such as ABA. The mean apertures of control and *prt6* mutants all reduced significantly following exposure of epidermal peels to exogenous ABA. However, *prt6* apertures were significantly smaller than control apertures after being incubated with 1 and 5 μM ABA suggesting that *prt6* stomata have enhanced ABA-induced stomatal closure responses. Because the *prt6* stomatal apertures were smaller in the control solution, without the addition of ABA, the data have analysed further. Expressing the same data as a ratio of ABA-treated to control (no added ABA) for each genotype indicated that the *prt6* stomata closed to a greater extent than wild-type stomata, suggesting that lack of *PRT6* confers stomatal hypersensitivity to ABA (**Figure 3-11 A and B**). To investigate the possibility that *prt6* may have smaller sized stomata rather than more closed stomatal pores, stomatal pore lengths were also measured. The average length of control and

prt6 stomatal pores was not significantly different (**Figure 3-11 C**) suggesting that their guard cells are of a similar size and that *prt6* stomatal closure is hypersensitive to ABA.

3.9.3 *prt6* stomatal aperture responses to CO₂ concentration

The results presented above suggest that it is most likely that *prt6* stomata respond normally to low [CO₂] (**Figure 3-12 A**) but are hypersensitive to ABA. Epidermal bioassay experiments at differing CO₂ concentrations confirmed that *prt6* stomata could open as fully as wild-type stomata in response to light and CO₂ free or 200 ppm CO₂, and could close normally at 1000ppm CO₂ (**Figure 3-12 A**). However the results suggested that atmospheric [CO₂] induced slightly but significantly greater stomatal closure in *prt6* mutants compared to wild-type. This enhanced closure, seen only at ambient [CO₂], could be explained by the hypersensitivity to endogenous ABA observed in (**Figure 3-11 A and B**). Thus *prt6* stomata are either more sensitive to [CO₂] induced closure at atmospheric CO₂ conditions (but behave normally at sub-ambient or elevated [CO₂]) or more likely they are hypersensitive to endogenous ABA when present (**Figure 3-12 A**).

3.9.4 *prt6* stomatal opening in response to light

Plants were removed from the growth room and kept in the dark overnight. In the morning epidermal peels were taken in dim light and floated on resting buffer, supplied with CO₂-free air, in the absence of light for an hour. Peels were transferred to opening buffer in the 300μmol m⁻² s⁻¹ light and stomatal apertures recorded at intervals for 180 minutes. The results showed that stomatal apertures of both wild type and *prt6* plants increased during exposure of epidermal peels to light (**Figure 3-12 B**). However, between 45 and 180 minutes incubation in light, the wild-type stomata were significantly more open than those of *prt6* suggesting that *prt6* stomata may have slightly impaired light-induced opening, or alternatively and as suggested above, *prt6* stomata are hypersensitive to endogenous ABA when present. The experiments presented above indicate that *prt6* stomata are able to close normally in response to darkness or on exposure to elevated [CO₂]. It clear from the experiment in (**Figure 3-11 A and B**), that *prt6* stomata are hypersensitive to ABA-induced closure, but it is less clear from the other experiments in (**Figure 3-12 A and B**) whether *prt6* stomatal opening responses to light or ambient CO₂ are also impaired. As the stomata of *prt6* plants sampled during their photoperiod, were able to open fully in response to

light and CO₂ free air in the experiment shown in **(Figure 3-12)**, it is unlikely that *prt6* stomata have impaired light and sub-ambient CO₂-induced opening responses. However, under similar conditions *prt6* stomata were more closed than wild-type, in the control experiment presented in **(Figure 3-12 A)**. It is possible that these enhanced levels of stomatal closure observed in some experiments in the absence of added ABA, are as a result of the hypersensitive *prt6* response to endogenous ABA production in some samples, rather than an impairment in stomatal opening.

3.9.5 Analysis of stomatal development in *prt6*

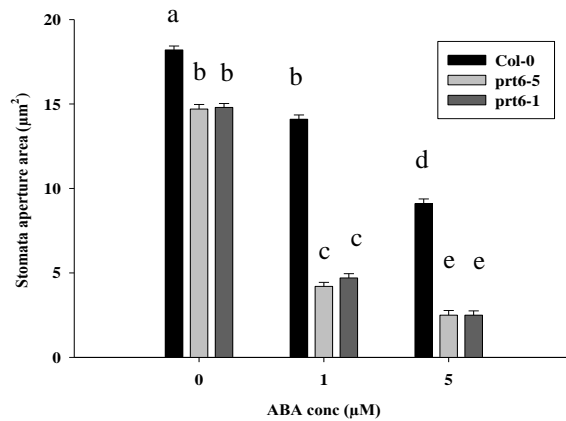
Impressions were created of the abaxial and adaxial surfaces of mature leaves for stomatal and epidermal cell counting. *prt6* mutants (*prt6-1*, *prt6-5*) were found to have approximately 30% fewer stomata on fully expanded leaves compared to Col-0 **(Figure 3-13)**. A reduction in stomatal density could be explained by an amplified size of epidermal cells or decreased formation of stomata (Nilson and Assmann, 2010). The stomatal index provide a measure of stomatal development. Stomatal indices were calculated from the stomatal frequency (number of stomata per unit area) divided by the epidermal cell density plus stomatal densities per unit area. Although the *prt6* epidermis had a much reduced density of epidermal pavement cells, suggesting larger pavement cells, stomatal indices were significantly reduced in *prt6* mutants in comparison to Col-0 **(Figure 3-14)** suggesting reduced numbers of all types of epidermal cells but particularly guard cells. To test whether this is a feature of other ABA hypersensitive plants, *abh1* stomatal density was analysed. A similar reduction in stomatal frequency to that obtained for the N-end rule pathway component mutants was found for *abh1*. It has been suggested by, (Lake and Woodward, 2008) that stomatal development is affected by transpiration rate and that plants that have reduced transpiration (due to growth at high humidity, low [CO₂], or in the presence of ABA) produce fewer stomata. Thus the significantly reduced stomatal density of *prt6* and *abh1* could result from the reduced transpiration rate due the stomatal ABA-hypersensitivity, or be as a direct effect of ABA hypersensitivity on cell division and or expansion in the epidermis during development.

3.9.6 Relative water content of *prt6*

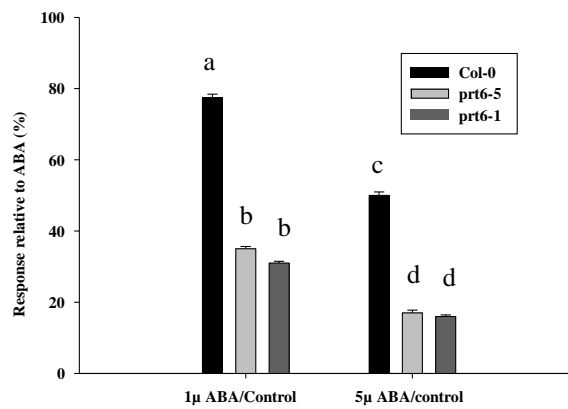
Relative water content (RWC) is an indication of plant-water status. The relative water content of *prt6-1* and *prt6-5* under both well watered and drought conditions was calculated from wet, fresh and dry weights of rosette leaves from 10 plants of

each genotype. The RWC of *prt6* plants was significantly higher than wild type plants under both watering conditions. These results indicate that *prt6* mutants are more able to conserve water than the wild-type plants. This evidence is consistent with the *prt6* reduced stomatal density and enhanced stomatal sensitivity to ABA (**Figure 3-15** and **Figure 3-11**). Together the results presented in this chapter, indicate that *PRT6* normally controls plant ABA responses, and suggest that *prt6* plants may be expected to have reduced transpiration and enhanced drought tolerance.

A



B



C

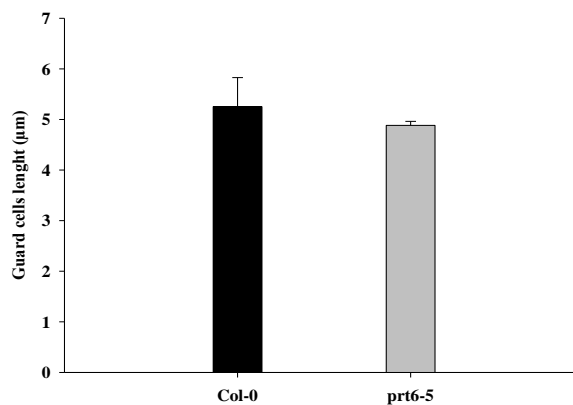
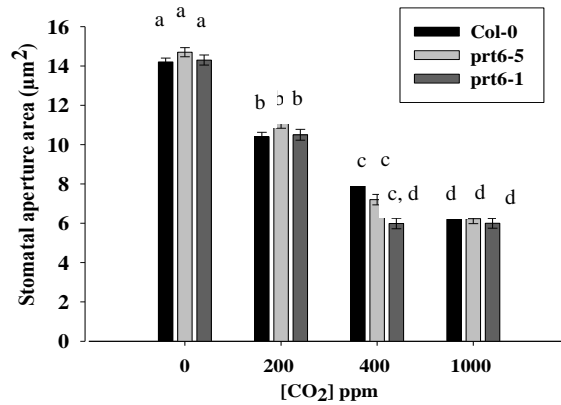


Figure 3-11 Stomatal aperture measurements taken from epidermal peels of *prt6-5*, *prt6-1* and control plants in response to A) ABA; B) expressing the same data as a ratio of ABA-treated to control (no added ABA) for each genotype; C) pore length of open stomata of *prt6* and control

For each experiment, epidermal peels were taken from three different plants, and each experiment was repeated three times. Mean apertures calculated from measurements of 120 stomata for each genotype at each time point or treatment are shown. Error bars represent the standard error. Values were statistically tested using one way ANOVA ($P < 0.0001$) and Tukey's Multiple Comparison Test. Different letters denote statistically significant differences ($p < 0.05$).

A



B

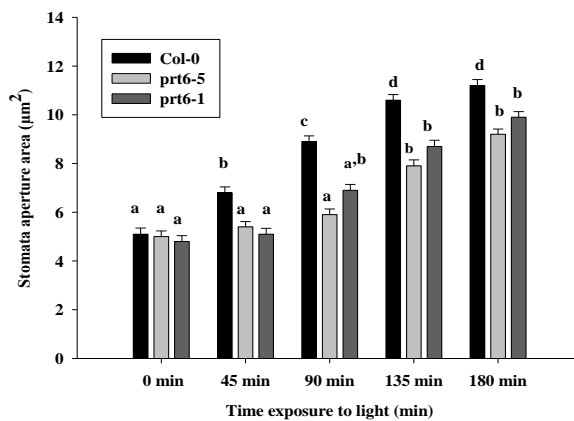


Figure 3-12 Stomatal aperture measurements taken from epidermal peels of prt6-5, prt6-1 and control plants in response to A) CO₂ B) Light

For each experiment, epidermal peels were taken from three different plants, and each experiment was repeated three times. Mean apertures calculated from measurements of 120 stomata for each genotype at each timepoint or treatment are shown. Error bars represent the standard error. Values were statistically tested using one way ANOVA ($P < 0.0001$) and Tukey's Multiple Comparison Test. Different letters denote statistically significant differences ($p < 0.05$).

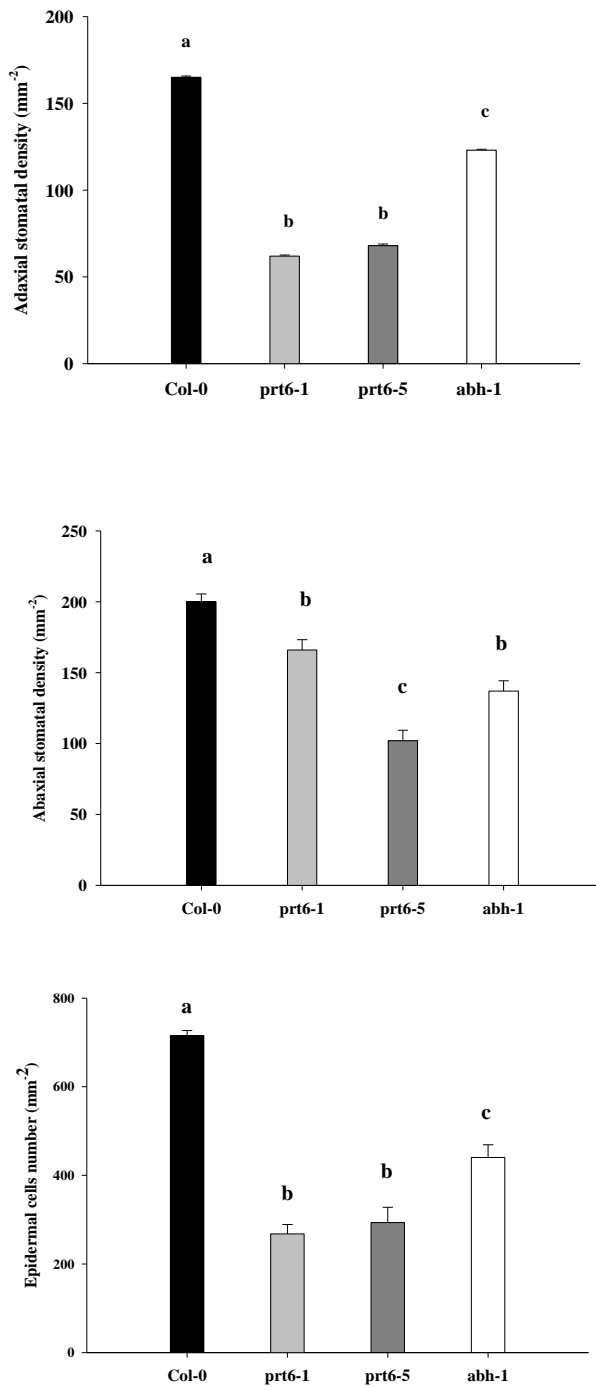


Figure 3-13 Stomatal and epidermal cell densities of Col-0, prt6-1, prt6-5 and abh-1 leaves

Adaxial and abaxial stomatal densities of *prt6-1*, *prt6-5* and wild type (Col-0) fully expanded leaves. Error bars represent the standard error. Stomatal and epidermal cell densities of 120 stomata for each genotype at each time point are shown. Values were statistically tested using one way ANOVA ($P < 0.0001$) and Tukey's Multiple Comparison Test. Different letters denote statistically significant differences ($p < 0.05$).

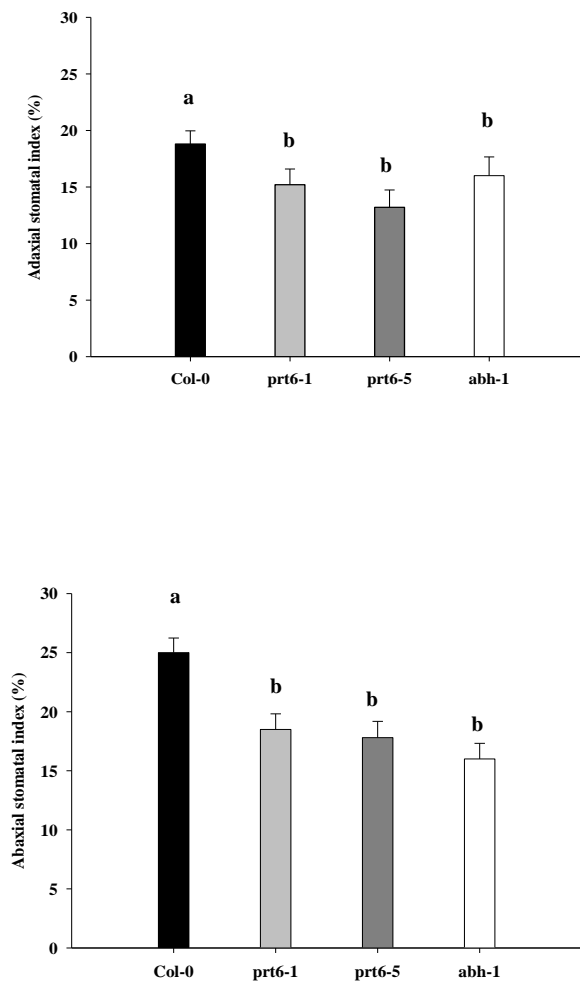
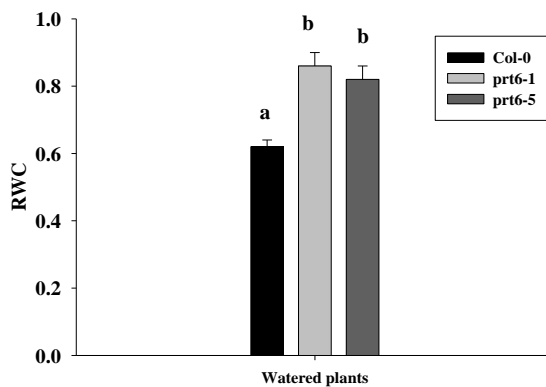


Figure 3-14 Stomatal indices of Col-0, prt6-1, prt6-5 and abh-1 leaves

Adaxial and abaxial stomatal indices of *prt6-1*, *prt6-5* and wild types (Col-0) of three areas of three fully expanded leaves of three plants. Error bars represent the standard error. Stomatal and epidermal cell densities of 120 stomata for each genotype at each time point are shown. Values were statistically tested using one way ANOVA ($P < 0.0001$) and Tukey's Multiple Comparison Test. Different letters denote statistically significant differences ($p < 0.05$).

A



B

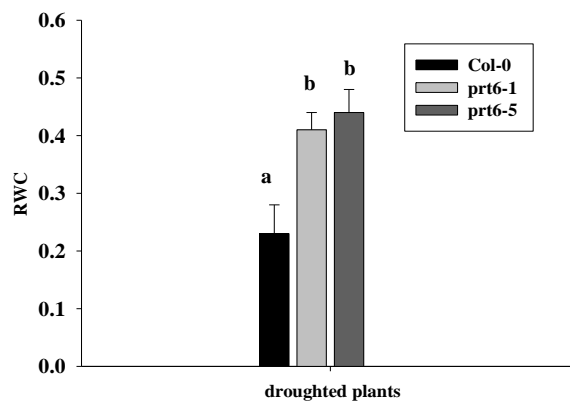
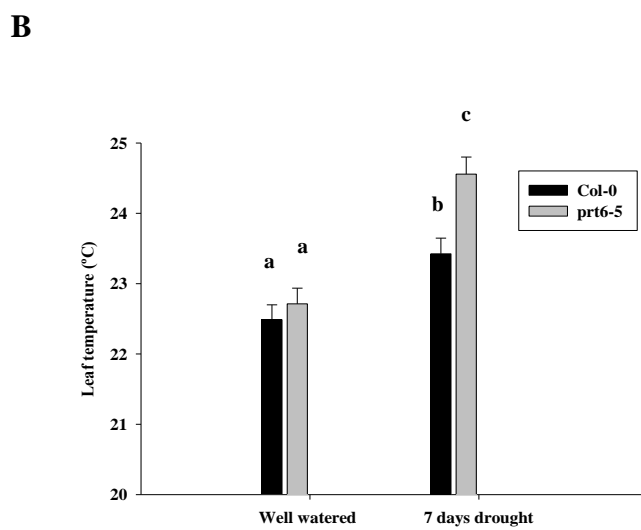
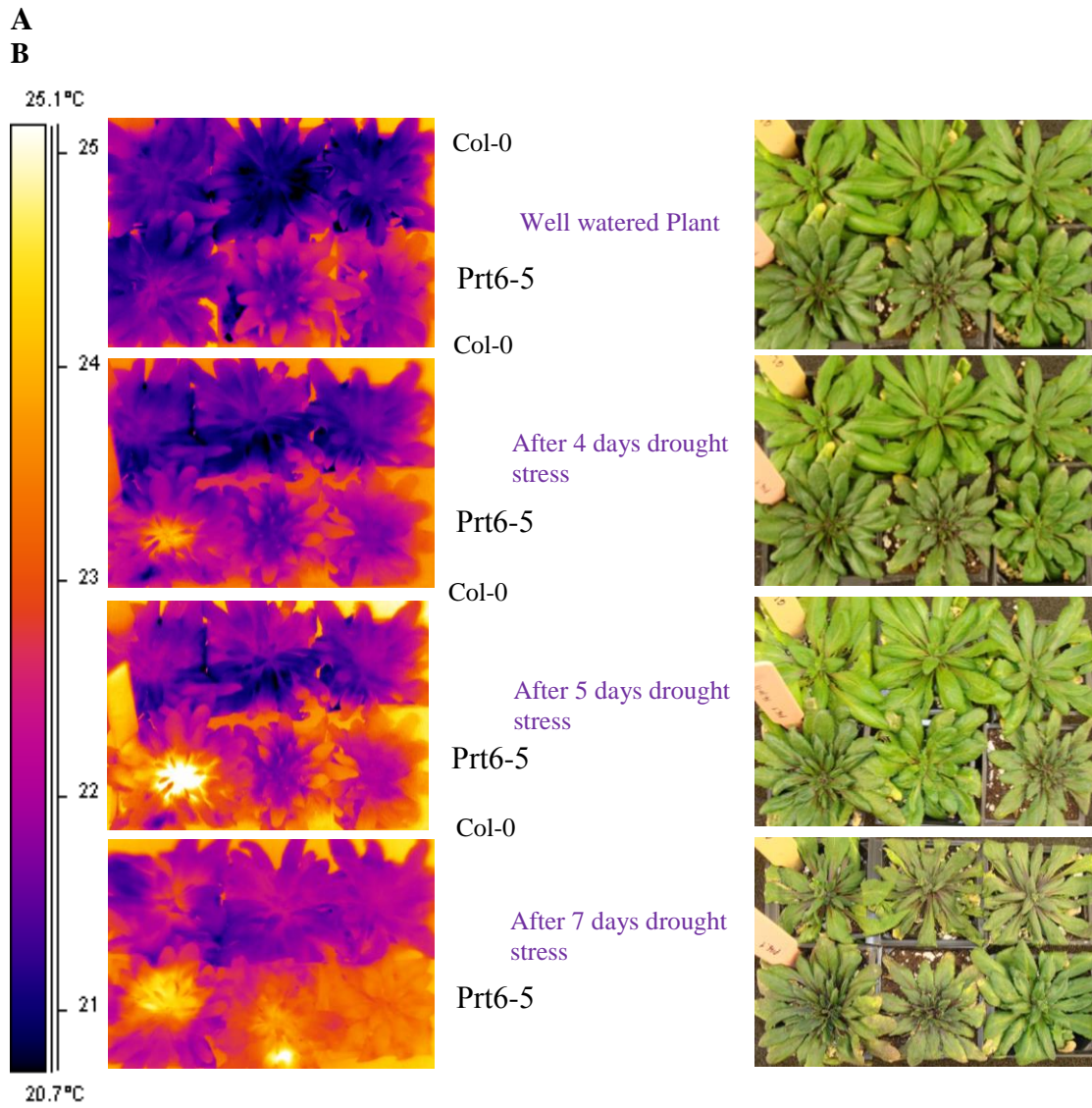


Figure 3-15 Measurements of leaf relative water content of control, prt6-1 and prt6-5

A) RWC under normal watering conditions for *prt6* mutants and control plants. B) RWC of *prt6* mutants and control plants after one week severe drought stress with no water supplied. The values are a mean of 4 measurements of 10 leaves from 10 plants. Values were statistically tested using one way ANOVA ($P < 0.0001$) and Tukey's Multiple Comparison Test. Different letters denote statistically significant differences ($p < 0.05$).

3.10 Thermal imaging of *prt6* leaf evapotranspiration

Infra thermal imaging was used to investigate whether the reduced stomatal density and enhanced stomatal closure of *prt6* plants as described above, would result in a reduction in evapotranspiration. A reduction in transpiration can cause an increase in leaf temperature (Lake and Woodward, 2008). Therefore, infrared thermal imaging is a powerful tool to estimate plant evapotranspiration. An experiment was set up with three wild type and three *prt6* plants and watering was withheld for a week (**Figure 3-16 A and B**) A Thermacam FLIR 660 camera was mounted vertically at approximately 40 cm above the leaf rosettes, and was connected to a colour screen for visualisation of plant temperatures. Subsequently, ThermaCAM Researcher 2.9 software was used for analysing the leaf temperature. The software supplies the function of measuring spot, line and area. In this study, a square area was drawn to measure the overall leaf temperature. The thermal images in (**Figure 3-16A**) suggest that *prt6* plants were hotter than controls throughout the experiment both when well-watered, and following 4, 5 or 7 days drought stress, suggesting a lower level of evapotranspiration. However, *prt6* plant temperatures were not significantly different to controls when the plants were well watered but they were over 1 °C hotter follow 7 days of drought (**Figure 3-16B**). These results are in line with the *prt6* stomatal ABA hypersensitivity shown in (**Figure 3-11 A**) and the *prt6* reduced stomatal density shown in (**Figure 3-13**). A second drought experiment was carried out where water was with-held for longer to investigate whether *prt6* plants are drought tolerant (**Figure 3-16 C**). After 10 days without water the plants were re-watered and imaged again after a further 2 days. On re-watering the *prt6* plant presumably was able to restore, its transpiration rate, to a level similar to pre-drought. In contrast, most of the wild-type plant leaves are dead and were unable to regain control of their temperature. The results of these experiments suggest that plants lacking PRT6 have decreased evapotranspiration when well-watered which is consistent with their reduced stomatal density. The further decrease in evapotranspiration that was observed on imposition of drought is consistent with the enhanced *prt6* stomatal sensitivity to the drought signal ABA. Together these differences in stomatal density and sensitivity give the *prt6* plants enhanced drought tolerance.



C

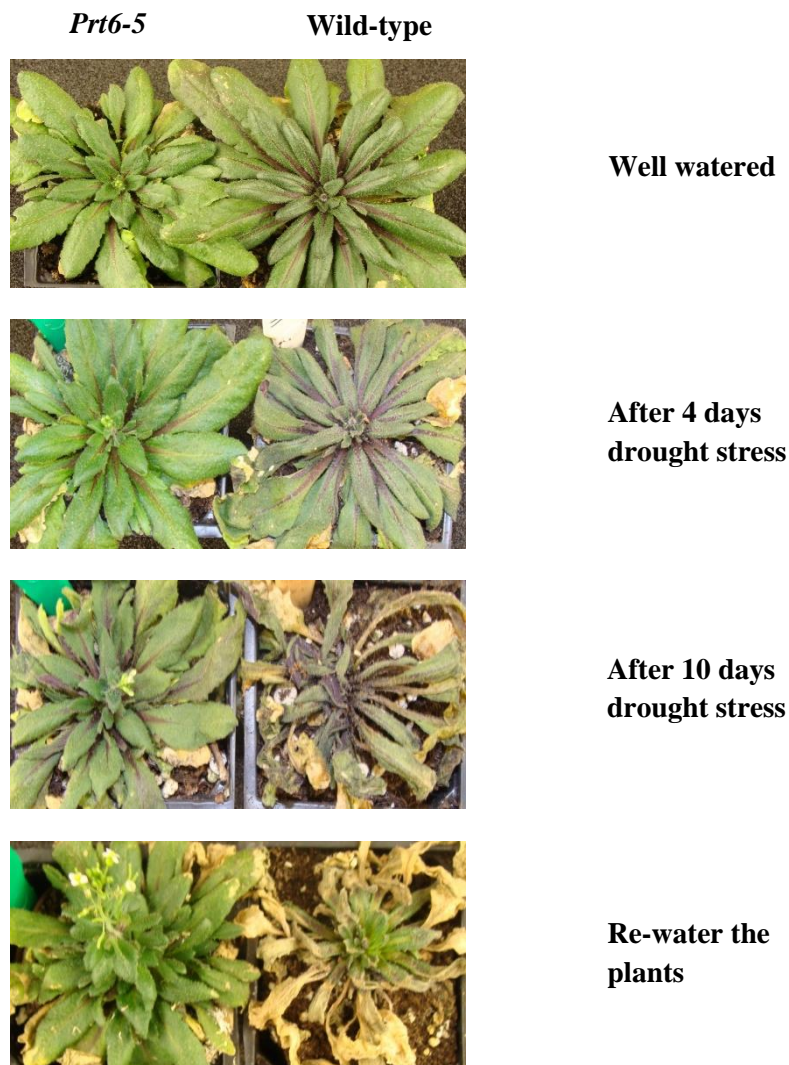


Figure 3-16 *prt6-5* mutants are defective in the regulation of transpiration during water stress

A) Infra-red thermographic image of droughted Col-0 and *prt6-5* plants. B) Leaf temperature measurement of *prt6-5* mutants and control plants. Four square areas were drawn to measure the overall each leaf temperature. False colour temperature scale: 20.7 to 25.1 °C. Error bars represent the standard errors. Values were statistically tested using one way ANOVA ($P < 0.0001$) and Tukey's Multiple Comparison Test. Different letters denote values that are statistical significance ($p < 0.05$). C) 6 weeks old plant, *prt6-5* (left hand) and wild-type (right hand) were subjected to drought for 10 days and plants were re-watered and imaged again after a further 2 days.

3.11 Nitric oxide is an endogenous signalling intermediate in ABA-induced stomatal closure

Recent evidence proposes the existence of crosstalk between NO and ABA signalling pathways during adaptive responses to plant biotic and abiotic stresses. NO has been shown to be significant during ABA-induced stomatal closure as observed in *Pisum sativum*, *Vicia faba* and *Arabidopsis* (Gonugunta *et al.*, 2008). Exogenous application of NO, supplied in the form of sodium nitroprusside (SNP), increases plant tolerance to drought stress by restricting stomatal apertures (Gonugunta *et al.*, 2008). The stomatal closure induced by SNP is believed to be similar to stomatal closure induced by ABA, based on both dose-response and timescale (Garcia-Mata and Lamattina, 2009).

3.11.1 *Prt6* stomatal aperture responses to NO

The results presented previously in this chapter show that PRT6 regulates the stomatal response to ABA. To investigate the role of NO in ABA-induced stomatal closing, we studied the effects of exogenous ABA and NO on *prt6* stomata in epidermal strip bioassays. NO is typically applied to plants through NO-releasing compounds such as SNP (sodium nitroprusside) or GSNO (S-nitrosoglutathione). Wild type and *prt6-5* epidermal strips were treated for 2.5 h with the NO donor SNP (100 μ M) in the presence or absence of ABA. Stomatal apertures were then measured. As expected from previously published results, SNP treatment of wild-type stomata resulted in significantly reduced stomatal apertures (**Figure 3-17**). The presence of 5 μ M ABA also led to a further reduction in stomatal aperture. In contrast, *prt6* stomata showed no response to NO alone but in the presence of ABA, stomatal closure was observed. Thus NO responses appear to be impaired in the absence of PRT6. To investigate whether endogenous NO was responsible for ABA-induced stomatal closure as a signalling intermediate, epidermal peels from wild type and *prt6-5* were incubated in 1 μ M ABA and endogenous NO was removed by the NO-scavenger c-PTIO (2-carboxy phenyl-4, 4, 5, 5-tetramethylimidazoline-1-oxyl-3-oxide). In published experiments the presence of 200 μ M cPTIO almost completely prevents ABA-induced stomatal closure (Neill *et al.*, 2003). Interestingly, co-incubation in 200 μ M c-PTIO demonstrated that *prt6* ABA inducible stomatal closure is not inhibited by cPTIO implying that *prt6* does not require NO as a secondary intermediate in ABA-inducible

stomatal closure. In contrast, NO stomatal closure was impaired in wild type stomata in response to 1 μ M ABA when c-PTIO was present (**Figure 3-18**).

3.11.2 ABA induces NO synthesis in *Arabidopsis* guard cells

3.11.2.1 Measurement of nitric oxide using DAF2-DA

The above experiments revealed that *prt6* stomata are insensitive to NO. In order to detect whether levels of NO synthesis are normal in *prt6* guard cells, *Arabidopsis* epidermal fragments were loaded with the NO-indicator dye DAF-2DA (diaminofluorescein diacetate), subsequently exposed to ABA and imaged using fluorescent microscopy. DAF-2DA is a dye that reacts particularly with NO and has been used to demonstrate NO generation in plant cells (Gonugunta *et al.*, 2008). In untreated wild-type *Arabidopsis* guard cells, little fluorescence was visible in the guard cells but the level of fluorescence in *prt6* was significantly higher than in WT guard cells. Fluorescence levels were almost 4x higher in the *prt6* guard cells. Exposure to 5 μ M ABA induced an increase in the fluorescence of guard cells of both *prt6* and WT after only 10 minutes (**Figure 3-19**). But again the level of fluorescence was much higher in the *prt6* guard cells. These results suggest that *prt6* stomata are not defective in their synthesis of NO, but their higher levels of NO are consistent with a defect in their response to NO as shown in (**Figure 3-19**).

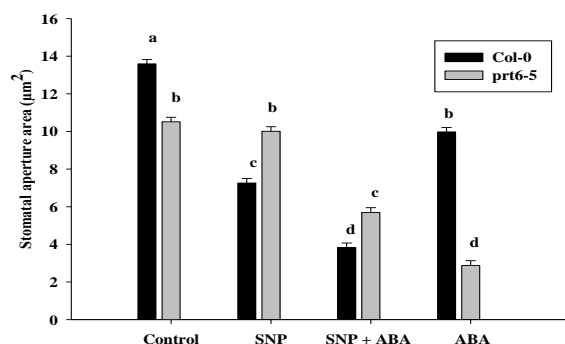


Figure 3-17 Effects of ABA and NO donor on stomatal closure of *prt6-5* and control plants

The effect of the NO donor sodium nitroprusside (SNP, 100 μ M) with or without ABA (5 μ M) on stomatal apertures in epidermal strips from *Arabidopsis*. Error bars represent the standard error. Mean apertures calculated from measurements of 120 stomata for each genotype at each time point are shown. Values were statistically tested using one way ANOVA ($P < 0.0001$) and Tukey's Multiple Comparison Test. Different letters denote values that are statistical significance ($p < 0.05$).

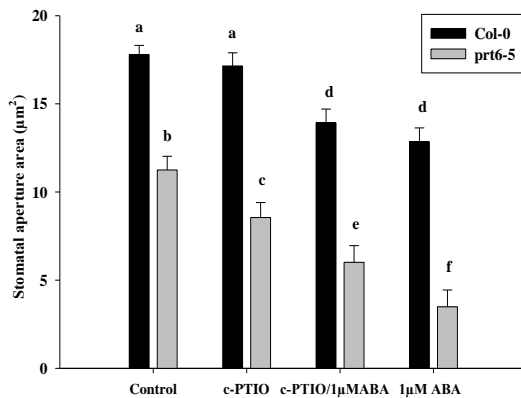
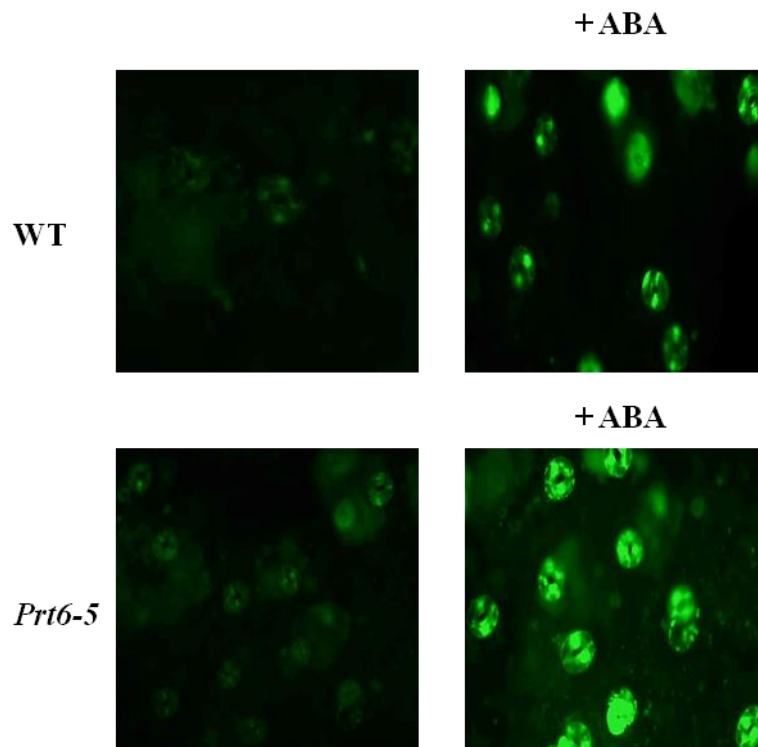


Figure 3-18 Effects of ABA and NO scavenger on stomatal closure of prt6 and control plants

NO scavenger 2-carboxy phenyl-4, 4, 5, 5-tetramethylimidazoline-1-oxyl-3-oxide (c-PTIO, 200 µM), with or without ABA (1 µM) on stomatal aperture in epidermal strips from *Arabidopsis*. Error bars represent the standard error. Mean apertures calculated from measurements of 120 stomata for each genotype at each time point are shown. Values were statistically tested using one way ANOVA ($P < 0.0001$) and Tukey's Multiple Comparison Test. Different letters denote statistically significant differences ($p < 0.05$).

A



B

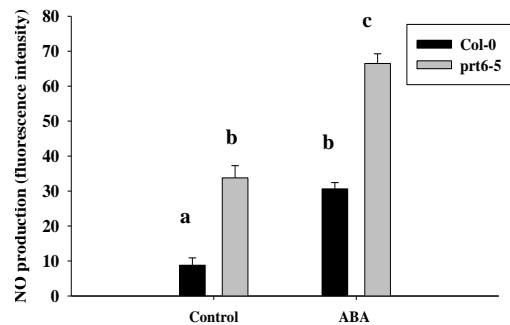


Figure 3-19 ABA induces NO synthesis in *Arabidopsis* guard cells.

A) Epidermal fragments were loaded in MES buffer with 10 μM DAF-2DA with or without ABA treatment then peels were examined with a fluorescence microscope a) *prt6* b) *prt6*+5 μM ABA c) WT d) WT+5 μM ABA. B) NO generation was observed by quantification of the level of DAF-2DA fluorescence of wild type and *prt6* mutant guard cells in the presence or absence of ABA. Fluorescent intensity calculated from measurements of 120 stomata for each genotype at each time point are shown. Values were statistically tested using one way ANOVA ($P < 0.0001$) and Tukey's Multiple Comparison Test. Different letters denote statistically significant differences ($p < 0.05$).

3.12 Genetic interactions of *PRT6* with ABA signal transduction components

Genetic cross-talk between the N-end rule pathway and ABA signalling has been demonstrated during seed germination. Holman *et al.* 2009 showed that two copies of the GCC box (GCCGCC) are present in the 5'UTR of the *ABI5* gene which encodes a transcription factor that enhances seed sensitivity to ABA. *ABI5* expression is believed to be controlled by substrates of the N-end rule pathway. The GCC box is the consensus binding sequence for the group VII ERFs which initiate with MC- at their N-terminal and these are substrates for the N-end rule pathway (Neill *et al.*, 2003). Remarkably, the GCC box motif is present in the 5'UTR of other ABA signalling genes including PP2Cs and the SnRK phosphorylated bZIP factors AREB2/ABF4, and other stress-related genes (Gibbs *et al.*, 2011). Thus, it is possible that these genes may also be regulated by group VII ERFs and the N-end rule pathway although this remains to be demonstrated. In the following experiments, the possibility of genetic interactions of the N-end rule pathway with stomatal ABA signalling components were investigated by using double mutants of ABA signal components such as *OST1* (OPEN STOMATA 1) and other SnRKs, and *ABI1* in combination with *PRT6* mutation. These homozygous double, and in one case triple, mutant lines were kindly provided by Dr D. Gibbs, University of Nottingham. Unfortunately, it was not possible to obtain all of the required mutants in exactly the same genetic background. However, the differences in stomatal ABA-responses resulting from the lack of *OST1* or the presence of constitutively active *ABI1* are extreme, and much greater than the slight differences that occur between background ecotypes. For each of the experiments the most appropriate control available was used (Col-2 for *ost1-4 prt6-4*, Col-0 for *Snrk2.2 Snrk2.3 prt6-1* and Ler for *abi1-1 prt6-4*. *OST1* (*SnRK2.6/SnRK2E*) encodes a protein kinase that is crucial for ABA-mediated stomatal closure (Yoshida *et al.*, 2010). *ost1-4* used in this study, originated from an M2 population of an EMS (ethyl methanesulphonate) mutagenized population (Xie *et al.*, 2006) and has stomata with a high degree of insensitivity to ABA. In epidermal strip bioassays *ost1-4 prt6-1* double mutant lines, showed stronger ABA-induced closure in response to 5 and 10 μ M ABA in comparison to the *ost1-4* single mutant stomata. Thus *PRT6* appears to be epistatic to *OST1* (**Figure 3-20**). Lack of *PRT6* was able to restore and possibly enhance ABA sensitivity in the absence of *OST1* activity, suggesting that *PRT6* may normally act downstream of *OST1* to regulate guard cell ABA sensitivity. SnRK2.2

and SnRK2.3 are closely related protein kinases to OST1 which are known to be involved in ABA-signalling responses during seed germination (Fujii *et al.*, 2007). The ABA-induced stomatal closure response in the double mutant, *snrk2.2snrk2.3* (**Figure 3-21**) was similar to wild type. This is unsurprising as *SnRK2.2* and *SnRK2.3* although close relatives of *OST1*, are not believed to play a significant role in stomatal closure. Stomata of the triple mutant, *snrk2.2 snrk2.3 prt6* were hypersensitive to ABA (showing a similar phenotype to the *prt6* single mutant) suggesting that they normally exert no effect on PRT6 activity in stomatal ABA responses. The ABI1 protein phosphatase acts upstream of OST1 in the ABA signalling pathway. The *abi1-1* mutation dominantly represses ABA signalling by constitutively activating the phosphatase. As expected *abi1-1* stomata were relatively insensitive to ABA in the stomatal ABA response (**Figure 3-22**). The stomatal apertures of double mutant *abi1-1 prt6-4* plants were significantly reduced in comparison to *abi1-1* plants under 10 μ M exogenous ABA treatment in epidermal bioassays, suggesting that lack of *PRT6* can restore ABA sensitivity to *abi1-1* mutants. Thus, *PRT6* appears to be epistatic to *ABI1*, as well as *OST1*. In summary, the above experiments indicate that the N-end rule pathway genetically interacts with at least two known components of stomatal ABA signalling; *OST1* and *ABI1*. It is possible that a substrate which is normally selected for degradation by the N-rule pathway is stabilised in *prt6* mutant plants. It appears likely that this presumed substrate (or substrates) induces ABA-signalling responses via a mechanism that does not require the activity of ABI1 or OST1.

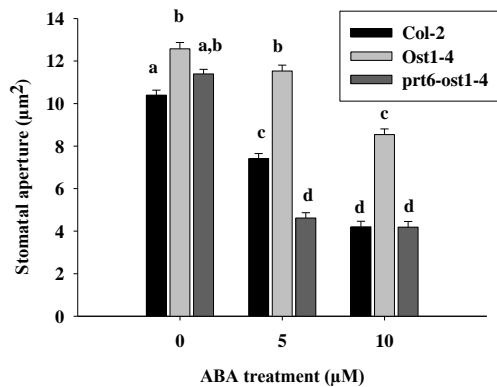


Figure 3-20 Stomatal ABA-responses of the ost1-4 mutant in combination with prt6-1

Comparison of stomatal responses to ABA in the wild type (Col-2), *ost1-4* and *prt6 ost1-4*. The values are a mean of 120 aperture measurements taken in three experiments. For each experiment, epidermal peels were taken from three different plants. Error bars represent the standard error. Values were statistically tested using one way ANOVA ($P < 0.0001$) and Tukey's Multiple Comparison Test. Different letters denote statistically significant differences ($p < 0.05$).

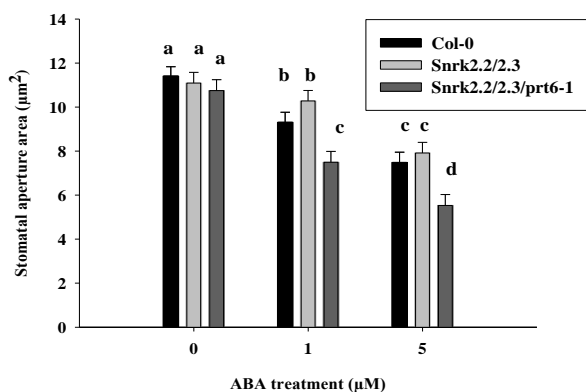


Figure 3-21 Stomatal ABA-responses of snrk2 mutants in combination with prt6-1

Comparison of stomatal responses to ABA in the wild type (Col-0), *snrk2.2snrk2.3* double mutant, and *snrk2.2 2.3prt6-1* triple mutant. The values are means of 120 aperture measurements taken over three experiments. For each experiment, epidermal peels were taken from three different plants. Error bars represent the standard error. Values were statistically tested using one way ANOVA ($P < 0.0001$) and Tukey's Multiple Comparison Test. Different letters denote statistically significant differences ($p < 0.05$).

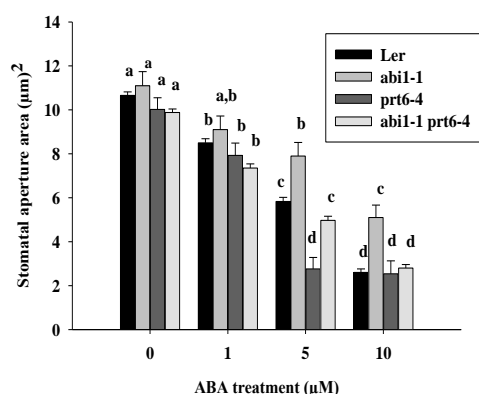


Figure 3-22 Stomatal ABA-responses of *abi1-1* mutant in combination with *prt6-4*

Comparison of stomatal responses to ABA in the *Landsberg erecta* background (L.er), *prt6-4*, *abi1-1* and *abi1-1 prt6-4*. The values are a mean of 120 aperture measurements taken in over three experiments. For each experiment, epidermal peels were taken from three different plants. Error bars represent the standard error. Values were statistically tested using one way ANOVA ($P < 0.0001$) and Tukey's Multiple Comparison Test. Different letters denote statistically significant differences ($p < 0.05$).

3.13 Conclusion

In summary the results presented in this chapter show that the gene encoding the plant N-recognin, *PRT6*, is expressed at a low level in most plant tissues. A *PRT6* promoter fusion experiment suggested that *PRT6* expression occurs in guard cells, and may be ABA-inducible in seedlings. Experiments with a series of mutant alleles lacking *PRT6* expression revealed that *prt6* stomata are hypersensitive to ABA-induced closure, that *prt6* plants have reduced stomatal density, and are drought tolerant. Plants lacking *PRT6* are able to synthesis NO but their stomata do not close in response to NO suggesting that *PRT6* is required for stomatal aperture responses to NO. Double mutant studies suggested that *PRT6* (and by implication the N-end rule pathway) genetically interacts with known guard cell ABA signalling components *OST1* and *ABII*, and that it may act downstream in the same signalling pathway. In conclusion *PRT6*, and perhaps the N-end rule pathway, is shown to be important in regulating stomatal ABA-responses, in addition to its previously described roles in germination and hypoxia.

4 Chapter 4-The N-end rule pathway of protein degradation regulates ABA-induced stomatal closure

The results presented in the Chapter 3 showed that plants lacking the N-degron PRT6, have ABA-hypersensitive stomata. This suggests that the N-end rule pathway may normally inactivate components of stomatal ABA signalling by selecting and directing them for protein degradation. As *prt6* stomata have an enhanced stomatal closure, it follows that PRT6 substrate(s) normally act to maintain stomatal opening, or prevent stomatal closure. In this chapter, the involvement of further components of the N-end rule pathway is investigated, and putative substrates for degradation by the pathway are explored.

4.1 The role of methionine aminopeptidases in the N-end rule pathway and stomatal ABA signalling

In living organisms, cellular proteins are synthesised with methionine (Met) as the first amino acid residue, occupying the N-terminal position of each nascent protein. This first Met is often removed from mature proteins (Giglione and Meinnel, 2001). Recently, components of the N-terminal methionine removal machinery have been identified in higher plants which are homologous to the bacterial system. Methionine aminopeptidases (MetAPs) are the enzymes responsible for removing amino-terminal Met. These enzymes form part of the N-end rule pathway as described in Chapter 1 (**Figure 1-6**) by acting on ‘tertiary destabilizing residues’ in proteins beginning with methionine cysteine sequences (MC-proteins), to target substrates into this protein degradation pathway (Gibbs *et al.*, 2011; Hu *et al.*, 2005). Out of the 13 destabilizing residues of the mammalian N-end rule pathway, only N-terminal cysteines can be produced by MetAP activity (Graciet *et al.*, 2010). After methionine cleavage, proteins with an N-terminal cysteine residue can be substrates for N-terminal arginylation to produce a ‘primary destabilising residue’ as described below (**Figure 4-1**). Unlike bacteria, which have only one type of MetAP activity (MAP1), eukaryotes possess a second enzymic activity, MAP2, which has the same substrate specificity as MAP1 (Kendall and Bradshaw, 1992). Thus two classes of MetAP enzymes have been described which are encoded by different gene families. In *Arabidopsis*, the two MetAP classes have similar enzymatic roles but their amino acid sequences vary significantly (Giglione and Meinnel, 2001; Giglione *et al.*, 2004). MAP1s are found in both the cytoplasm and the organelles of all higher organisms but

MAP2s are located only in the cytoplasm (Giglione *et al.*, 2004). The cytoplasmic MAP2s are the particular cellular targets of antitumor or immunosuppressive compounds including fumagillin, produced by the fungus *Aspergillus fumigates* (Ingber *et al.*, 1990; McCowen *et al.*, 1951). This natural compound covalently binds and inactivates MAP2s, and has no other physiological effects (Griffith *et al.*, 1997).

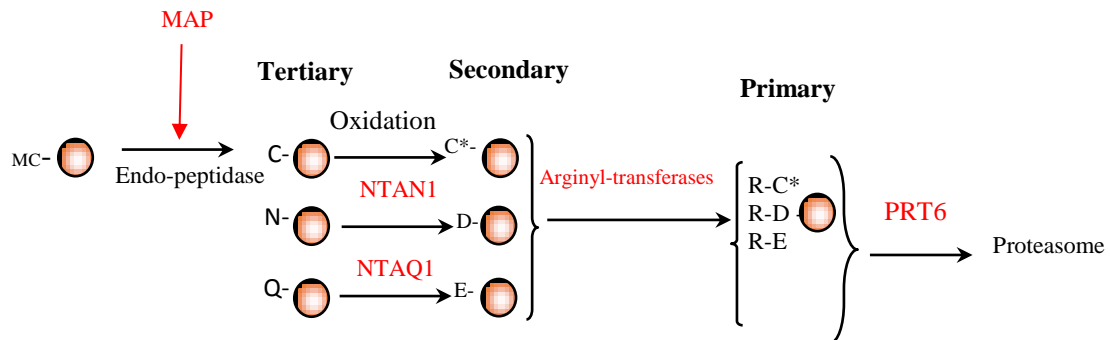


Figure 4-1 Simplified representation of Arginine branch of the N-end rule pathway associated with Cysteine oxidation of MC-substrate proteins (S).

Substrates are depicted as pink shapes with only their N-terminal amino acid residues shown in the single letter code; C- cysteine (C* indicates oxidised C), N- asparagine, Q- glutamine, D- aspartate, E- glutamate, and R- arginine. Enzymes are shown in red, MAP, methionine amino-peptidase; NTAN1 and NTAQ1 are two distinct Nt-amidasases, ATE, arginyl tRNA protein transferase); PRT6, the N-recognin proteolysis 6. Figure taken by Hu *et al.*, 2005.

4.2 Expression of methionine aminopeptidase genes in guard cells

The *Arabidopsis* genome contains one *MAP1* gene (*MAP1A*) and two *MAP2* genes (*MAP2A* and *MAP2B*). Existing transcriptomic data was used to examine expression patterns of the *Arabidopsis* *MAP1A*, *MAP2A* and *MAP2B* genes. The publically available transcriptomic data deposited in the eFP browser suggested that all these of genes are expressed throughout the plant including in guard cell protoplasts but their expression pattern does not change considerably with ABA treatment (**Figure 4-2**). In view of their relatively strong expression in guard cells, and their activity in the arginine branch of the N-end rule pathway (**Figure 4-1**) it was decided to further study the potential role of MetAPs in stomatal ABA-responses.

4.3 Stomatal aperture response of *map1a* to ABA

In *Arabidopsis*, MAP1 and MAP2 cytoplasmic MetAP enzyme activities appear to be redundant. An *Arabidopsis* T-DNA insertion mutant lacking MAP1A expression has been isolated but *map1a-1* plants have no detectable phenotype (Ross *et al.*, 2005). However, *map1a* plants are extremely sensitive to fumagillin. Treatment of the *map1a* mutant with fumagillin to remove MAP2 activity (from MAP2A and MAP2B) causes multiple phenotypes including dwarfism, and germination defects. In the current study, the *map1a-1* mutant and fumagillin were used in epidermal strip bioassays to investigate a potential role for MetAP activity in stomatal ABA-responses. Fumagillin alone did not induce wild-type stomatal closure (**Figure 4-3 A**). However, *map1a-1* stomata had significantly increased closure in response to 1 μ M and 5 μ M exogenous ABA, and stomata of *map1a-1* exposed to fumagillin showed even greater ABA hypersensitivity (in comparison to *map1a-1* stomata treated with ABA alone) (**Figure 4-3 A**). These results suggest that both classes of MetAPs, MAP1 and MAP2 are, like PRT6, involved in regulating stomatal ABA responses. To begin to investigate whether MetAPs might act in the same pathway as PRT6 an experiment was carried out to investigate *prt6-5* stomatal closure in the presence of fumagillin. *prt6-5* stomata remained ABA-hypersensitive in the presence of fumagillin (**Figure 4-3 B**). As there was no additive affect these results suggest that both PRT6 and MAP2s could act in the same pathway. However as MAP1 is still active in these stomata the results are not conclusive and how these components influence ABA stomatal aperture responses is not yet clear.

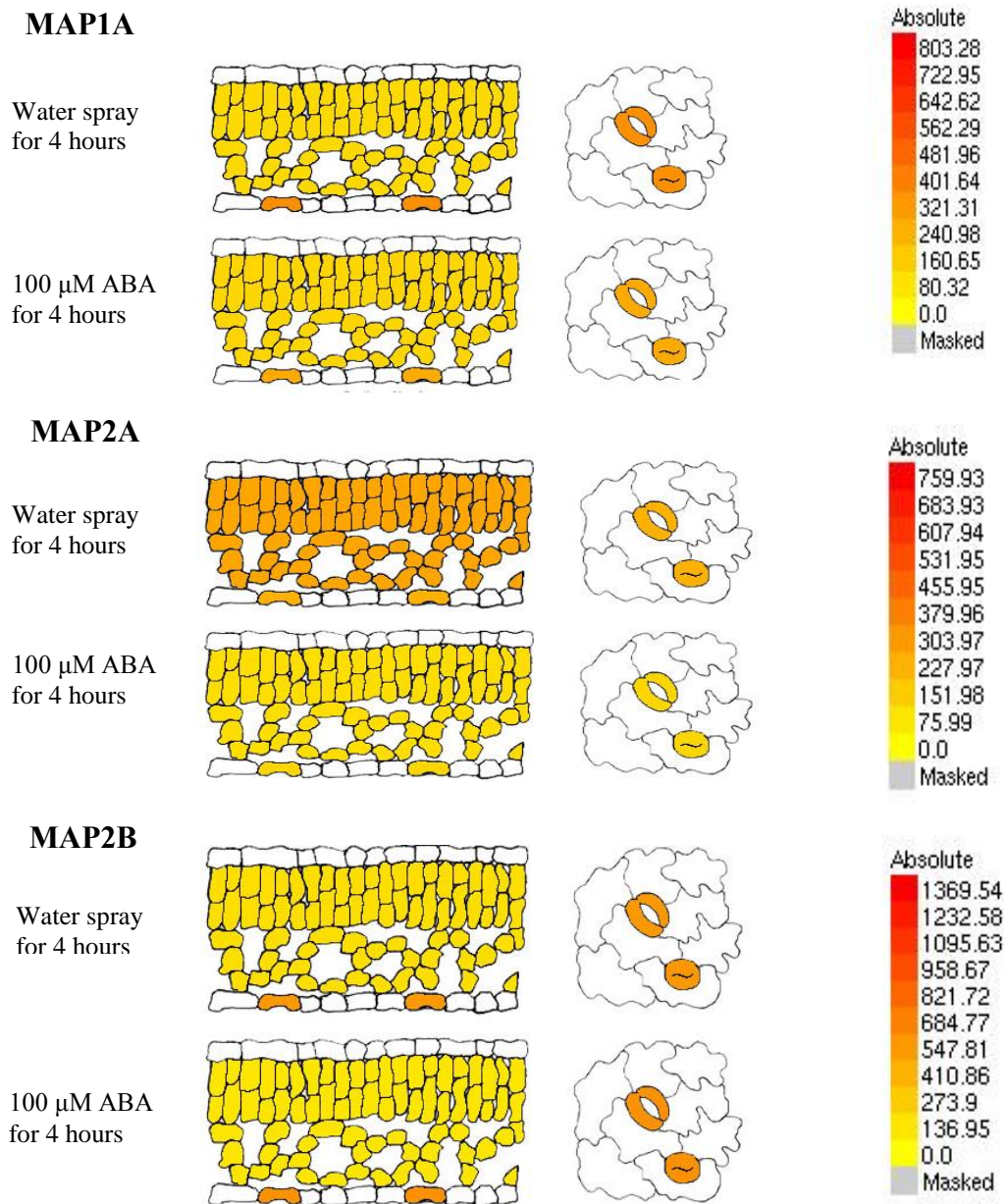
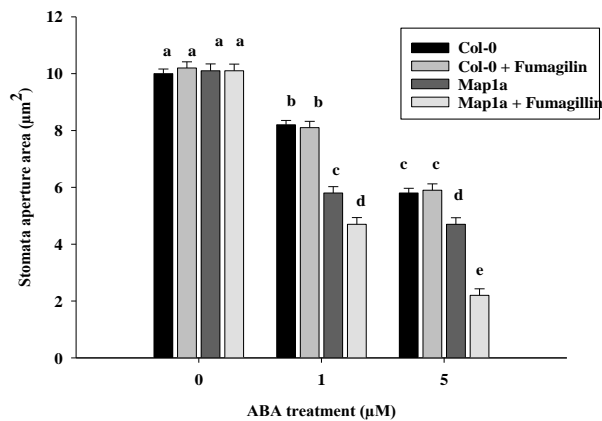


Figure 4-2 Expression patterns of *MAP1A*, *MAP2A* and *MAP2B* genes in guard and mesophyll cells from a transcriptomic analysis of protoplast extracts

Schematic illustration of the expression levels of the *MAP1A*, *MAP2A* and *MAP2B* genes in guard and mesophyll cell protoplasts before and after treatment with 100 μ M ABA. Darker colours represent relatively higher gene expression levels as shown in the scale bar to the right. Data was taken from the eFP-browser and is based on results from experiments carried out by (Winter *et al.*, 2007; Yang *et al.*, 2008).

A



B

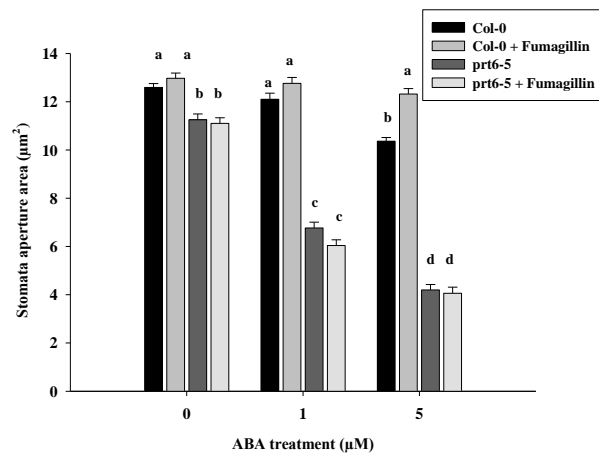


Figure 4-3 Stomatal aperture measurements taken from epidermal peels of *map1a*, *prt6-5* and control plants in response to ABA

A) Stomatal aperture response of *map1a* and control plants to fumagillin and/or ABA (1 µM and 5 µM). B). Stomatal aperture response of *prt6-5* and control plants to fumagillin and/or ABA (1 µM and 5 µM). The values are a mean of 120 aperture measurements taken in over three experiments. Error bars represent the standard error. Values were statistically tested using one way ANOVA ($P < 0.0001$) and Tukey's Multiple Comparison Test. Different letters denote statistically significant differences ($p < 0.05$).

4.4 *Arabidopsis* NTAN and NTAQ amidases

The plant N-end rule pathway has a hierarchical structure similar to the N-end rule pathway organization in fungi and mammals (Hu *et al.*, 2005, Varshavsky, 2011, Varshavsky and Byrd, 1996, Wang *et al.*, 2009). Protein substrates starting with N-terminal asparagine or glutamine, tertiary destabilizing residues can be deamidated into secondary destabilising residues aspartate or glutamate, which are in turn

substrates for an arginyl-transferase which adds the primary destabilising residue arginine to their N-terminus (**Figure 4-1**). Nt^N-amidases (NTANs) and Nt^Q-amidases (NTAQs) are involved in the deamidation of N-terminal asparagine or glutamine, respectively (Graciet *et al.*, 2010). Nt^N-amidase, was originally characterized by (Grigoryev *et al.*, 1996) in mouse tissues, which could not deamidate N-terminal asparagine Kwon *et al.* 2000 and Wang *et al.* 2009 identified activity of Nt^Q-amidase, again in mouse tissues. The sequence of NTAQ1 is extremely conserved among mammals, plants and some fungi but is different from sequences of other amidases including the N-terminal amidase NTAN1 (Wang *et al.*, 2009). Graciet *et al.* 2010 isolated *Arabidopsis* cDNAs encoding putative Nt^N and Nt^Q amidases, and showed that their expression could restore activity of the N-end rule using a Asn-βGal and/or Gln-βGal reporter in a yeast *ntan1* mutant (Kwon *et al.*, 2000). Expression of the putative Nt^N-amidase resulted in degradation of the Asn-βGal, but not Gln-βGal, indicating that this enzyme is specific for substrates with N-terminal asparagine tertiary destabilizing residues, whereas expression of the putative Nt^Q amidase led to degradation of the Gln-βGal reporter, but not of Asn-βGal. These results confirmed that At2g44420 and At2g41760 encode *Arabidopsis* Nt^N and Nt^Q amidases (Graciet *et al.*, 2010). It is believed likely that Nt^N and Nt^Q amidases target plant proteins for degradation by the N-end rule pathway and facilitate the desensitization of plant tissues to ABA (Holman *et al.*, 2009). The experiments presented below were aimed at investigating whether these enzymes could be involved in regulating stomatal ABA-responses.

4.4.1 The expression of *NTAN* and *NTAQ* genes in guard cells

NTAN1 and *NTAQ1* expression patterns were investigated using the transcriptomic data available from the *Arabidopsis* eFP browser. *NTAN1* was expressed in all tissues, including guard cell and mesophyll cell protoplasts, both before and after treatment with 100μM ABA (**Figure 4-4**) However, *NTAQ1* appeared to be expressed at very low level guard cell protoplasts.

4.4.2 The role of *NTAN1* and *NTAQ1* in stomatal ABA-responses.

ntan1-1 is a tilling line of *NTAN1*, and *ntaq1-1*, *ntaq1-2* are T-DNA insertion mutants of *NTAQ1*. These unpublished mutant lines were obtained from Dr. Gibbs at the University of Nottingham and used to study stomatal ABA-signalling. To analyze stomatal responses to ABA, epidermal peels of *ntan1-1* and the Col-Big Mama (or

BM) wild-type background, were exposed to different concentrations of ABA. Similar, experiments were carried out for *ntaq1-1* and *ntaq1-2* alongside their Col-0 background. The stomata of *ntan1-1*, *ntaq1-1* and *ntaq1-2* all showed significantly hypersensitive responses to ABA in comparison to their wild type controls (**Figure 4-5**). These results indicate that Nt^N-amidation and Nt^Q-amidation of N-terminal asparagine or glutamine could be involved in regulation of ABA-induced stomatal closure. Thus, in combination with the results presented in the above sections, it appears that several activities of the arginine branch of the N-end rule pathway that prepares substrates with N-terminal asparagine, glutamine or cysteine tertiary destabilizing residues for degradation maybe involved in the stomatal ABA-response. It also suggests that the degradation of more than one substrate normally occurs to desensitize stomata to ABA-induced closure responses.

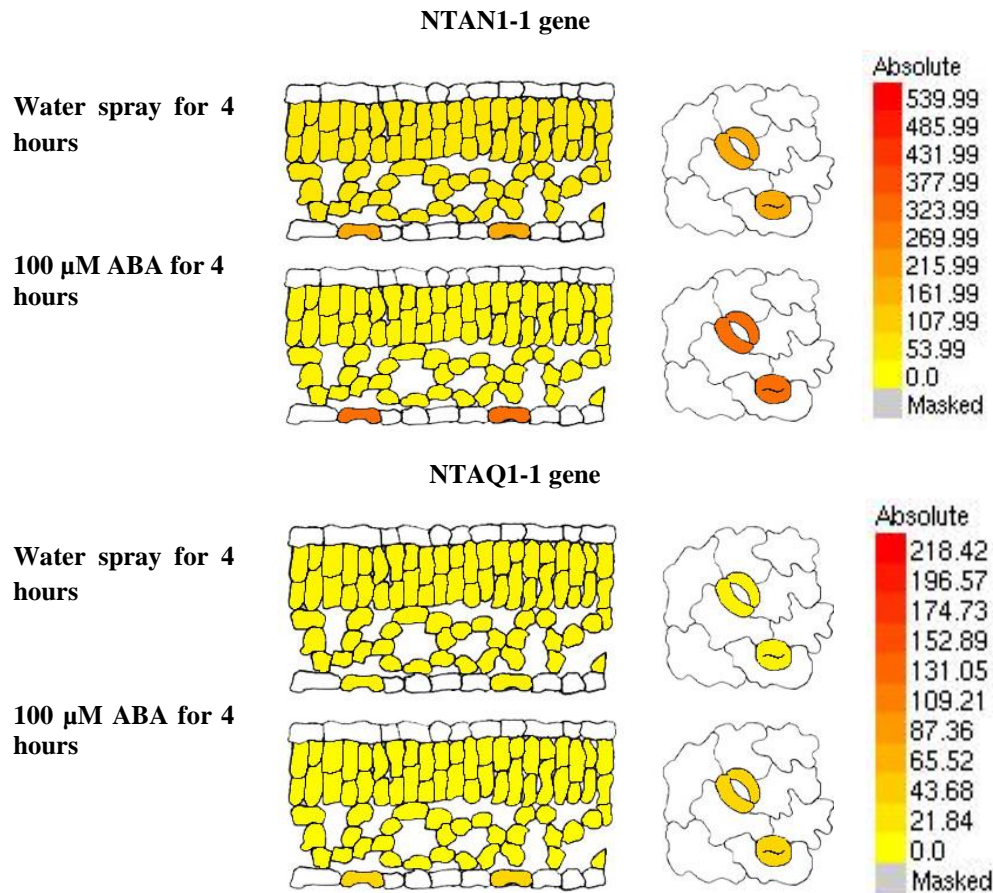
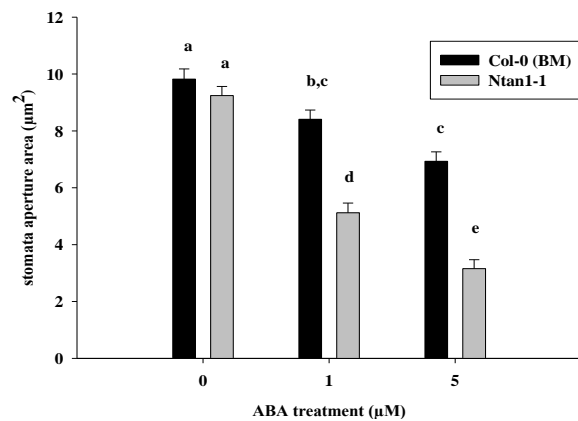


Figure 4-4 Expression patterns of the *NTAN1* and *NTAQ1* genes in mesophyll and guard cells from a transcriptomic analysis of protoplast extracts

Schematic illustration of the expression levels of the *NTAN1* and *NTAQ1* genes in the guard and mesophyll cell protoplasts before and after treatment with 100 μ M ABA. Darker colours represents relatively for higher gene expression levels as demonstrated in the scale bar to the right. Data was taken from the eFP-browser and is based on results from experiments carried out by (Winter *et al.*, 2007; Yang *et al.*, 2008).

A



B

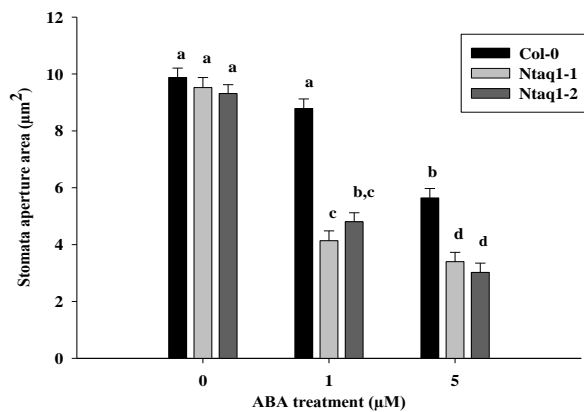


Figure 4-5 Stomatal aperture measurements taken from epidermal peels of *ntan1-1*, *ntaq1-1*, *ntaq1-2* and control plants in response to ABA.

A) Stomatal aperture response of *ntan1-1* and control plants to ABA (1µM and 5µM). B) Stomatal aperture response of *ntaq1-1* *ntaq1-2* and control plants to ABA (1µM and 5µM). For each experiment, epidermal peels were taken from three different plants. The values are a mean of 120 aperture measurements taken in over three experiments. Error bars represent the standard error. Values were statistically tested using one way ANOVA ($P < 0.0001$) and Tukey's Multiple Comparison Test. Different letters denote statistically significant differences ($p < 0.05$).

4.5 N-terminal arginylation in the N-end rule pathway

Primary destabilizing N-terminal residues can be generated via specific proteolytic cleavage, or created through chemical modifications or successive enzymatic additions to the N terminus. The most common primary destabilising residue in eukaryotes is arginine, which is often added to secondary destabilising residues by the activity of an arginyl transferase enzyme (**Figure 4-1**). The *Arabidopsis* genome contains two Arg-tRNA-protein transferase genes, *ATE1* and *ATE2* encoding enzymes which catalyse the conjugation of the carboxyl group of Arg to the α -amino group of a polypeptide N-terminal residue (Varshavsky, 2011) The *Arabidopsis ATE1* gene is disrupted in the null mutant *delayed leaf senescence1 (dls1)* in which leaf senescence is abnormally slow (Yoshida *et al.*, 2002). Yoshida *et al.* 2002 suggested that *ATE2* a putative arginyl transferase which has 58% the amino acid sequence similarity to *ATE1*, including all the conserved cysteine residues, may also have arginyl transferase activity. Recent studies employing double mutant plants, lacking *ATE1* and *ATE2*, indicated that this branch of the N-end rule pathway has several functions, including controlling different aspects of leaf and shoot development and removal of ABA sensitivity in seed germination (Graciet *et al.*, 2009; Holman *et al.*, 2009). Several of these arginyl transferase functions require the activity of PRT6, suggesting that this N-recognin acts downstream of arginyl transferases in the plant N-end rule pathway (Garzon *et al.*, 2007; Graciet *et al.*, 2009; Holman *et al.*, 2009). In the present study, the stomatal ABA-responses of the *Arabidopsis* double mutant lacking both arginyl transferases *ATE1* and *ATE2* were studied.

4.5.1 The expression of arginyl transferases genes in guard cells

The expression pattern of the closely related *ATE1* and *ATE2* genes were investigated. Data obtained from the eFP browser suggested that both were expressed in mesophyll and guard protoplasts and their expression pattern did not change before and after treatment with 100 μ M ABA (**Figure 4-6**). Generally, both genes appeared to be expressed at low levels in all tissues.

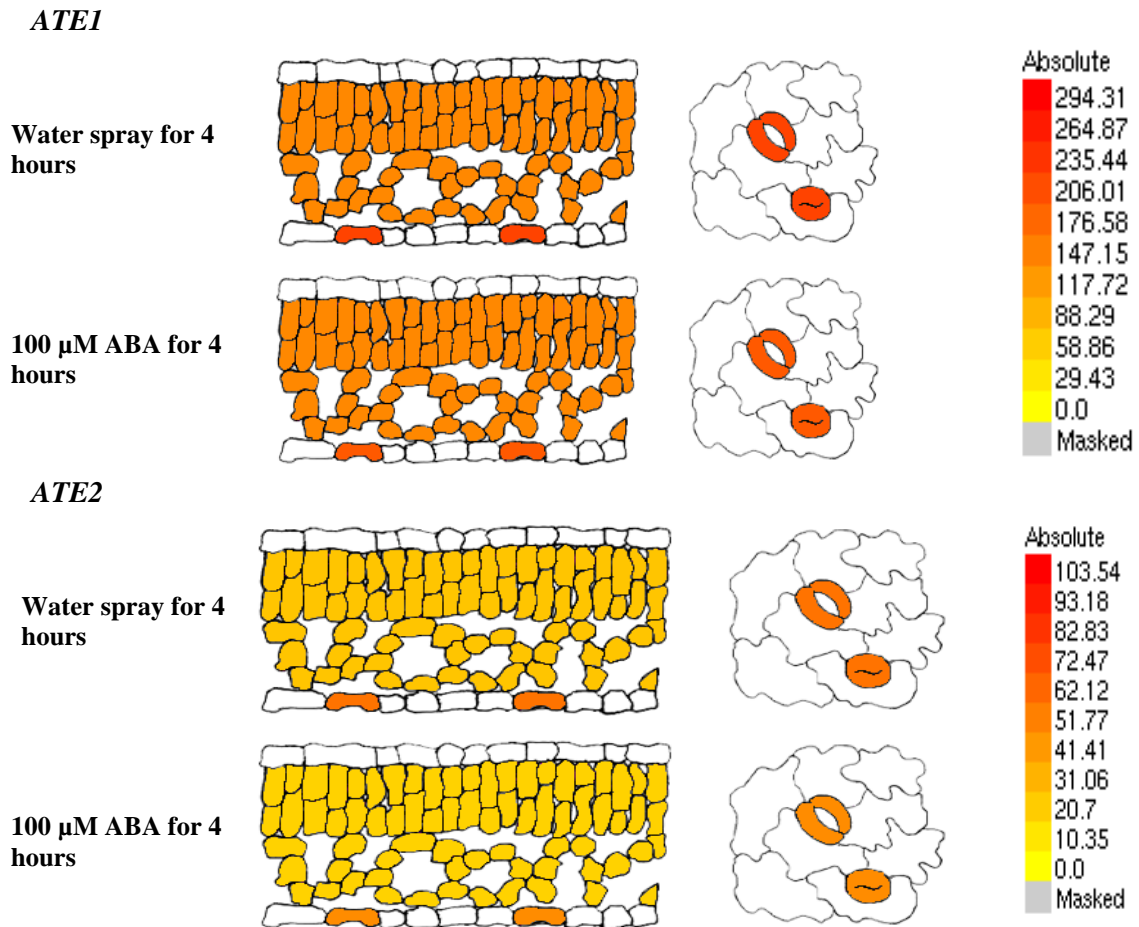


Figure 4-6 Expression patterns of the *ATE1* and *ATE2* genes in mesophyll and guard cells from a transcriptomic analysis of protoplast extracts

Schematic illustration of the expression levels of *ATE1* and *ATE2* genes in mesophyll and guard cell protoplasts before and after treatment with 100 μ M ABA. Darker colour represents relatively for higher gene expression levels as demonstrated in the scale bar to the right. Data was taken from the eFP-browser and is based on results from experiments carried out by (Yang *et al.*, 2008).

4.5.2 Role of arginyl transferases in stomatal ABA-signalling

Arabidopsis *ATE1* and *ATE2* have been shown to be involved in promoting seed germination and establishment through the removal of sensitivity to ABA (Holman *et al.*, 2009; Yoshida *et al.*, 2002). In the present study, the stomatal ABA-responses of the double mutant lacking arginyl transferase were examined. Epidermal peel bioassays showed that *ate1-2 ate2-1* stomata were hypersensitive to 1 μ M and 5 μ M exogenous ABA, which is consistent with the results for other N-end rule pathway mutants presented above. However the stomatal response assays shown in (**Figure 4-7**) suggest that *ate1-2 ate2-1* stomata are not as hypersensitive to ABA as *prt6* stomata. This result indicates that not all of the substrates for PRT6 involved in this ABA response are also substrates for arginyl transferases. Thus, again, the stomatal

responses of the *Arabidopsis* N-rule pathway mutants analysed in this chapter suggest that more than one protein is normally degraded by this pathway in order to reduce stomatal ABA-sensitivity. It appears that at least one substrate has an N-terminal Arg residue added by an arginyl transferase, and at least one substrate does not.

4.5.3 Analysis of stomatal numbers

Stomatal and epidermal cell density measurements were performed on fully expanded leaves. *ate1-2 ate2-1* mutant plants had significantly lower stomatal densities than control plants (**Figure 4-8**). Stomatal indices were also significantly reduced in *ate1-2 ate2-1* in comparison to Col-0 (**Figure 4-9**) but here there was no significant difference between the mutant phenotypes. These results are similar to those shown for *prt6* mutants in chapter 3, suggesting that both ATE and PRT6 activities are involved, either directly or indirectly in the control of stomatal development.

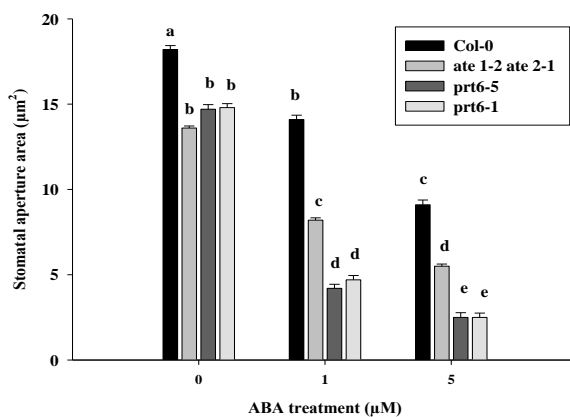


Figure 4-7 Stomatal aperture measurements taken from epidermal peels of *ate1-2ate2-1*, *prt6-5*, *prt6-1* and control plants in response to ABA

For each experiment, epidermal peels were taken from three different plants. The values are a mean of 120 aperture measurements taken in over three experiments. Error bars represent the standard error. Values were statistically tested using one way ANOVA ($P < 0.0001$) and Tukey's Multiple Comparison Test. Different letters denote statistically significant differences ($p < 0.05$).

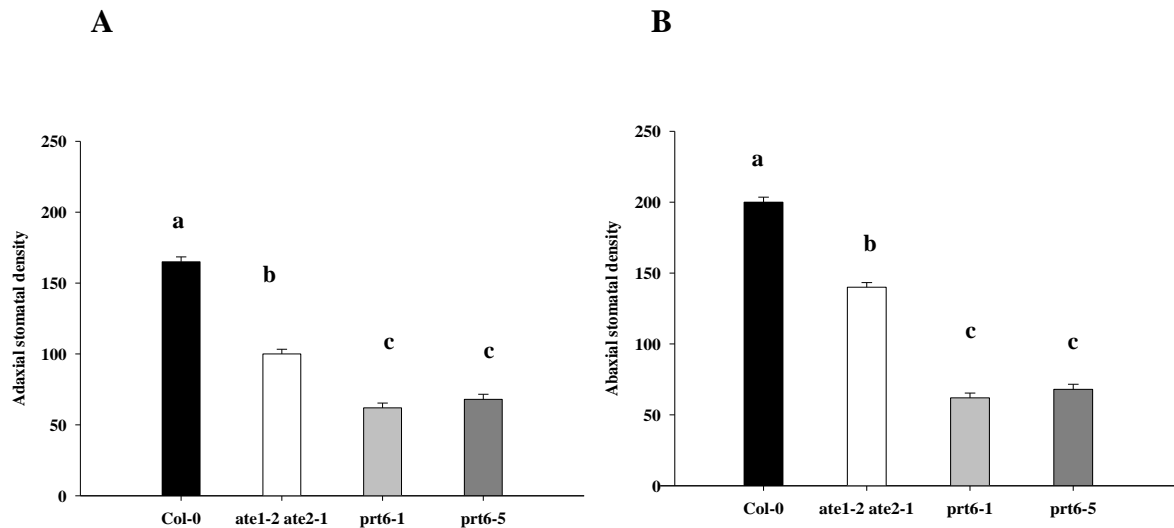


Figure 4-8 Analysis of stomatal density in Col-0, *ate1-2ate2-1*, *prt6-1* and *prt6-5*

A) Adaxial stomatal density B) Abaxial stomatal density of *ate1-2ate2-1*, *prt6-1*, *prt6-5* and wild types (Col-0). Three areas of three leaves of three plants were sampled and the mean density calculated. Error bars represent the standard error. Stomatal and epidermal cell densities of 120 stomata for each genotype at each time point are shown. Values were statistically tested using one way ANOVA ($P < 0.0001$) and Tukey's Multiple Comparison Test. Different letters denote statistically significant differences ($p < 0.05$).

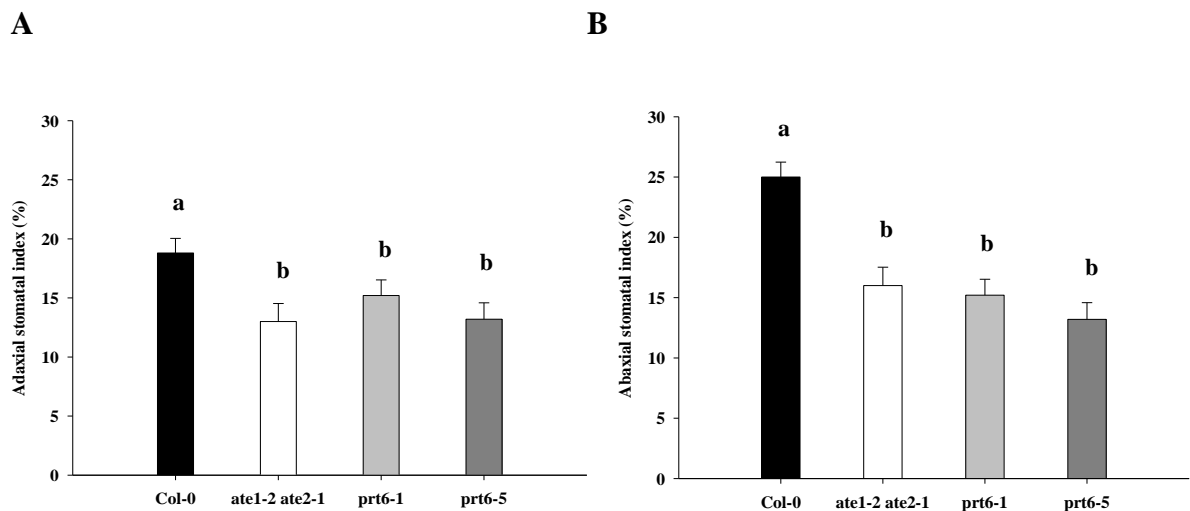


Figure 4-9 Analysis of stomatal indices in Col-0, *ate1-2ate2-1*, *prt6-1* and *prt6-5*

A) Adaxial stomatal indices B) Abaxial stomatal indices of *ate1-2ate2-1*, *prt6-1*, *prt6-5* and wild types (Col-0) of three areas of three leaves of three plants. Error bars represent the standard error. Stomatal and epidermal cell densities of 120 stomata for each genotype at each time point are shown. Values were statistically tested using one way ANOVA ($P < 0.0001$) and Tukey's Multiple Comparison Test. Different letters denote statistically significant differences ($p < 0.05$).

4.6 Putative substrates of the N-End Rule Pathway

Results presented, in both Chapters 3 and above in Chapter 4, indicate that several components of the N-end rule pathway of protein degradation are involved in removing stomatal ABA-sensitivity. The results are consistent with several guard cell proteins normally being targeted for degradation by this pathway. However the proteins that are degraded are unknown for stomatal ABA responses. The experiments presented in the remainder of Chapter 4 were aimed at examining putative protein substrates. The experiment shown in **(Figure 4-3)** indicated that removal of MetAP activity confers stomatal ABA hypersensitivity. Because of the substrate specificity of these enzymes, this indicates that at least one of the protein(s) that confer ABA hypersensitivity must have methionine and cysteine residues at the N-terminus. As MetAPs do not act on proteins initiating with MN or MQ N-terminal sequences, the only remaining N-terminal sequence they could cleave to produce a substrate for the arginine branch of the N-end rule pathway is MC **(Figure 4-1)**. Proteins that initiate with MC appear to be under-represented in nature, and the *Arabidopsis* genome sequence only encodes 247 such proteins. The major group of 'MC-proteins' in plant genomes are the MC-ERFs, a subgroup of the AP2 or Ethylene Response Factor family of transcription factors. It has been shown that the MC-ERFs regulate ABA-responses in seed and that other ERF transcription factors affect drought stress responses. It is also known that the group VII Ethylene Response Factors (which are MC-ERFs) are commonly engaged in enhancing *Arabidopsis* stress responses, through GCC-box elements (Ohmetakagi and Shinshi, 1995). Recently, the MC-ERFs, HYPOXIA RESPONSIVE 1 & 2 (HRE1 and HRE2), and RELATED TO AP2 2 (RAP2.2) have been shown to improve plant responses during hypoxia or anoxia, a process which is regulated by the N-end rule pathway (Bailey-Serres *et al.*, 2012; Gibbs *et al.*, 2011; Hinz *et al.*, 2010). These MC-ERFs show homology to the agronomically significant rice ERFs SUBMERGENCE 1A, B and C (Xu *et al.*, 2006) and SNORKEL 1 and 2 (Hattori *et al.*, 2009). The SUBMERGENCE 1 (SUB1) locus contains SUB1A-1 which is a main determinant of survival of rice plants under entire submergence (Xu *et al.*, 2006). With the exemption of SUB1C, all SUB1 proteins initiate with MC- (Gibbs *et al.*, 2011). The main focus of the following experiments was to find out whether the MC-ERFs could be involved in stomatal ABA-responses **(Figure 4-11)**. There are five group VII ERFs (HRE1, HRE2, RAP2.12, RAP2.2 and EBP) and one other *ERF* (*ABR1*) that initiate with MC-. *HRE1* and 2 are induced on

hypoxia whereas the two MC-ERFs RAP2.12 and RAP2.2 are constitutively expressed. The expression pattern of four group VII ERFs genes *HRE1*, *HRE2*, *RAP2.12* and *RAP2.2* were investigated. Data obtained from the eFP browser suggested that these genes were expressed in mesophyll and guard protoplasts and their expression pattern did not change before and after treatment with 100 μM ABA (**Figure 4-10**). The *RAP2.12* gene is highly expressed in guard cell protoplasts but had low expression levels in mesophyll protoplasts. From the above analysis of N-end rule pathway mutants (*prt6*, *map1*, or *ate1 ate2*) it was predicted that protein substrate(s) which are stabilised when their degradation pathway is disrupted, confer ABA hypersensitivity. Thus it is expected that plants lacking the predicted substrate(s) would be less sensitive to ABA. However, because more than one substrate is predicted from the above results it is unlikely that a phenotype would be apparent in a single knock-out mutant. It was also expected that these experiments could be complicated by problems with redundancy.

4.7 The role of MC-ERFs in stomatal ABA-responses

Several MC-ERF mutants were kindly provided by Dr Gibbs (Nottingham) and these were examined in preliminary experiments to investigate whether MC-ERFs might be involved in stomatal ABA responses. RAP2.2 is involved in plant responses to hypoxia, and its degradation is known to be regulated by the N-end rule pathway (Gibbs *et al.*, 2011; Hinz *et al.*, 2010). RAP2.12 is highly homologous to RAP2.2. The stomatal ABA responses of T-DNA insertion mutants *rap2.12-1* and *rap2.2* were studied. Unexpectedly, the stomata of both mutants showed significant hypersensitivity to 1 and 5 μM ABA concentration. The two hypoxia associated MC-ERFs were also studied. Surprisingly, the stomata of *hre1 hre2* double mutants, which lack HRE activity (Gibbs *et al.*, 2011), also showed significantly greater stomatal closure responses in 5 μM ABA (but not in response to 1 μM ABA). Although the results from these experiments with plants lacking one or two of the MC-ERFs suggest that these transcription factors could be involved in regulating stomatal ABA responses, they are difficult to interpret in the light of our knowledge of the function of the N-end rule pathway. Previous results with mutants defective in the N-end rule pathway (**Figure 4-7**) indicated that enhanced stability of substrates should promote rather than remove ABA hypersensitivity. Thus the substrates for the N-end rule pathway that experiments in Chapter 3 suggested could enhance plant water use

efficiency and drought tolerance were not identified by these experiments. Further experiments are required to determine whether a different MC-ERF, or combinations of MC-ERFs may be responsible for stomatal ABA-hypersensitivity. Alternatively, other unstudied MC-proteins may be responsible for this phenotype.

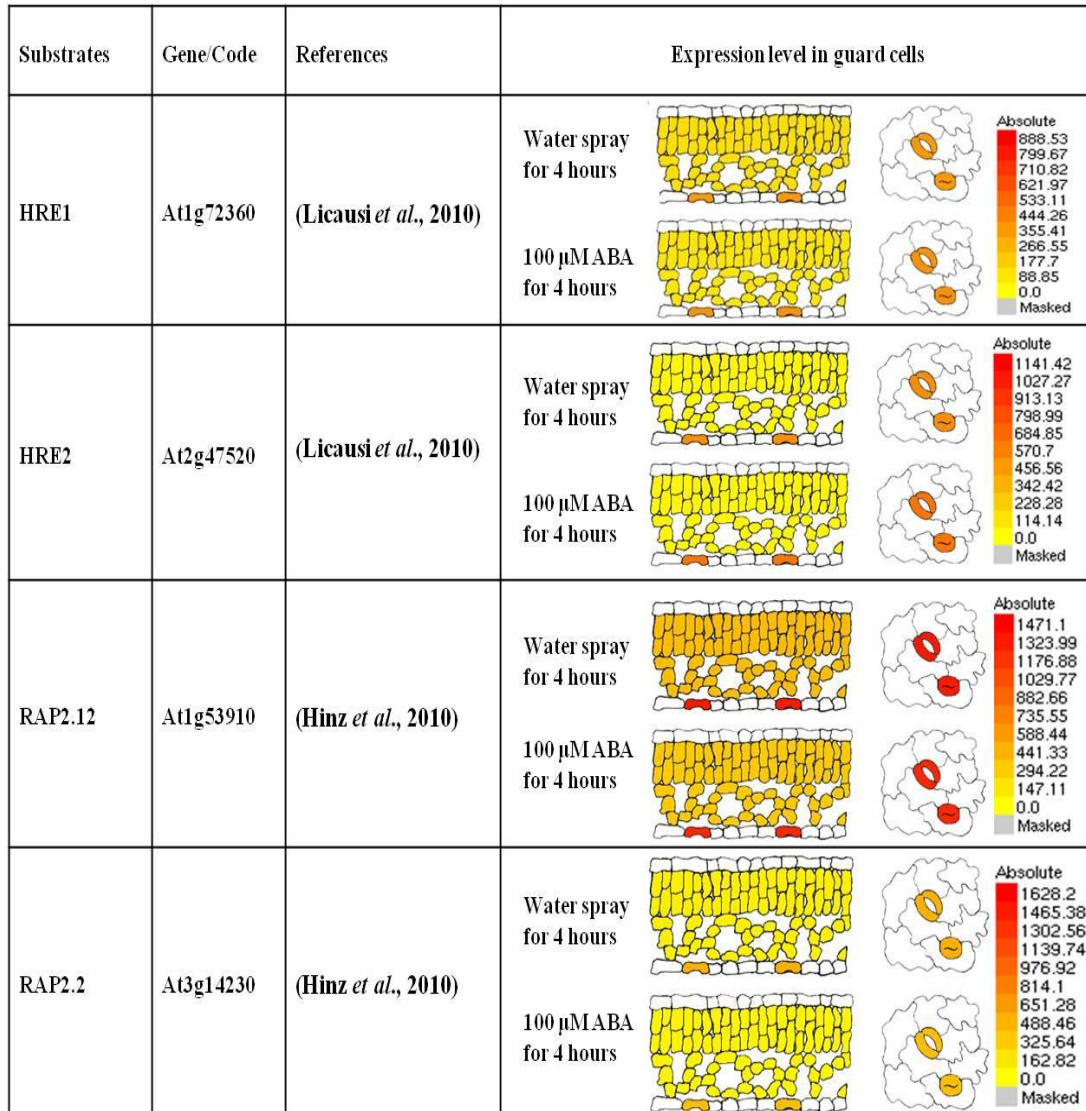


Figure 4-10 Expression patterns of the HRE1, HRE2, RAP2.12 and RAP2.2 genes in mesophyll and guard cells from a transcriptomic analysis of protoplast extracts

Schematic illustration of the expression levels of *HRE1*, *HRE2*, *RAP2.12* and *RAP2.2* genes in mesophyll and guard cells before and after treatment with 100 μM ABA. Darker colour represents relatively for higher gene expression levels as demonstrated in the scale bar to the right. Data was taken from the eFP-browser and is based on results from experiments carried out by (Yang *et al.*, 2008).

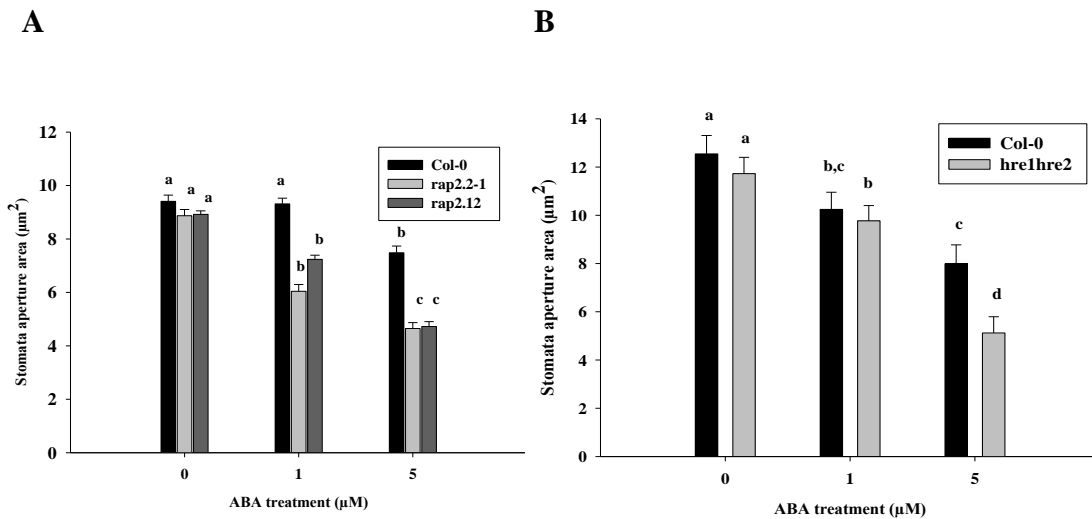


Figure 4-11 Stomatal aperture measurements taken from epidermal peels of *rap2.2-1*, *rap2.12*, *hre1hre2* and control plants in response to ABA

A) Stomatal aperture response of *rap2.2-1*, *rap2.12* and control plants to ABA (1 μM and 5 μM). B) Stomatal aperture response of *hre1hre2* and control plants to ABA (1 μM and 5 μM). For each experiment, epidermal peels were taken from three different plants. The values are a mean of 120 aperture measurements taken in over three experiments. Error bars represent the standard error. Values were statistically tested using one way ANOVA ($P < 0.0001$) and Tukey's Multiple Comparison Test. Different letters denote statistically significant differences ($p < 0.05$).

4.8 Conclusion

Taken together the physiological responses of mutants lacking several N-end rule pathway activities; methionine amino peptidase, N-terminal amidase, or arginyl transferase, all support the conclusion from Chapter 3 that there is a link between the function of the N-end rule pathway and drought tolerance in removing responsiveness to ABA. However preliminary attempts to determine protein substrates for this pathway via an investigation of the Group VII MC-ERFs were not successful.

5 Chapter- 5 The mechanisms of ABA and CO₂ induced stomatal closure appears to have been conserved throughout land plant evolution.

5.1 Introduction

Stomata are found on the aerial surface of higher plants and on the sporophyte of mosses, an early land plant group (Peterson *et al.*, 2010, Rensing *et al.*, 2008) (**Figure 5-1**). Mosses are the most ancient, and non-vascular, plant lineage to form stomata which are found in a ring around the base of their sporophyte structures, or spore capsule (Berry *et al.*, 2010; Edwards *et al.*, 1998). Higher plant stomatal apertures respond to a range of environmental signals allowing plants to regulate water loss. The control of plant water status is believed to have been a key acquisition in enabling plants to colonise the land masses of the earth. However, the function of stomata on moss spore capsules is unclear and their responses to environmental signals were poorly documented at the start of this project (Raven, 2002). Studies of moss stomata over 30 years ago reported that they could respond to ABA by reducing their apertures (Garner and Paolillo, 1973). The extent of homology between the ABA signalling cascades in “lower” non-vascular plants and the higher plant core ABA signalling network is beginning to be revealed from genome sequences (Komatsu *et al.*, 2009). The ABA signalling pathway of the gametophyte (protonema) of *Physcomitrella patens*, the first moss species to have its genome sequenced, appears to be similar to *Arabidopsis* seed-specific ABA signalling, which suggests that during the evolution of land plants, ABA signalling in the vegetative organs of their last common ancestor has been functionally diverted to seeds (Komatsu *et al.*, 2009). In essence, there are three major players in the core ABA signalling pathway in higher plant guard cells - the ABA receptors of the PYR/PYL/RCAR family, the ABA signal repressors of the ABI1 family, and the ABA signal transducer OST1 (Belin *et al.*, 2006; Cutler *et al.*, 2010). In the absence of the phytohormone ABA, ABI1 (a PP2C phosphatase enzyme) is free to inhibit OST1 kinase activity (also named SnRK2.6 and SnRK2E). In the presence of ABA, PYR/PYL/RCARs identify and bind to ABI1-related PP2Cs (Mustilli *et al.*, 2002). Subsequently, the OST1 kinase auto-activates and can phosphorylate and activate downstream substrates to generate ABA induced stomatal closure (Miyazono *et al.*, 2009; Sheard and Zheng, 2009). In the absence of ABA, ABI1 represses OST1 kinase activity and stomata remain open. The

interactions between ABA, the PP2Cs as negative regulators and the interacting SnRK2s as positive regulators, all engaged in ABA signalling in higher plants, are also becoming well characterised in the moss *Physcomitrella* (Sakata *et al.*, 2009). Recently, it was demonstrated that the apertures of these moss stomata close in response to ABA (Chater *et al.*, 2011). Other recent work has shown that the vascular plant stomatal aperture response to CO₂, like the ABA response, also requires OST1 (Xue *et al.*, 2011), and earlier work showed that ABI1 also acts in the stomatal CO₂ signalling pathway (Webb and Hetherington, 1997). The OST1 protein kinase is a regulator of CO₂-induced stomatal closing and CO₂ activation of SLAC1-mediated anion channels in guard cells, leading to a model for CO₂ regulation of gas exchange in plants (Lee *et al.*, 2009; Xue *et al.*, 2011). The aim of the experiments described in this chapter was to identify whether signalling components similar to OST1 and ABI1 are functional in the ancient plant stomatal responses to both ABA and CO₂. By using an *Arabidopsis* genetic complementation approach this study suggests conservation of the core ABA and CO₂ signalling module in guard cells of higher and lower plants. Some of the moss ABA signalling experiments outlined below have been described in the publication by Chater *et al.* 2011.

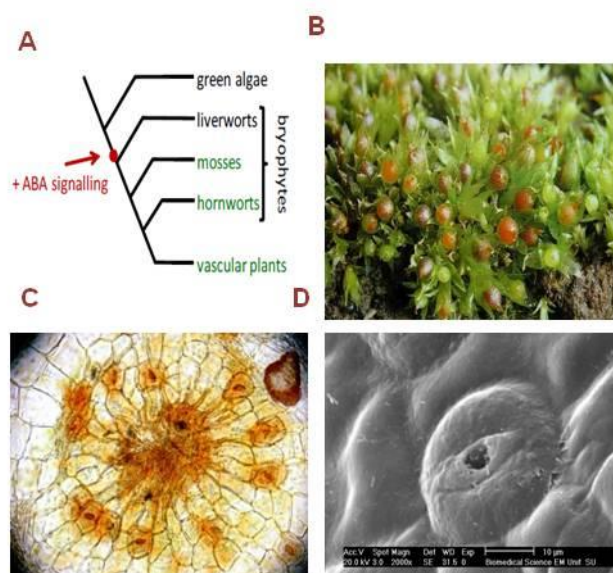


Figure 5-1 Moss stomata

A and B Mosses are the most basal group of extant land plants to possess stomata. C. The stomata of *Physcomitrella patens* are located in a ring around the base of the spore capsule of the sporophyte. D. Electron microscope image of *P. patens* stoma (taken from Chater *et al.*, 2011).

5.2 Moss stomata respond to ABA and CO₂

It has been shown that, stomatal apertures of *Physcomitrella* reduce significantly in a dose dependant manner on addition of ABA from 0 μ M to 100 μ M (**Figure 5-2 A**). Similar reductions in stomatal aperture area are detected as the CO₂ concentration increases from 0 ppm to 1000 ppm, with the strongest response between 0 and 400 ppm (Chater *et al.*, 2011) (**Figure 5-2 B**). This evidence and other related experiments Chater *et al.*, 2011 suggest that active stomatal responses to CO₂ and ABA occurs in mosses in similar way to that reported for stomata of vascular plants.

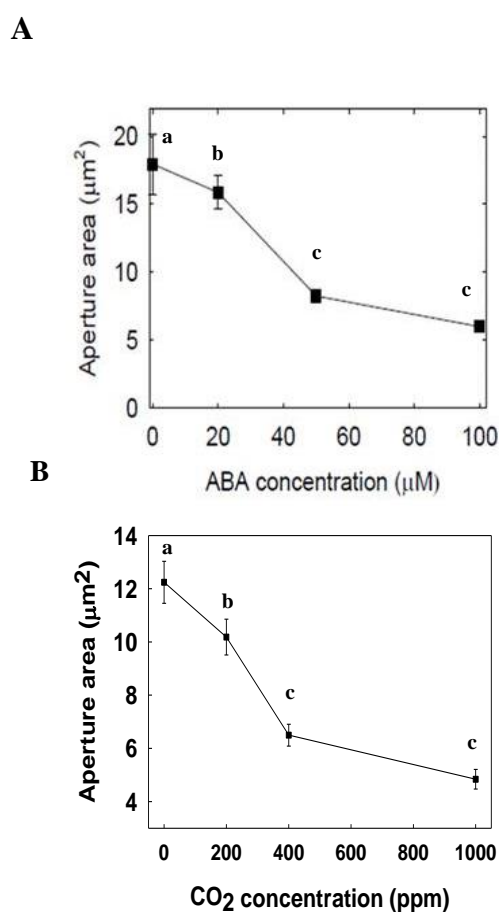


Figure 5-2 Moss stomatal responses to ABA and increasing [CO₂].

The stomata of *P. patens* are responsive to both ABA and [CO₂] in a dose dependent manner. Spore capsules were incubated with **A.** ABA or **B.** CO₂ concentrations as indicated for 2 hours before stomatal aperture measurement. Values were statistically tested using one way ANOVA ($P < 0.0001$) and Tukey's Multiple Comparison Test. Different letters denote statistical significance ($p < 0.05$) (taken from Chater *et al.*, 2011).

5.3 Methods Summary

Detailed methods are provided in Chapter 2. Cross-species complementation experiments were carried out in collaboration with Dr. Caspar Chater (University of Sheffield) as follows. Gateway constructs were designed containing full-length coding sequences of *PpOST1-1* and *PpABI1A* respectively. These were transformed into *Agrobacterium* strain GV3101RK by electroporation and then into their respective *Arabidopsis* backgrounds. Two constructs were made for each gene complementation, *PpOST1-1* and *PpABI1A* were inserted under the control of the *Arabidopsis* OST1 promoter region (p\$POHA) (Belin *et al.*, 2006; Mustilli *et al.*, 2002) and also under the control of the CaMV 35S promoter (CTAPi) (Rohila *et al.*, 2004). The destination vector p\$POHA(gw) was kindly provided by Doctor Sébastien Thomine (CNRS, France). This construct contained the *AtOST1* promoter which drives gene expression in the guard cells (Belin *et al.*, 2006; Mustilli *et al.*, 2002). Expression of *PpOST1* was carried out in the *Arabidopsis ost1-4* background (Xie *et al.*, 2006), and expression of *PpABI1A* was undertaken in the *Arabidopsis hab1-1:abi1-2* background (Saez *et al.*, 2006). Xie *et al.* 2006 identified *ost1-4* from a screen M2 plants from an (ethyl methanesulphonate) EMS- mutagenized population by thermal imaging the effect of relative humidity on stomatal aperture and seed were kindly supplied by Prof A Hetherington (University of Bristol). The double *hab1 abi1* mutant, which was kindly provided by Pedro L. Rodriguez, was used for these experiments as its reported ABA hypersensitivity phenotype is greater than that of single mutants. Transformed plants were generated and plants expressing the moss *PpOST1* or *PpABI1A* genes under the control of the *AtOST1* guard cell promoter were used for phenotype analysis. As phenotypic complementation was observed in these plants (see below) no further work was carried out on the plants transformed with the CaMV 35S promoter. T₂ lines were selected by GFP fluorescence in seed, and mature plant leaves were analyzed for a stomatal phenotype. Detailed studies of *Arabidopsis* stomatal aperture responses were performed by direct measurement of stomatal apertures using an epidermal strip bioassay as described in Chapter 2. In the *ost1 Arabidopsis* complementation experiments 20 µM ABA was used to observe restoration of ABA insensitivity. ABA concentrations of 0.1 µM and 1.0 µM were used in the *hab1-labi1-2* complementation experiments to discern restoration of the ABA hypersensitive phenotype.

5.3.1 *Atost1-4* complementation with *PpOST1-1*

Expression of *PpOST1-1* in the *Arabidopsis ost1-4* mutant background (Xie *et al.*, 2006) under the control of the *Arabidopsis OST1* promoter (Belin *et al.*, 2006) were carried out to assess whether transforming *Arabidopsis* ABA-signalling mutants with *PpOST1-1* could restore the normal higher plant stomatal ABA-response. Following the introduction of the *PpOST1-1* gene, the ABA-insensitive stomata of *Arabidopsis ost1-4* became more sensitive to ABA (Chater *et al.*, 2011). ABA-induced stomatal closure was compared between wild-type, the *Arabidopsis* mutant *ost1-4* and the mutant complemented with the moss *PpOST1-1* gene. Stomatal aperture measurements taken from epidermal strip bioassays show that *ost1-4* stomatal closure was, as expected, insensitive to ABA (**Figure 5-3**) (Xie *et al.*, 2006). The response of *ost1-4* plants expressing *PpOST1A* under the control of the *AtOST1* promoter was more sensitive than *ost1-4* to ABA. The moss *PpOST1-1* at least partly rescued ABA-induced stomatal closure in two independently transformed T2 generation *Arabidopsis* lines, with significant reductions in stomatal aperture observed following exposure to 20 μ M ABA (**Figure 5-3**). Similar results were also obtained in prior experiments with T1 generation plant lines (not shown).

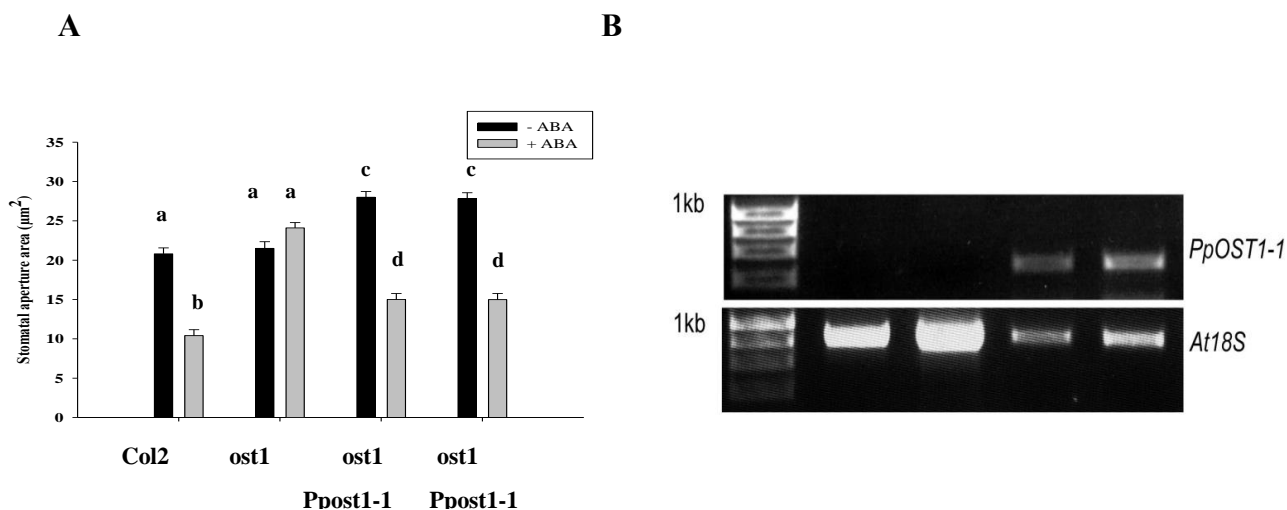


Figure 5-3 Stomatal aperture measurements of cross-species complementation of *ost1* mutant with *PpOST1-1* in *Arabidopsis* response to ABA.

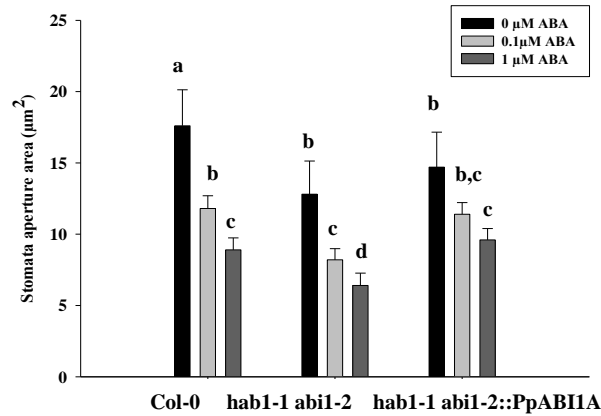
Cross-species complementation of *Arabidopsis ost1* mutant with *PpOST1-1* restores stomatal sensitivity to ABA. Stomatal aperture measurements of *Arabidopsis* lines treated with or without 20 μ M ABA for 2h in CO₂-free air. For each experiment, epidermal peels were taken from three different plants. The values are a mean of 120 aperture measurements taken in over three experiments. Error bars represent the standard error. Values were statistically tested using one way ANOVA ($P < 0.0001$) and Tukey's Multiple Comparison Test. Different letters denote statistical significance ($p < 0.05$). (B) RT-PCR verification of *PpOST1-1* expression in *Arabidopsis ost1* mutant, also shown on left of gel Col-2

WT and *ost1* from comparison. Positive RT-PCR control of *At18S rRNA* is also shown below. The experiment in B. was performed with the help of Dr C. Chater.

5.4 PpABI1A Complementation of *Arabidopsis hab1-1abi1-2*

Investigation of the *Physcomitrella* genome revealed that *PpABI1A* (JGI ID 32342) is related to the higher plant *ABI1*, a negative regulator of ABA signalling (Komatsu *et al.*, 2009) but its function in moss stomata has not been previously studied. To determine conservation of gene function between the moss and the higher plant an experiment was carried out to assess the ability of *Arabidopsis* lines transformed with *PpABI1* to close their stomata in response to exogenous ABA. This experiment was designed to ascertain whether genetic complementation provided a phenotypic complementation. Analyses were carried out to assess responses in wild-type and the different mutant backgrounds. T-DNA insertion mutant lines of *ABI1* and its close relative *HABI1* (*hab1* and *abi1-2*) were identified and characterised by Saez *et al.* 2006. In physiological studies of the double mutant *hab1-1 abi1-2* transformed with *PpABI1A* ABA-induced stomatal closure was compared between wild-type, (Col-0), double mutant *hab1-1 abi1-2* and the double mutant complemented with the moss gene *PpABI1A*. Stomatal aperture measurements indicated that the double mutant *hab1-1abi1-2* (in comparison to Col-0) was as expected hypersensitive to ABA-induced stomatal closure in the range of 0 to 0.1 μ M exogenously added ABA. However, the response of *hab1-1abi1-2::PpABI1A* to 0.1 and 1 μ M ABA was less sensitive than the *hab1-1 abi1-2* mutant (**Figure 5-4**). Although, wild-type responses to ABA were not fully restored in the absence of added ABA it can be concluded that the function of ABI1-related PP2C as a negative regulator of stomatal ABA signalling is not specific to higher plants but is also evolutionary conserved in the basal land plant *Physcomitrella*. It demonstrates that not only can the *Physcomitrella* SnRK2 PpOST1-1 positively regulate angiosperm guard cell ABA signalling, but *Physcomitrella* PP2Cs can also regulate it negatively. This conservation of function suggests that the core guard cell ABA stomatal signalling toolkit was present in the last common ancestor of *Physcomitrella* and *Arabidopsis*.

A



B

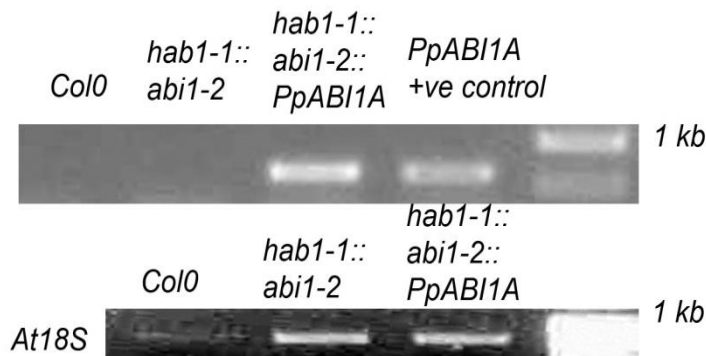


Figure 5-4 Stomatal aperture measurements of cross-species complementation of double mutant *hab1-1abi1-2* with *PpABI1A* in *Arabidopsis* response to ABA.

Complementation of ABA hypersensitive *hab1-1abi1-2* mutant with *PpABI1A* in the stomatal sensitivity response to 0.1 µM and 1.0 µM exogenous ABA in epidermal bioassays. For each experiment, epidermal peels were taken from three different plants. Error bars represent the standard error. The values are a mean of 120 aperture measurements taken in over three experiments. Values were statistically tested using one way ANOVA ($P < 0.0001$) and Tukey's Multiple Comparison Test. Different letters denote statistical significance ($p < 0.05$). (B) RT-PCR verification of *PpABI1A* expression in *Arabidopsis hab1-1abi1-2* mutant also shown on left of gel Col-0 WT and *hab1-1abi1-2* for comparison. Positive RT-PCR control of *At18S rRNA* is also shown below.

5.5 CO₂ Signalling

Both OST1 and ABI1 have been shown to act in the stomatal CO₂ signalling pathway in *Arabidopsis* (Xue *et al.*, 2011, Webb and Hetherington, 1997). Experiments were carried out to investigate whether the *Physcomitrella* OST1 and ABI1 orthologs could fulfil the same functions in moss stomata. Assays of CO₂-induced stomatal closure indicated that expression of *PpOST1-1* in the *Arabidopsis ost1-4* background restored stomatal sensitivity to elevated [CO₂] but not to sub-ambient [CO₂] (**Figure 5-5**). Furthermore, expression of *PpABI1* in the *Arabidopsis hab1-1 abi1-2* background restored normal CO₂ sensitivity to sub-ambient [CO₂] at 0 and 200ppm (but did not affect the response to ambient CO₂ which was not affected in the *hab1-1 abi1-2* mutant (**Figure 5-6**). These data indicate that the guard cell CO₂ and ABA signalling pathways in moss and *Arabidopsis* both converge at the level of the ABI1 protein phosphatases and the OST1 protein kinases. This suggests that stomatal ABA and CO₂ signalling responses both arose early in land plant evolution and have continued to function in a similar manner for over 400M years.

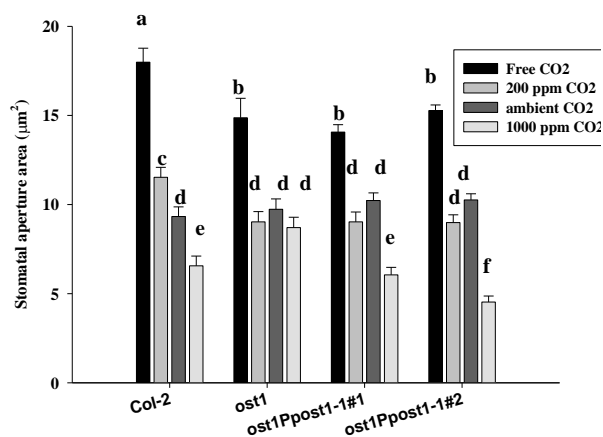


Figure 5-5 Stomatal aperture measurements of Cross-species complementation of *ost1* mutant with *PpOST1-1* in *Arabidopsis* response to CO₂.

Cross-species complementation of *Arabidopsis ost1* mutant with *PpOST1-1* restores stomatal were exposed to CO₂-free air, 200 ppm, ambient and 1000 ppm CO₂ in air. Stomatal aperture measurements were performed after two hours in the light. For each experiment, epidermal peels were taken from three different plants. For each experiment, epidermal peels were taken from three different plants. The values are a mean of 120 aperture measurements taken in over three experiments. Error bars represent the standard error. Values were statistically tested using one way ANOVA (P<0.0001) and Tukey's Multiple Comparison Test. Different letters denote statistical significance (p<0.05).

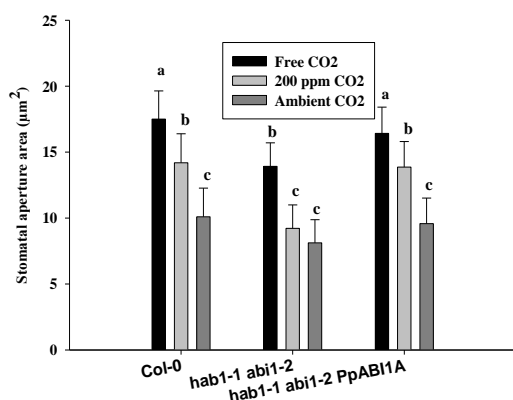


Figure 5-6 Stomatal aperture measurements of Cross-species complementation of ABA hypersensitive *hab1-1abi1-2* mutant with *PpABI1A* in *Arabidopsis* response to CO₂.

Complementation of ABA hypersensitive *hab1-1abi1-2* mutants with *PpABI1A* were exposed to CO₂-free air, 200 ppm and ambient CO₂ in air. Stomatal aperture measurements were performed after two hours in the light. For each experiment, epidermal peels were taken from three different plants. The values are a mean of 120 aperture measurements taken in over three experiments. Error bars represent the standard error. Values were statistically tested using one way ANOVA ($P < 0.0001$) and Tukey's Multiple Comparison Test. Different letters denote statistical significance ($p < 0.05$).

5.6 Conclusion

Expression of moss genes homologous to vascular plant OST1 or ABI1 was able to at least partially restore ABA- and CO₂-induced stomatal aperture responses to vascular plants lacking these components. These data indicate that the guard cell CO₂ and ABA signalling pathways in moss and *Arabidopsis* both converge the level of the ABI1 protein phosphatases and the OST1 protein kinases. It therefore appears that mosses may actively regulate their stomatal apertures in a similar way to later-evolving vascular plants. Experimental evidence in Chater *et al.* 2011 shown in **(Figure 5-2)** indicates that moss stomata close in response to ABA and CO₂. To test this further Chater *et al.* 2011 created moss knockout mutants lacking the *PpOST1-1* gene. The stomata of *Ppost1* exhibited significantly reduced aperture closure in response to ABA, confirming the involvement of PpOST1-1 in moss stomatal aperture responses **(Figure 5-7)**. This result suggested that the moss OST1 is well-conserved and functional in the higher plant stomatal ABA-response. The evidence suggests that the function of ABI1 and OST1, as key regulators of stomatal ABA signalling, have been conserved throughout plant evolution since the last common ancestor of moss and vascular plants over 400 million years ago (Chater *et al.*, 2011; Kenrick and Crane, 1997). Other recent experiments suggest that ABA and CO₂ signalling

pathways are present in guard cells of *Selaginella* species of the lycophyte lineage (Ruszala *et al.*, 2011). However, other studies have been unable to find active stomatal responses in lycophyte species (McAdam and Brodribb, 2012a; McAdam and Brodribb, 2012b). It is possible that this is due to differences in methodology and growth conditions or the particular species studied (Haworth *et al.*, 2012). Although, the field remains controversial there is a growing body of evidence to support the hypothesis that lower plant stomata close in response to both ABA and [CO₂] by activating a similar signalling pathway to that of higher plants. The data presented in this Chapter add weight to the argument that stomatal ABA and CO₂ signalling responses both arose early in land plant evolution and have continued to function in a similar manner for over 400M years.

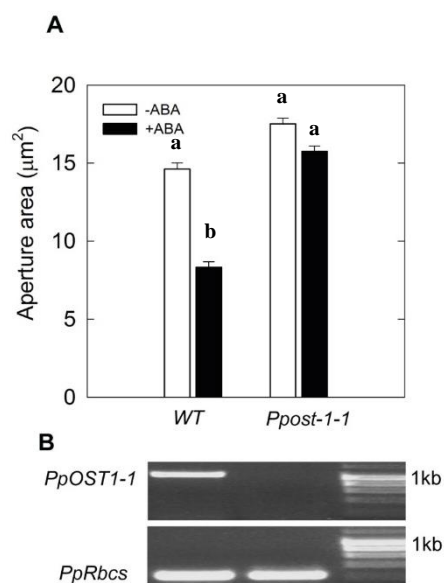


Figure 5-7 Stomatal aperture measurements and RT-PCR verification of *Physcomitrella* wild-type and *Ppost1-1* sporophytes

A) Stomatal aperture measurements of *Physcomitrella*, wild-type and *Ppost1-1* sporophytes treated with or without 100 µM ABA for 2h in CO₂-free air. Error bars represent the standard error. Values were statistically tested using one way ANOVA ($P < 0.0001$) and Tukey's Multiple Comparison Test. Different letters denote statistical significance ($p < 0.05$).

B) RT-PCR verification of *Physcomitrella Ppost1-1* knockout mutant. *PpOST1-1* and wild-type cDNA amplified with primers specific to *PpOST1-1* or positive control *PpRbcs* (Chater *et al.*, 2011).

6 Chapter 6– Discussion

6.1 Discussion

Guard cell signal transduction networks consist of a variety of molecular components and regulatory mechanisms as introduced in Chapter 1. Stomatal movement analyses have the potential to quantify and identify mechanisms which have an effect on guard cell signalling and such research will clarify novel approaches for engineering improved water-use efficiency and desiccation avoidance in crop plants. In this study (Chapters 3 and 4), the role of the N-end rule pathway was investigated in stomatal ABA signalling, the results presented suggest that this pathway inactivates components of higher plant stomatal signalling pathways by selecting and directing them for protein degradation. A related study presented in Chapter 5, suggests that both positive and negative regulatory components of the stomatal ABA signalling network previously characterised in higher plants form an ancient core signalling module that has been conserved throughout stomatous land plant evolution.

6.1.1 The N-recognin *PRT6* mediates ABA-induced stomatal closure and drought susceptibility

As introduced in Chapter 1, the N-end rule pathway was discovered in yeast and animal cells where it is known to control a diverse range of regulatory events (Graciet and Wellmer, 2010; Tasaki and Kwon, 2007; Varshavsky and Byrd, 1996). Our understanding of the functions of N-end rule pathway in plants is less well developed, although a number of components of this pathway have been identified in plants and their physiological functions have recently begun to emerge (Graciet *et al.*, 2009; Yoshida *et al.*, 2002). Undoubtedly, many substrates of the plant N-end rule pathway probably remain to be discovered. Evidence for the involvement of the N-end rule pathway in plants functions was revealed by Holman *et al.* 2009 who recognized a mutant allele of the N-recognin *PRT6*. *prt6* mutant plants have reduced germination potential with a hypersensitive response to exogenously added abscisic acid (ABA). The identification of a further function for the N-recognin *PRT6* in the regulation of ABA-induced stomatal closure and drought responses presented in Chapter 3 are consistent with this pathway being required for key aspects of ABA-inducible plant responses. Preliminary experiments using a *pPRT6::GUS* reporter gene, identified *PRT6* as an ABA-inducible gene although its mechanism of induction remains

unknown. They also confirmed *PRT6* gene expression in guard cells and many other cell types. Thus, it appears that *PRT6* is a negative regulator of ABA-inducible stomatal closure and water stress responses (**Figure 3-7**). Furthermore, the *prt6* mutants which exhibit hypersensitivity to ABA-induced stomatal closure also had reduced stomatal density (**Figure 3-11**, **Figure 3-13** and **Figure 3-14**), and reduced evapotranspiration as shown by infrared thermal imaging of (**Figure 3-15**). Perhaps more importantly they also showed enhanced drought tolerance. Interestingly, the *prt6* mutants had NO-insensitive phenotypes in stomatal aperture regulation. The response of *prt6* stomata to ABA and NO together was comparable to that of wild type leaves (**Figure 3-17** and **Figure 3-18**) suggesting that *prt6* may exert a negative effect on the ABA signalling pathway downstream of nitric oxide's effect. This suggests that during ABA induced stomatal closure nitric oxide may be involved in selecting a protein for degradation that is normally involved in promoting stomatal opening. In mouse cells nitric oxide has been shown to oxidise cysteine residues of N-end rule pathway substrates converting them to secondary destabilising residues (Hu *et al.*, 2005). This observation may provide an explanation for why stomata lacking the N-recognin *PRT6* are apparently blind to NO. To begin to elucidate the genetic relationship between *PRT6* and known ABA signal transduction components multiple mutant studies were carried out. Stomatal behaviours of the *prt6-1 ost1-4* double mutant line were similar to those of the *snrk2.2 snrk2.3 prt6-1* triple mutant in response to ABA. In addition, the double mutant *abi1-1 prt6-4* exhibited a hypersensitive stomatal response to ABA (**Figure 3-22**). These results strongly suggest that the N-end rule pathway inhibits ABA-signalling via a mechanism that does not require the activity of ABI1 or OST1. Thus the N-end rule pathway may act downstream, or independently of these core ABA signalling components to maintain stomatal opening (**Figure 6-1**). In summary, the results presented in Chapters 3 demonstrate that *PRT6* and the N-end rule pathway, are significant in regulating stomatal ABA-responses, in addition to the previously described roles in germination and hypoxia (Gibbs *et al.*, 2011; Holman *et al.*, 2009; Licausi *et al.*, 2010). The potential substrates of *PRT6* in guard cells are currently unknown. The identification, of the N-end rule target proteins is required to understand how the UBR box-containing E3 ligase *PRT6* negative regulators mediate a drought stress response in *Arabidopsis*.

6.1.2 The N-end rule pathway of protein degradation is a mediator of ABA-induced stomatal closure

The results of the experiments presented in Chapter 4, demonstrated that several enzymatic components of the plant N-end rule pathway are involved in removing stomatal ABA-sensitivity including arginyl transferase and methionine amino peptidase activities. Treatment of stomata of the *map1A* mutant with fumagillin resulted in ABA hypersensitivity (**Figure 4-3 A**). This result suggests that N end rule substrates initiating MC- are stabilised in these mutants, and indicates that the MC-ERFs may be regulators of plant responses to water availability, and this regulation is integrated through the N-end rule pathway. Further experiments should aid in the systematic identification of substrate proteins to determine whether a different MC-ERF, or combinations of MC-ERFs or indeed a non-ERF MC- protein might play key role in stomatal ABA-sensitivity. There are a further 200 *Arabidopsis* proteins with amino acid sequences that start with Met-Cys. In conclusion, the data presented in Chapters 3 and 4 suggest that the N-end rule pathway is critically involved in regulation of ABA protective mechanisms against drought stress in *Arabidopsis*. Evidence from hypoxia studies (Gibbs *et al.*, 2011) implicated ERF/AP2 transcription factors as potential substrates for the N-end rule pathways but experiments described in Chapter 3 could find no evidence for this in the stomatal closure response.

6.1.3 The mechanisms of ABA and CO₂ induced stomatal closure appears to have been conserved throughout land plant evolution.

The drought phytohormone ABA is responsible for promoting reductions in stomatal aperture, therefore allowing higher plants to conserve water (Kim *et al.*, 2010). The role of ABA in controlling the stomata of lower plants is much less well described. However, the presence of *PpOST1* and *PpABII* genes, in addition to a range of other known components of ABA signalling cascades (e. g. H⁺-ATPase, and 14-3-3 proteins) in the *Physcomitrella* genome suggest that similar signalling pathways are possible (Wurtele *et al.*, 2003). Secondly, the strong evidence of negative regulation of *Physcomitrella* ABA signalling by expression of the dominant negative *Atabi1-1* (Komatsu *et al.*, 2009) suggests that stomatal ABA signalling components are active, at least in the gametophytic tissues of moss species. In the current study, experiments were carried out to determine whether ABA signalling components identified in higher plants, regulate stomatal apertures of *Physcomitrella*, and thus whether moss stomata show similar control of stomatal function to that of higher plants. The cross-

species genetic complementation experiments presented in Chapter 5 support the proposition that the function of both positive (*AtOST1*-like SnRKs) and negative (*AtABI1*-like PP2Cs) regulatory components of the core ABA signalling cascade are conserved between the stomata of the lower plant *Physcomitrella* and the higher plant *Arabidopsis* (**Figure 5-3**, **Figure 5-4** and **Figure 5-5**). Interestingly, in a separate study OST1, Ca²⁺, and ROS which are involved in higher plant guard cell intracellular signalling were recently shown to be involved in the stomatal responses of a lycophyte early land plant lineage (Ruszala *et al.*, 2011). In *Arabidopsis*, OST1 plays a key role to activate the S-type onion channel SLAC1, triggering depolarization of the guard cell membrane, and a significant step in stomatal closure (Kim *et al.*, 2010). It will be interesting to discover whether PpOST1 phosphorylates an orthologous ion channel in *Physcomitrella*. The CO₂ concentration in the atmosphere is an additional significant environmental signal to which stomata in flowering plants are recognized to respond actively (Kim *et al.*, 2010). In Chapter 5, it was investigated whether *Physcomitrella* stomatal apertures are able to respond to the concentration of atmospheric CO₂ in a similar manner to the stomata of higher plants. The recognition and characterisation of a number of shared guard cell ABA and CO₂ signalling genes, has been confirmed for higher plants (Kim *et al.*, 2010; Webb and Hetherington, 1997; Xue *et al.*, 2011). Again the results suggested that moss orthologs of OST1 and ABI1 were able to at least partly compensate for the lack of *AtOST1* or *AtABI1* in *Arabidopsis* mutant backgrounds. The experiments presented here begin to shed light on the ancient signalling pathway that evolved prior to the divergence of higher and lower stomatous land plants. The results in the current study and indeed others cited here Ruszala *et al.* 2011 demonstrate that the stomata of the moss *Physcomitrella* and the lycophyte *Selaginella* (Ruszala *et al.*, 2011) respond to ABA and CO₂ using a signalling pathway that appears to be directly comparable to that of the model flowering plant *Arabidopsis thaliana*. This evidence would be consistent with a monophyletic origin for stomata.

6.2 Prospects for future work

Preliminary experiments presented in (Chapters 3 and 4) together with other published experiments indicate that MC-proteins, and probably other proteins are N-end rule substrates related to stomatal ABA responsiveness (Gibbs *et al.*, 2011; Licausi *et al.*, 2011) (**Figure 6-1**). The function of the 5 Group VII ERF MC-proteins in particular,

in drought and ABA responses, requires further study. Dr D. Gibbs (University of Nottingham) has created multiple combinations of knock-out mutants of the MC-ERFs, RAP2.12, RAP2.2, and EBP in the *prt6* background. In future experiments it will be investigated whether the lack of ERF expression can suppress the *prt6* hypersensitive stomatal response to ABA, and the stomatal insensitivity to nitric oxide. This will confirm whether the MC-ERFs are involved in nitric oxide and ABA signalling, and define the MC-ERF combination(s) which provide functionality to enhance plant responses to decreased water availability. Experiments are also underway to define and characterise possible substrates enhancing drought tolerance for the N-end rule pathway in the barley. Initial informatics analyses illustrate that the barley genome encodes a similar number of group VII MC-ERFs. These experiments will attempt to define the level of evolutionary conservation of the plant N-end rule pathway and its potential use in modifying crop performance to changing water availability. The results presented here indicate a function for the N-end rule pathway in drought tolerance, a significant discovery in plant signalling biology, providing an improved understanding of how plants respond to abiotic stress. This gives an opportunity to establish how targeted proteolysis homeostatically co-ordinates plant responses to water stress. Water logging and drought plant responses are key determinants of food security and stability of yield. Characterisation of the conserved role of the N-end rule pathway and its substrates will propose new approaches for delivery of abiotic stress resistance in crops, providing strategies to overcome these negative environmental conditions.

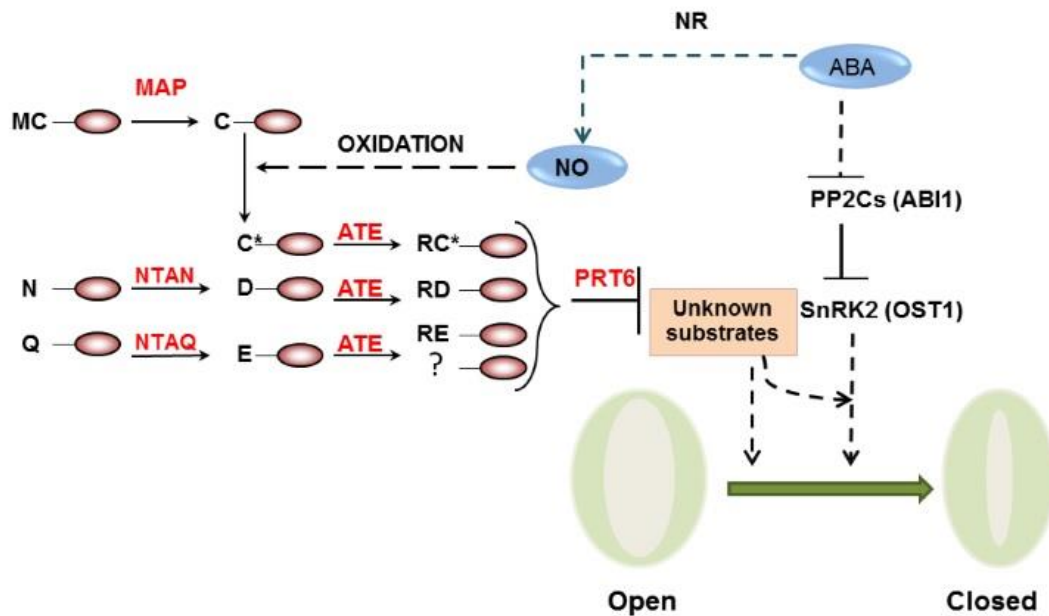


Figure 6-1 Model to illustrate how the N-end rule pathway and its currently unknown substrates may interact with known components of the core guard cell ABA signalling pathway to regulate stomatal aperture.

This model incorporates the results from experiments presented in this thesis which indicate that: (i) Plants lacking components of the N-end rule pathway have stomata that are hypersensitive to ABA. (ii) Plants lacking an intact N-end rule pathway have stomata that are completely insensitive to nitric oxide (NO). (iii) N-end rule pathway substrates act to prevent stomatal closure either downstream of or independently of OST1 and ABI1. Schematic representation of the N-end rule pathway in plants. Ovals denote a protein substrate. N-terminal residues are indicated by single-letter abbreviations. N-terminal methionine residues (M) may be removed by an endo-peptidase (e.g. MAP1A) to reveal tertiary destabilising residues. The tertiary destabilizing N-terminal residues asparagine and glutamine (N and Q) are deamidated through two distinct enzymes NTAN1 and NTAQ1 into aspartic acid and glutamic acid (D and E) respectively. C denotes N-terminal cysteine residues. Cysteine residues may be oxidised by oxygen and/or nitric oxide (shown as C*). Arginyl-tRNA:protein arginyltransferase (e.g. ATE1) is responsible for converting N-terminal aspartate and glutamate secondary destabilizing residues to the primary destabilizing N-terminal residues through arginylation.

7 References

- ASSMANN, S. M. 1993. Signal transduction in guard cells. *In*: PALADE, G. E. (ed.) *Annual Review of Cell Biology*.
- BACHMAIR, A., FINLEY, D. & VARSHAVSKY, A. 1986. In vivo half-life of a protein is a function of its amino-terminal residue. *Science*, 234, 179-186.
- BAILEY-SERRES, J., FUKAO, T., GIBBS, D. J., HOLDSWORTH, M. J., LEE, S. C., LICAUSI, F., PERATA, P., VOESENEK, L. A. C. J. & VAN DONGEN, J. T. 2012. Making sense of low oxygen sensing. *Trends in Plant Science*, 17, 129-138.
- BARRERO, J. M., PIQUERAS, P., GONZALEZ-GUZMAN, M., SERRANO, R., RODRIGUEZ, P. L., PONCE, M. R. & MICOL, J. L. 2005. A mutational analysis of the ABA1 gene of *Arabidopsis thaliana* highlights the involvement of ABA in vegetative development. *Journal of Experimental Botany*, 56, 2071-2083.
- BELIN, C., DE FRANCO, P.-O., BOURBOUSSE, C., CHAIGNEPAIN, S., SCHMITTER, J.-M., VAVASSEUR, A., GIRAUDAT, J., BARBIER-BRYGOO, H. & THOMINE, S. 2006. Identification of features regulating OST1 kinase activity and OST1 function in guard cells. *Plant Physiology*, 141, 1316-1327.
- BERRY, J. A., BEERLING, D. J. & FRANKS, P. J. 2010. Stomata: key players in the earth system, past and present. *Current Opinion in Plant Biology*, 13, 233-240.
- BRADSHAW, R. A., BRICKEY, W. W. & WALKER, K. W. 1998. N-terminal processing: the methionine aminopeptidase and N-alpha-acetyl transferase families. *Trends in Biochemical Sciences*, 23, 263-267.
- BRANDT, B., BRODSKY, D. E., XUE, S., NEGI, J., IBA, K., KANGASJARVI, J., GHASSEMIAN, M., STEPHAN, A. B., HU, H. & SCHROEDER, J. I. 2012. Reconstitution of abscisic acid activation of SLAC1 anion channel by CPK6 and OST1 kinases and branched ABI1 PP2C phosphatase action. *Proceedings of the National Academy of Sciences of the United States of America*, 109, 10593-10598.

- BREARLEY, J., VENIS, M. A. & BLATT, M. R. 1997. The effect of elevated CO₂ concentrations on K⁺ and anion channels of *Vicia faba* L. guard cells. *Planta*, 203, 145-154.
- BRIGGS, W. R. & CHRISTIE, J. M. 2002. Phototropins 1 and 2: versatile plant blue-light receptors. *Trends in Plant Science*, 7, 204-210.
- CHATER, C., KAMISUGI, Y., MOVAHEDI, M., FLEMING, A., CUMING, A. C., GRAY, J. E. & BEERLING, D. J. 2011. Regulatory Mechanism Controlling Stomatal Behavior Conserved across 400 Million Years of Land Plant Evolution. *Current Biology*, 21, 1025-1029.
- CHOI, W. S., JEONG, B. C., JOO, Y. J., LEE, M. R., KIM, J., ECK, M. J. & SONG, H. K. 2010. Structural basis for the recognition of N-end rule substrates by the UBR box of ubiquitin ligases. *Nature Structural & Molecular Biology*, 17, 1175-+.
- CHRISTMANN, A., HOFFMANN, T., TEPLOVA, I., GRILL, E. & MULLER, A. 2005. Generation of active pools of abscisic acid revealed by in vivo Imaging of water-stressed Arabidopsis. *Plant Physiology*, 137, 209-219.
- COMINELLI, E., GALBIATI, M., VAVASSEUR, A., CONTI, L., SALA, T., VUYLSTEKE, M., LEONHARDT, N., DELLAPORTA, S. L. & TONELLI, C. 2005. A guard-cell-specific MYB transcription factor regulates stomatal movements and plant drought tolerance. *Current Biology*, 15, 1196-1200.
- CUMING, A. C., CHO, S. H., KAMISUGI, Y., GRAHAM, H. & QUATRANO, R. S. 2007. Microarray analysis of transcriptional responses to abscisic acid and osmotic, salt, and drought stress in the moss, *Physcomitrella patens*. *New Phytologist*, 176, 275-287.
- CUTLER, S. R., RODRIGUEZ, P. L., FINKELSTEIN, R. R. & ABRAMS, S. R. 2010. Abscisic Acid: Emergence of a Core Signaling Network. In: MERCHANT, S., BRIGGS, W. R. & ORT, D. (eds.) *Annual Review of Plant Biology*, Vol 61.
- DELLEDONNE, M. 2005. NO news is good news for plants. *Current Opinion in Plant Biology*, 8, 390-396.

- DELLEDONNE, M., XIA, Y. J., DIXON, R. A. & LAMB, C. 1998. Nitric oxide functions as a signal in plant disease resistance. *Nature*, 394, 585-588.
- DESIKAN, R., GRIFFITHS, R., HANCOCK, J. & NEILL, S. 2002. A new role for an old enzyme: Nitrate reductase-mediated nitric oxide generation is required for abscisic acid-induced stomatal closure in *Arabidopsis thaliana*. *Proceedings of the National Academy of Sciences of the United States of America*, 99, 16314-16318.
- DONALDSON, L., LUDIDI, N., KNIGHT, M. R., GEHRING, C. & DENBY, K. 2004. Salt and osmotic stress cause rapid increases in *Arabidopsis thaliana* cGMP levels. *Febs Letters*, 569, 317-320.
- EDWARDS, D., KERP, H. & HASS, H. 1998. Stomata in early land plants: an anatomical and ecophysiological approach. *Journal of Experimental Botany*, 49, 255-278.
- FINKELSTEIN, R. R., GAMPALA, S. S. L. & ROCK, C. D. 2002. Abscisic acid signaling in seeds and seedlings. *Plant Cell*, 14, S15-S45.
- FORSTBAUER, C. 2009. Photosynthesis - leaf and pigments. <http://fhs-bio-wiki.pbworks.com>.
- FUJII, H., CHINNUSAMY, V., RODRIGUES, A., RUBIO, S., ANTONI, R., PARK, S. Y., CUTLER, S. R., SHEEN, J., RODRIGUEZ, P. L. & ZHU, J. K. 2009. In vitro reconstitution of an abscisic acid signalling pathway. *Nature*, 462, 660-U138.
- FUJII, H., VERSLUES, P. E. & ZHU, J.-K. 2007. Identification of two protein kinases required for abscisic acid regulation of seed germination, root growth, and gene expression in *Arabidopsis*. *Plant Cell*, 19, 485-494.
- FUJITA, Y., FUJITA, M., SHINOZAKI, K. & YAMAGUCHI-SHINOZAKI, K. 2011. ABA-mediated transcriptional regulation in response to osmotic stress in plants. *Journal of Plant Research*, 124, 509-525.

- GARCIA-MATA, C. & LAMATTINA, L. 2009. Nitric Oxide Induces Stomatal Closure and Enhances the Adaptive Plant Responses against Drought Stress (vol 126, pg 1196, 2001). *Plant Physiology*, 150, 531-531.
- GARNER, D. L. B. & PAOLILLO, D. J. J. 1973. On the functioning of stomates in *Funaria*. *Bryologist*, 76, 423-427.
- GARZON, M., EIFLER, K., FAUST, A., SCHEEL, H., HOFMANN, K., KONCZ, C., YEPHREMOV, A. & BACHMAIR, A. 2007. PRT6/At5g02310 encodes an Arabidopsis ubiquitin ligase of the N-end rule pathway with arginine specificity and is not the CER3 locus. *Febs Letters*, 581, 3189-3196.
- GIBBS, D. J., LEE, S. C., MD ISA, N., GRAMUGLIA, S., FUKAO, T., BASSEL, G. W., CORREIA, C. S., CORBINEAU, F., THEODOULOU, F. L., BAILEY-SERRES, J. & HOLDSWORTH, M. J. 2011. Homeostatic response to hypoxia is regulated by the N-end rule pathway in plants. *Nature*, 479, 415-8.
- GIGLIONE, C., BOULAROT, A. & MEINNEL, T. 2004. Protein N-terminal methionine excision. *Cellular and Molecular Life Sciences*, 61, 1455-1474.
- GIGLIONE, C. & MEINNEL, T. 2001. Organellar peptide deformylases: universality of the N-terminal methionine cleavage mechanism. *Trends in Plant Science*, 6, 566-572.
- GODA, H., SASAKI, E., AKIYAMA, K., MARUYAMA-NAKASHITA, A., NAKABAYASHI, K., LI, W., OGAWA, M., YAMAUCHI, Y., PRESTON, J., AOKI, K., KIBA, T., TAKATSUTO, S., FUJIOKA, S., ASAMI, T., NAKANO, T., KATO, H., MIZUNO, T., SAKAKIBARA, H., YAMAGUCHI, S., NAMBARA, E., KAMIYA, Y., TAKAHASHI, H., HIRAI, M. Y., SAKURAI, T., SHINOZAKI, K., SAITO, K., YOSHIDA, S. & SHIMADA, Y. 2008. The AtGenExpress hormone and chemical treatment data set: experimental design, data evaluation, model data analysis and data access. *Plant Journal*, 55, 526-542.
- GONUGUNTA, V. K., SRIVASTAVA, N., PULI, M. R. & RAGHAVENDRA, A. S. 2008. Nitric oxide production occurs after cytosolic alkalization during

- stomatal closure induced by abscisic acid. *Plant Cell and Environment*, 31, 1717-1724.
- GRABOV, A. & BLATT, M. R. 1999. A steep dependence of inward-rectifying potassium channels on cytosolic free calcium concentration increase evoked by hyperpolarization in guard cells. *Plant Physiology*, 119, 277-287.
- GRACIET, E., MESITI, F. & WELLMER, F. 2010. Structure and evolutionary conservation of the plant N-end rule pathway. *Plant Journal*, 61, 741-751.
- GRACIET, E. & WELLMER, F. 2010. The plant N-end rule pathway: structure and functions. *Trends in Plant Science*, 15, 447-453.
- GRACIET, E., WALTER, F., O'MAOILEIDIGH, D., POLLMANN, S., MEYEROWITZ, E. M., VARSHAVSKY, A. & WELLMER, F. 2009. The N-end rule pathway controls multiple functions during Arabidopsis shoot and leaf development. *Proceedings of the National Academy of Sciences of the United States of America*, 106, 13618-13623.
- GRAY, J. E., HOLROYD, G. H., VAN DER LEE, F. M., BAHRAMI, A. R., SIJMONS, P. C., WOODWARD, F. I., SCHUCH, W. & HETERINGTON, A. M. 2000. The HIC signalling pathway links CO₂ perception to stomatal development. *Nature*, 408, 713-716.
- GRIFFITH, E. C., SU, Z., TURK, B. E., CHEN, S. P., CHANG, Y. H., WU, Z. C., BIEMANN, K. & LIU, J. O. 1997. Methionine aminopeptidase (type 2) is the common target for angiogenesis inhibitors AGM-1470 and ovalicin. *Chemistry & Biology*, 4, 461-471.
- GRIGORYEV, S., STEWART, A. E., KWON, Y. T., ARFIN, S. M., BRADSHAW, R. A., JENKINS, N. A., COPELAND, N. G. & VARSHAVSKY, A. 1996. A mouse amidase specific for N-terminal asparagine - The gene, the enzyme, and their function in the N-end rule pathway. *Journal of Biological Chemistry*, 271, 28521-28532.
- HANCOCK, J. T., NEILL, S. J. & WILSON, I. D. 2011. Nitric oxide and ABA in the control of plant function. *Plant science : an international journal of experimental plant biology*, 181, 555-9.

- HATTORI, Y., NAGAI, K., FURUKAWA, S., SONG, X.-J., KAWANO, R., SAKAKIBARA, H., WU, J., MATSUMOTO, T., YOSHIMURA, A., KITANO, H., MATSUOKA, M., MORI, H. & ASHIKARI, M. 2009. The ethylene response factors SNORKEL1 and SNORKEL2 allow rice to adapt to deep water. *Nature*, 460, 1026-U116.
- HAUSER, F., WAADTL, R. & SCHROEDER, J. I. 2011. Evolution of Abscisic Acid Synthesis and Signaling Mechanisms. *Current Biology*, 21, R346-R355.
- HAWORTH, M., ELLIOTT-KINGSTON, C., GALLAGHER, A., FITZGERALD, A. & MCELWAIN, J. C. 2012. Sulphur dioxide fumigation effects on stomatal density and index of non-resistant plants: Implications for the stomatal palaeo-CO₂ proxy method. *Review of Palaeobotany and Palynology*, 182, 44-54.
- HEDRICH, R. 2012. ION CHANNELS IN PLANTS. *Physiological Reviews*, 92, 1777-1811.
- HEDRICH, R. & MARTEN, I. 1993. Malate-induced feedback-regulation of plasma-membrane anion channels could provide a CO₂ sensor to guard-cells. *Embo Journal*, 12, 897-901.
- HEICHEL, G. H. & ANAGNOSTAKIS, S. L. 1978. Stomatal response to light of solanum-pennellii, lycopersicon-esculentum, and a graft-induced chimera. *Plant Physiology*, 62, 387-390.
- HETHERINGTON, A. M. & WOODWARD, F. I. 2003. The role of stomata in sensing and driving environmental change. *Nature*, 424, 901-908.
- HETHERINGTON, A. M. 2001. Guard cell signaling. *Cell*, 107, 711-714.
- HETHERINGTON, A. M. & QUATRANO, R. S. 1991. Mechanisms of action of abscisic-acid at the cellular-level. *New Phytologist*, 119, 9-32.
- HINZ, M., WILSON, I. W., YANG, J., BUERSTENBINDER, K., LLEWELLYN, D., DENNIS, E. S., SAUTER, M. & DOLFERUS, R. 2010. Arabidopsis RAP2.2: an ethylene response transcription factor that is important for hypoxia survival. *Plant Physiology*, 153, 757-72.

- HOLMAN, T. J., JONES, P. D., RUSSELL, L., MEDHURST, A., TOMAS, S. U., TALLOJI, P., MARQUEZ, J., SCHMUTHS, H., TUNG, S.-A., TAYLOR, I., FOOTITT, S., BACHMAIR, A., THEODOULOU, F. L. & HOLDSWORTH, M. J. 2009. The N-end rule pathway promotes seed germination and establishment through removal of ABA sensitivity in Arabidopsis. *Proceedings of the National Academy of Sciences of the United States of America*, 106, 4549-4554.
- HOSY, E., VAVASSEUR, A., MOULINE, K., DREYER, I., GAYMARD, F., POREE, F., BOUCHEREZ, J., LEBAUDY, A., BOUCHEZ, D., VERY, A. A., SIMONNEAU, T., THIBAUD, J. B. & SENTENAC, H. 2003. The Arabidopsis outward K⁺ channel GORK is involved in regulation of stomatal movements and plant transpiration (vol 100, pg 5549, 2003). *Proceedings of the National Academy of Sciences of the United States of America*, 100, 7418-7418.
- HOTH, S., MORGANTE, M., SANCHEZ, J. P., HANAFEY, M. K., TINGEY, S. V. & CHUA, N. H. 2002. Genome-wide gene expression profiling in Arabidopsis thaliana reveals new targets of abscisic acid and largely impaired gene regulation in the abi1-1 mutant. *Journal of Cell Science*, 115, 4891-4900.
- HU, H., BOISSON-DERNIER, A., ISRAELSSON-NORDSTROEM, M., BOEHMER, M., XUE, S., RIES, A., GODOSKI, J., KUHN, J. M. & SCHROEDER, J. I. 2011. Carbonic anhydrases are upstream regulators of CO₂-controlled stomatal movements in guard cells (vol 12, pg 87, 2010). *Nature Cell Biology*, 13, 734-734.
- HU, R. G., SHENG, J., QI, X., XU, Z. M., TAKAHASHI, T. T. & VARSHAVSKY, A. 2005. The N-end rule pathway as a nitric oxide sensor controlling the levels of multiple regulators. *Nature*, 437, 981-986.
- INGBER, D., FUJITA, T., KISHIMOTO, S., SUDO, K., KANAMARU, T., BREM, H. & FOLKMAN, J. 1990. Synthetic analogs of fumagillin that inhibit angiogenesis and suppress tumor-growth.. *Nature*, 348, 555-557.

- INOUE, S., TAKEMIYA, A. & SHIMAZAKI, K. 2010. Phototropin signaling and stomatal opening as a model case. *Current Opinion in Plant Biology*, 13, 587-593.
- ISRAELSSON, M., SIEGEL, R. S., YOUNG, J., HASHIMOTO, M., IBA, K. & SCHROEDER, J. I. 2006. Guard cell ABA and CO₂ signaling network updates and Ca²⁺ sensor priming hypothesis. *Current Opinion in Plant Biology*, 9, 654-663.
- JEFFERSON, R. A., KAVANAGH, T. A. & BEVAN, M. W. 1987. Gus fusions-beta-glucuronidase as a sensitive and versatile gene fusion marker in higher-plants. *Embo Journal*, 6, 3901-3907.
- KENDALL, R. L. & BRADSHAW, R. A. 1992. Isolation and characterization of the methionine aminopeptidase from porcine liver responsible for the cotranslational processing of proteins. *Journal of Biological Chemistry*, 267, 20667-20673.
- KENRICK, P. & CRANE, P. R. 1997. The origin and early evolution of plants on land. *Nature*, 389, 33-39.
- KIM, T. H., BOHMER, M., HU, H. H., NISHIMURA, N. & SCHROEDER, J. I. 2010. Guard Cell Signal Transduction Network: Advances in Understanding Abscisic Acid, CO₂, and Ca²⁺ Signaling. In: MERCHANT, S., BRIGGS, W. R. & ORT, D. (eds.) *Annual Review of Plant Biology*, Vol 61. Palo Alto: Annual Reviews.
- KARIMI, M., INZE, D. & DEPICKER, A. 2002. GATEWAY(TM) vectors for Agrobacterium-mediated plant transformation. *Trends in Plant Science*, 7, 193-195.
- KEENER, M. E. & KIRCHER, P. L. 1983. The use of canopy temperature as an indicator of drought stress in humid regions. *Agricultural Meteorology*, 28, 339-349.
- KILIAN, J., WHITEHEAD, D., HORAK, J., WANKE, D., WEINL, S., BATISTIC, O., D'ANGELO, C., BORNBERG-BAUER, E., KUDLA, J. & HARTER, K. 2007. The AtGenExpress global stress expression data set: protocols,

- evaluation and model data analysis of UV-B light, drought and cold stress responses. *Plant Journal*, 50, 347-363.
- KOMATSU, K., NISHIKAWA, Y., OHTSUKA, T., TAJI, T., QUATRANO, R. S., TANAKA, S. & SAKATA, Y. 2009. Functional analyses of the ABI1-related protein phosphatase type 2C reveal evolutionarily conserved regulation of abscisic acid signaling between *Arabidopsis* and the moss *Physcomitrella patens*. *Plant Molecular Biology*, 70, 327-340.
- KWON, Y. T., BALOGH, S. A., DAVYDOV, I. V., KASHINA, A. S., YOON, J. K., XIE, Y. M., GAUR, A., HYDE, L., DENENBERG, V. H. & VARSHAVSKY, A. 2000. Altered activity, social behavior, and spatial memory in mice lacking the NTAN1p amidase and the asparagine branch of the N-end rule pathway. *Molecular and Cellular Biology*, 20, 4135-4148.
- LAKE, J. A. & WOODWARD, F. I. 2008. Response of stomatal numbers to CO₂ and humidity: control by transpiration rate and abscisic acid. *New Phytologist*, 179, 397-404.
- LEE, J.-H. & KIM, W. T. 2011. Regulation of abiotic stress signal transduction by E3 ubiquitin ligases in *Arabidopsis*. *Molecules and Cells*, 31, 201-208.
- LEE, S. C., LAN, W. Z., BUCHANAN, B. B. & LUAN, S. 2009. A protein kinase-phosphatase pair interacts with an ion channel to regulate ABA signaling in plant guard cells. *Proceedings of the National Academy of Sciences of the United States of America*, 106, 21419-21424.
- LEUNG, J., MERLOT, S. & GIRAUDAT, J. 1997. The *Arabidopsis* ABSCISIC ACID-INSENSITIVE2 (ABI2) and ABI1 genes encode homologous protein phosphatases 2C involved in abscisic acid signal transduction. *Plant Cell*, 9, 759-771.
- LIANG, Y-K., DUBOS, C., DODD, I. C., HOLROYD, G. H., HETHERINGTON, A. M. & CAMPBELL, M. M. 2005. *AtMYB61*, an R2R3-MYB Transcription Factor Controlling Stomatal Aperture in *Arabidopsis thaliana*, *Current Biology*, 15, 1201-1206.

- LICAUSI, F., KOSMACZ, M., WEITS, D. A., GIUNTOLI, B., GIORGI, F. M., VOESENEK, L. A. C. J., PERATA, P. & VAN DONGEN, J. T. 2011. Oxygen sensing in plants is mediated by an N-end rule pathway for protein destabilization. *Nature*, 479, 419-22.
- LICAUSI, F., VAN DONGEN, J. T., GIUNTOLI, B., NOVI, G., SANTANIELLO, A., GEIGENBERGER, P. & PERATA, P. 2010. HRE1 and HRE2, two hypoxia-inducible ethylene response factors, affect anaerobic responses in *Arabidopsis thaliana*. *Plant Journal*, 62, 302-315.
- LOZANO-JUSTE, J. & LEON, J. 2010. Nitric oxide modulates sensitivity to ABA. *Plant signaling & behavior*, 5, 314-6.
- MA, Y., SZOSTKIEWICZ, I., KORTE, A., MOES, D., YANG, Y., CHRISTMANN, A. & GRILL, E. 2009. Regulators of PP2C Phosphatase Activity Function as Abscisic Acid Sensors. *Science*, 324, 1064-1068.
- MACROBBIE, E. A. C. 1998. Signal transduction and ion channels in guard cells. *Philosophical Transactions of the Royal Society of London Series B-Biological Sciences*, 353, 1475-1488.
- MAO, J., ZHANG, Y. C., SANG, Y., LI, Q. H. & YANG, H. Q. 2005. A role for *Arabidopsis* cryptochromes and COP1 in the regulation of stomatal opening. *Proceedings of the National Academy of Sciences of the United States of America*, 102, 12270-12275.
- MARELLA, H. H., SAKATA, Y. & QUATRANO, R. S. 2006. Characterization and functional analysis of ABSCISIC ACID INSENSITIVE3-like genes from *Physcomitrella patens*. *Plant Journal*, 46, 1032-1044.
- MCADAM, S. A. M. & BRODRIBB, T. J. 2012a. Fern and Lycophyte Guard Cells Do Not Respond to Endogenous Abscisic Acid. *Plant Cell*, 24, 1510-1521.
- MCADAM, S. A. M. & BRODRIBB, T. J. 2012b. Stomatal innovation and the rise of seed plants. *Ecology Letters*, 15, 1-8.

- MCAINSH, M. R., BROWNLEE, C. & HETHERINGTON, A. M. 1991. PARTIAL INHIBITION OF ABA-INDUCED STOMATAL CLOSURE BY CALCIUM-CHANNEL BLOCKERS. *Proceedings of the Royal Society B-Biological Sciences*, 243, 195-201.
- MCAINSH, M. R., CLAYTON, H., MANSFIELD, T. A. & HETHERINGTON, A. M. 1996. Changes in stomatal behavior and guard cell cytosolic free calcium in response to oxidative stress. *Plant Physiology*, 111, 1031-1042.
- MCAINSH, M. R., WEBB, A. A. R., TAYLOR, J. E. & HETHERINGTON, A. M. 1995. Stimulus-induced oscillations in guard-cell cytosolic-free calcium. *Plant Cell*, 7, 1207-1219.
- MCCOWEN, M. C., CALLENDER, M. E. & LAWLIS, J. F. 1951. FUMAGILLIN (H-3), A NEW ANTIBIOTIC WITH AMEBICIDAL PROPERTIES. *Science*, 113, 202-203.
- MELHORN, V., MATSUMI, K., KOIWAI, H., IKEGAMI, K., OKAMOTO, M., NAMBARA, E., BITTNER, F. & KOSHIBA, T. 2008. Transient expression of AtNCED3 and AAO3 genes in guard cells causes stomatal closure in *Vicia faba*. *Journal of Plant Research*, 121, 125-131.
- MERLOT, S., GOSTI, F., GUERRIER, D., VAVASSEUR, A. & GIRAUDAT, J. 2001. The ABI1 and ABI2 protein phosphatases 2C act in a negative feedback regulatory loop of the abscisic acid signalling pathway. *Plant Journal*, 25, 295-303.
- MEYER, S., MUMM, P., IMES, D., ENDLER, A., WEDER, B., AL-RASHEID, K. A. S., GEIGER, D., MARTEN, I., MARTINOIA, E. & HEDRICH, R. 2010. AtALMT12 represents an R-type anion channel required for stomatal movement in *Arabidopsis* guard cells. *Plant Journal*, 63, 1054-1062.
- MIYAZONO, K., MIYAKAWA, T., SAWANO, Y., KUBOTA, K., KANG, H. J., ASANO, A., MIYAUCHI, Y., TAKAHASHI, M., ZHI, Y. H., FUJITA, Y., YOSHIDA, T., KODAIRA, K. S., YAMAGUCHI-SHINOZAKI, K. & TANOKURA, M. 2009. Structural basis of abscisic acid signalling. *Nature*, 462, 609-U79.

- MOON, J., PARRY, G. & ESTELLE, M. 2004. The ubiquitin-proteasome pathway and plant development. *Plant Cell*, 16, 3181-3195.
- MORISON, J. I. L., BAKER, N. R., MULLINEAUX, P. M. & DAVIES, W. J. 2008. Improving water use in crop production. *Philosophical Transactions of the Royal Society B-Biological Sciences*, 363, 639-658.
- MOTT, K. A. 2009. Opinion: Stomatal responses to light and CO₂ depend on the mesophyll. *Plant Cell and Environment*, 32, 1479-1486.
- MOTT, K. A., SIBBERNSEN, E. D. & SHOPE, J. C. 2008. The role of the mesophyll in stomatal responses to light and CO₂. *Plant Cell and Environment*, 31, 1299-1306.
- MUSTILLI, A. C., MERLOT, S., VAVASSEUR, A., FENZI, F. & GIRAUDAT, J. 2002. Arabidopsis OST1 protein kinase mediates the regulation of stomatal aperture by abscisic acid and acts upstream of reactive oxygen species production. *Plant Cell*, 14, 3089-3099.
- NA, J.-K. & METZGER, J. D. 2005. Guard cell specific expression of arabidopsis ABF4 alters drought tolerance in tomato and tobacco. *Plant Biology (Rockville)*, 2005, 100.
- NEGI, J., MATSUDA, O., NAGASAWA, T., OBA, Y., TAKAHASHI, H., KAWAIYAMADA, M., UCHIMIYA, H., HASHIMOTO, M. & IBA, K. 2008. CO₂ regulator SLAC1 and its homologues are essential for anion homeostasis in plant cells. *Nature*, 452, 483-U13.
- NEILL, S., DESIKAN, R. & HANCOCK, J. 2003. Nitric oxide as a mediator of ABA signalling in stomatal guard cells. *Bulgarian Journal of Plant Physiology*, 124-132.
- NELSON, D. E., REPETTI, P. P., ADAMS, T. R., CREELMAN, R. A., WU, J., WARNER, D. C., ANSTROM, D. C., BENSON, R. J., CASTIGLIONI, P. P., DONNARUMMO, M. G., HINCHEY, B. S., KUMIMOTO, R. W., MASZLE, D. R., CANALES, R. D., KROLIKOWSKI, K. A., DOTSON, S. B., GUTTERSON, N., RATCLIFFE, O. J. & HEARD, J. E. 2007. Plant nuclear factor Y (NF-Y) B subunits confer drought tolerance and lead to improved corn

- yields on water-limited acres. *Proceedings of the National Academy of Sciences of the United States of America*, 104, 16450-16455.
- NEUMANN, P. M. 2008. Coping mechanisms for crop plants in drought-prone environments. *Annals of Botany*, 101, 901-907.
- NILSON, S. E. & ASSMANN, S. M. 2010. The alpha-Subunit of the Arabidopsis Heterotrimeric G Protein, GPA1, Is a Regulator of Transpiration Efficiency. *Plant Physiology*, 152, 2067-2077.
- NG, L.-M., SOON, F.-F., ZHOU, X. E., WEST, G. M., KOVACH, A., SUINO-POWELL, K. M., CHALMERS, M. J., LI, J., YONG, E.-L., ZHU, J.-K., GRIFFIN, P. R., MELCHER, K. & XU, H. E. 2011. Structural basis for basal activity and autoactivation of abscisic acid (ABA) signaling SnRK2 kinases. *Proceedings of the National Academy of Sciences of the United States of America*, 108, 21259-21264.
- OHMETAKAGI, M. & SHINSHI, H. 1995. Ethylene-Inducible DNA-Binding proteins that interact with an ethylene-responsive element. *Plant cell*, 7, 173-182.
- PARK, S. Y., FUNG, P., NISHIMURA, N., JENSEN, D. R., FUJII, H., ZHAO, Y., LUMBA, S., SANTIAGO, J., RODRIGUES, A., CHOW, T. F. F., ALFRED, S. E., BONETTA, D., FINKELSTEIN, R., PROVART, N. J., DESVEAUX, D., RODRIGUEZ, P. L., MCCOURT, P., ZHU, J. K., SCHROEDER, J. I., VOLKMAN, B. F. & CUTLER, S. R. 2009. Abscisic Acid Inhibits Type 2C Protein Phosphatases via the PYR/PYL Family of START Proteins. *Science*, 324, 1068-1071.
- PETERSEN, K. L., FUCHS, M., MORESHET, S., COHEN, Y. & SINOQUET, H. 1992. Computing transpiration of sunlit and shaded cotton foliage under variable water-stress. *Agronomy Journal*, 84,91-97.
- PETERSON, K. M., RYCHEL, A. L. & TORII, K. U. 2010. Out of the Mouths of Plants: The Molecular Basis of the Evolution and Diversity of Stomatal Development. *Plant Cell*, 22, 296-306.

- POTUSCHAK, T., STARY, S., SCHLOGELHOFER, P., BECKER, F., NEJNSKAIA, V. & BACHMAIR, A. 1998. PRT1 of *Arabidopsis thaliana* encodes a component of the plant N-end rule pathway. *Proceedings of the National Academy of Sciences of the United States of America*, 95, 7904-7908.
- RASCHKE, K., SHABAHANG, M. & WOLF, R. 2003. The slow and the quick anion conductance in whole guard cells: their voltage-dependent alternation, and the modulation of their activities by abscisic acid and CO₂. *Planta*, 217, 639-650.
- RAVEN, J. A. 2002. Selection pressures on stomatal evolution. *New Phytologist*, 153, 371-386.
- RENSING, S. A., LANG, D., ZIMMER, A. D., TERRY, A., SALAMOV, A., SHAPIRO, H., NISHIYAMA, T., PERROUD, P.-F., LINDQUIST, E. A., KAMISUGI, Y., TANAHASHI, T., SAKAKIBARA, K., FUJITA, T., OISHI, K., SHIN-I, T., KUROKI, Y., TOYODA, A., SUZUKI, Y., HASHIMOTO, S.-I., YAMAGUCHI, K., SUGANO, S., KOHARA, Y., FUJIYAMA, A., ANTEROLA, A., AOKI, S., ASHTON, N., BARBAZUK, W. B., BARKER, E., BENNETZEN, J. L., BLANKENSHIP, R., CHO, S. H., DUTCHER, S. K., ESTELLE, M., FAWCETT, J. A., GUNDLACH, H., HANADA, K., HEYL, A., HICKS, K. A., HUGHES, J., LOHR, M., MAYER, K., MELKOZERNOV, A., MURATA, T., NELSON, D. R., PILS, B., PRIGGE, M., REISS, B., RENNER, T., ROMBAUTS, S., RUSHTON, P. J., SANDERFOOT, A., SCHWEEN, G., SHIU, S.-H., STUEBER, K., THEODOULOU, F. L., TU, H., VAN DE PEER, Y., VERRIER, P. J., WATERS, E., WOOD, A., YANG, L., COVE, D., CUMING, A. C., HASEBE, M., LUCAS, S., MISHLER, B. D., RESKI, R., GRIGORIEV, I. V., QUATRANO, R. S. & BOORE, J. L. 2008. The *Physcomitrella* genome reveals evolutionary insights into the conquest of land by plants. *Science*, 319, 64-69.
- ROELFSEMA, M. R. G., HANSTEIN, S., FELLE, H. H. & HEDRICH, R. 2002. CO₂ provides an intermediate link in the red light response of guard cells. *Plant Journal*, 32, 65-75.
- ROELFSEMA, M. R. G. & HEDRICH, R. 2005. In the light of stomatal opening: new insights into 'the Watergate'. *New Phytologist*, 167, 665-691.

- ROHILA, J. S., CHEN, M., CERNY, R. & FROMM, M. E. 2004. Improved tandem affinity purification tag and methods for isolation of protein heterocomplexes from plants. *Plant Journal*, 38, 172-181.
- RUBIO, S., RODRIGUES, A., SAEZ, A., DIZON, M. B., GALLE, A., KIM, T. H., SANTIAGO, J., FLEXAS, J., SCHROEDER, J. I. & RODRIGUEZ, P. L. 2009. Triple Loss of Function of Protein Phosphatases Type 2C Leads to Partial Constitutive Response to Endogenous Abscisic Acid. *Plant Physiology*, 150, 1345-1355.
- RUSZALA, E. M., BEERLING, D. J., FRANKS, P. J., CHATER, C., CASSON, S. A., GRAY, J. E. & HETHERINGTON, A. M. 2011. Land Plants Acquired Active Stomatal Control Early in Their Evolutionary History. *Current Biology*, 21, 1030-1035.
- SAEZ, A., ROBERT, N., MAKTABI, M. H., SCHROEDER, J. I., SERRANO, R. & RODRIGUEZ, P. L. 2006. Enhancement of abscisic acid sensitivity and reduction of water consumption in Arabidopsis by combined inactivation of the protein phosphatases type 2C ABI1 and HAB1. *Plant Physiology*, 141, 1389-1399.
- SAKATA, Y., KOMATSU, K., TAJI, T. & TANAKA, S. 2009. Role of PP2C-mediated ABA signaling in the moss *Physcomitrella patens*. *Plant signaling & behavior*, 4, 887-9.
- SALOMON, M., CHRISTIE, J. M., KNIEB, E., LEMPERT, U. & BRIGGS, W. R. 2000. Photochemical and mutational analysis of the FMN-binding domains of the plant blue light receptor, phototropin. *Biochemistry*, 39, 9401-9410.
- SCHMID, M., DAVISON, T. S., HENZ, S. R., PAPE, U. J., DEMAR, M., VINGRON, M., SCHOLKOPF, B., WEIGEL, D. & LOHMANN, J. U. 2005. A gene expression map of Arabidopsis thaliana development. *Nature Genetics*, 37, 501-506.
- SCHROEDER, J. I., ALLEN, G. J., HUGOUVIEUX, V., KWAK, J. M. & WANER, D. 2001. Guard cell signal transduction. *Annual Review of Plant Physiology and Plant Molecular Biology*, 52, 627-658.

- SCHROEDER, J. I. & KELLER, B. U. 1992. 2 TYPES OF ANION CHANNEL CURRENTS IN GUARD-CELLS WITH DISTINCT VOLTAGE REGULATION. *Proceedings of the National Academy of Sciences of the United States of America*, 89, 5025-5029.
- SHEARD, L. B. & ZHENG, N. 2009. PLANT BIOLOGY Signal advance for abscisic acid. *Nature*, 462, 575-576.
- SHIMAZAKI, K.-I., DOI, M., ASSMANN, S. M. & KINOSHITA, T. 2007. Light regulation of stomatal movement. *Annual Review of Plant Biology*.
- SOKOLOVSKI, S. & BLATT, M. R. 2004. Nitric oxide block of outward-rectifying K⁺ channels indicates direct control by protein nitrosylation in guard cells. *Plant Physiology*, 136, 4275-84.
- SONG, C. P., AGARWAL, M., OHTA, M., GUO, Y., HALFTER, U., WANG, P. C. & ZHU, J. K. 2005. Role of an Arabidopsis AP2/EREBP-type transcriptional repressor in abscisic acid and drought stress responses. *Plant Cell*, 17, 2384-2396.
- SRIRAM, S. M., KIM, B. Y. & KWON, Y. T. 2011. The N-end rule pathway: emerging functions and molecular principles of substrate recognition. *Nature Reviews Molecular Cell Biology*, 12, 735-747.
- STARY, S., YIN, X. J., POTUSCHAK, T., SCHLOGELHOFER, P., NIZHYNSKA, V. & BACHMAIR, A. 2003. PRT1 of Arabidopsis is a ubiquitin protein ligase of the plant N-end rule pathway with specificity for aromatic amino-terminal residues. *Plant Physiology*, 133, 1360-1366.
- STONE, S. L., WILLIAMS, L. A., FARMER, L. M., VIERSTRA, R. D. & CALLIS, J. 2006. KEEP ON GOING, a RING E3 ligase essential for Arabidopsis growth and development, is involved in abscisic acid signaling. *Plant Cell*, 18, 3415-3428.
- TASAKI, T. & KWON, Y. T. 2007. The mammalian N-end rule pathway: new insights into its components and physiological roles. *Trends in Biochemical Sciences*, 32, 520-528.

- TASAKI, T., ZAKRZEWSKA, A., DUDGEON, D. D., JIANG, Y. H., LAZO, J. S. & KWON, Y. T. 2009. The Substrate Recognition Domains of the N-end Rule Pathway. *Journal of Biological Chemistry*, 284, 1884-1895.
- TOUGANE, K., KOMATSU, K., BHYAN, S. B., SAKATA, Y., ISHIZAKI, K., YAMATO, K. T., KOHCHI, T. & TAKEZAWA, D. 2010. Evolutionarily Conserved Regulatory Mechanisms of Abscisic Acid Signaling in Land Plants: Characterization of ABSCISIC ACID INSENSITIVE1-Like Type 2C Protein Phosphatase in the Liverwort *Marchantia polymorpha*. *Plant Physiology*, 152, 1529-1543.
- UMEZAWA, T. 2011. Systems biology approaches to abscisic acid signaling. *Journal of Plant Research*, 124, 539-548.
- VAHISALU, T., KOLLIST, H., WANG, Y. F., NISHIMURA, N., CHAN, W. Y., VALERIO, G., LAMMINMAKI, A., BROSCHE, M., MOLDAU, H., DESIKAN, R., SCHROEDER, J. I. & KANGASJARVI, J. 2008. SLAC1 is required for plant guard cell S-type anion channel function in stomatal signalling. *Nature*, 452, 487-U15.
- VANKIRK, C. A. & RASCHKE, K. 1978. Release of malate from epidermal strips during stomatal closure. *Plant Physiology*, 61, 474-475.
- VARSHAVSKY, A. 2005. Regulated protein degradation. *Trends in Biochemical Sciences*, 30, 283-286.
- VARSHAVSKY, A. 2008. Discovery of Cellular Regulation by Protein Degradation. *Journal of Biological Chemistry*, 283, 34469-34489.
- VARSHAVSKY, A. 2011. The N-end rule pathway and regulation by proteolysis. *Protein Science*, 20, 1298-1345.
- VARSHAVSKY, A. & BYRD, C. 1996. The N-end rule: Functions, mysteries, uses. *Molecular Biology of the Cell*, 7, 2946-2946.
- VIERSTRA, R. D. 2009. The ubiquitin-26S proteasome system at the nexus of plant biology. *Nature Reviews Molecular Cell Biology*, 10, 385-397.

- WANG, Y. B., HOLROYD, G., HETHERINGTON, A. M. & NG, C. K. Y. 2004. Seeing 'cool' and 'hot'-infrared thermography as a tool for non-invasive, high-throughput screening of Arabidopsis guard cell signalling mutants. *Journal of Experimental Botany*, 55, 1187-1193.
- WANG, F. F., LIAN, H. L., KANG, C. Y. & YANG, H. Q. 2010. Phytochrome B Is Involved in Mediating Red Light-Induced Stomatal Opening in Arabidopsis thaliana. *Molecular Plant*, 3, 246-259.
- WANG, H. Q., PIATKOV, K. I., BROWER, C. S. & VARSHAVSKY, A. 2009. Glutamine-Specific N-Terminal Amidase, a Component of the N-End Rule Pathway. *Molecular Cell*, 34, 686-695.
- WASILEWSKA, A., VLAD, F., SIRICHANDRA, C., REDKO, Y., JAMMES, F., VALON, C., FREY, N. F. D. & LEUNG, J. 2008. An update on abscisic acid signaling in plants and more. *Molecular Plant*, 1, 198-217.
- WEBB, A. A. R. & HETHERINGTON, A. M. 1997. Convergence of the abscisic acid, CO₂, and extracellular calcium signal transduction pathways in stomatal guard cells. *Plant Physiology*, 114, 1557-1560.
- WEYERS, J. D. B. & HILLMAN, J. R. 1980. Effects of abscisic-acid on RB-86⁺ fluxes in commelina-communis 1 leaf epidermis. *Journal of Experimental Botany*, 31, 711-720.
- WINTER, D., VINEGAR, B., NAHAL, H., AMMAR, R., WILSON, G. V. & PROVART, N. J. 2007. An "Electronic Fluorescent Pictograph" Browser for Exploring and Analyzing Large-Scale Biological Data Sets. *Plos One*, 2.
- WOODWARD, F. I., LAKE, J. A. & QUICK, W. P. 2002. Stomatal development and CO₂: ecological consequences. *New Phytologist*, 153, 477-484.
- WURTELE, M., JELICH-OTTMANN, C., WITTINGHOFER, A. & OECKING, C. 2003. Structural view of a fungal toxin acting on a 14-3-3 regulatory complex. *EMBO J*, 22, 987-994.
- XIE, X. D., WANG, Y. B., WILLIAMSON, L., HOLROYD, G. H., TAGLIAVIA, C., MURCHIE, E., THEOBALD, J., KNIGHT, M. R., DAVIES, W. J.,

- LEYSER, H. M. O. & HETHERINGTON, A. M. 2006. The identification of genes involved in the stomatal response to reduced atmospheric relative humidity. *Current Biology*, 16, 882-887.
- XIONG, L. M. & ZHU, J. K. 2003. Regulation of abscisic acid biosynthesis. *Plant Physiology*, 133, 29-36.
- XUE, S., HU, H., RIES, A., MERILO, E., KOLLIST, H. & SCHROEDER, J. I. 2011. Central functions of bicarbonate in S-type anion channel activation and OST1 protein kinase in CO₂ signal transduction in guard cell. *Embo Journal*, 30, 1645-1658.
- XU, K., XU, X., FUKAO, T., CANLAS, P., MAGHIRANG-RODRIGUEZ, R., HEUER, S., ISMAIL, A. M., BAILEY-SERRES, J., RONALD, P. C. & MACKILL, D. J. 2006. Sub1A is an ethylene-response-factor-like gene that confers submergence tolerance to rice. *Nature*, 442, 705-708.
- YANG, Y., COSTA, A., LEONHARDT, N., SIEGEL, R. S. & SCHROEDER, J. I. 2008. Isolation of a strong Arabidopsis guard cell promoter and its potential as a research tool. *Plant Methods*, 4,6.
- YOSHIDA, T., FUJITA, Y., SAYAMA, H., KIDOKORO, S., MARUYAMA, K., MIZOI, J., SHINOZAKI, K. & YAMAGUCHI-SHINOZAKI, K. 2010. AREB1, AREB2, and ABF3 are master transcription factors that cooperatively regulate ABRE-dependent ABA signaling involved in drought stress tolerance and require ABA for full activation. *Plant Journal*, 61, 672-685.
- YOSHIDA, S., ITO, M., CALLIS, J., NISHIDA, I. & WATANABE, A. 2002. A delayed leaf senescence mutant is defective in arginyl-tRNA : protein arginyltransferase, a component of the N-end rule pathway in *Arabidopsis*. *Plant Journal*, 32, 129-137.
- YOSHIDA, R., UMEZAWA, T., MIZOGUCHI, T., TAKAHASHI, S., TAKAHASHI, F. & SHINOZAKI, K. 2006. The regulatory domain of SRK2E/OST1/SnRK2.6 interacts with ABI1 and integrates abscisic acid (ABA) and osmotic stress signals controlling stomatal closure in *Arabidopsis*. *Journal of Biological Chemistry*, 281, 5310-5318

- ZEIGER, E., TALBOTT, L. D., FRECHILLA, S., SRIVASTAVA, A. & ZHU, J. X. 2002. The guard cell chloroplast: a perspective for the twenty-first century. *New Phytologist*, 153, 415-424.
- ZHANG, X. R., GARRETON, V. & CHUA, N. H. 2005. The AIP2 E3 ligase acts as a novel negative regulator of ABA signaling by promoting ABI3 degradation. *Genes & Development*, 19, 1532-1543.
- ZHANG, Y. Y., YANG, C. W., LI, Y., ZHENG, N. Y., CHEN, H., ZHAO, Q. Z., GAO, T., GUO, H. S. & XIE, Q. 2007. SDIR1 is a RING finger E3 ligase that positively regulates stress-responsive abscisic acid signaling in Arabidopsis. *Plant Cell*, 19, 1912-1929.
- ZHANG, Y. Y., ZHU, H. Y., ZHANG, Q., LI, M. Y., YAN, M., WANG, R., WANG, L. L., WELTI, R., ZHANG, W. H. & WANG, X. M. 2009. Phospholipase D alpha 1 and Phosphatidic Acid Regulate NADPH Oxidase Activity and Production of Reactive Oxygen Species in ABA-Mediated Stomatal Closure in Arabidopsis. *Plant Cell*, 21, 2357-2377.
- ZHU, M. M., SIMONS, B., ZHU, N., OPPENHEIMER, D. G. & CHEN, S. X. 2010. Analysis of abscisic acid responsive proteins in Brassica napus guard cells by multiplexed isobaric tagging. *Journal of Proteomics*, 73, 790-805.